TiAM

kwartalnik naukowo-techniczny

e-ISSN-2450-8217

TECHNOLOGIA I AUTOMATYZACJA MONTAŻU

ZESPOŁÓW • MASZYN • URZĄDZEŃ

3/2021

Wydawca: Łukasiewicz - IMBiGS • Wydawnictwo SIGMA-NOT • Patronat: SIMP • Istnieje od 1993 r. • Open Access on www.sigma-not.pl • Zeszyt nr 3-2021 (113)

WYDAWNICTWO SIGMA-NOT

Łukasiewicz IMBiGS

TiAM kwartalnik naukowo-techniczny
TECHNOLOGIA I AUTOMATYZACJA MONTAŻU
ZESPOŁÓW • MASZYN • URZĄDZEŃ

ASSEMBLY TECHNIQUES AND TECHNOLOGIES

e-ISSN-2450-8217

ADRES REDAKCJI:
Kwartalnik „Technologia i Automatyzacja Montażu"
ul. Ratuszowa 11, pok. 740, 03-450 Warszawa
Tel. 22 853 81 13
e-mail: tiam@sigma-not.pl
www.tiam.pl

PRENUMERATA:
Zakład Poligrafi i Kolportażu Wydawnictwa SIGMA-NOT Sp. z o.o.
ul. Ks. J. Popiełuszki 19/21, 01-595 Warszawa
tel. 22 840 30 86
tel./fax: 22 827 43 65, 619 22 41 w. 215
e-mail: prenumerata@sigma-not.pl
portal: www.sigma-not.pl

REKLAMA:
Redakcja: tel. 22 853 81 13
e-mail: tiam@sigma-not.pl
Dział Reklamy i Marketingu
tel./fax: 22 827 43 65
e-mail: reklama@sigma-not.pl

SKŁAD I ŁAMANIE:
Wydawnictwo SIGMA-NOT
ul. Ratuszowa 11, 03-450 Warszawa
e-mail: sekretariat@sigma-not.pl

WYDAWCA:

Łukasiewicz IMBiGS

Sieć Badawcza Łukasiewicz
Instytut Mechanizacji Budownictwa i Górnictwa Skalnego
ul. Racjonalizacji 6/8, 02-673 Warszawa

WYDAWNICTWO SIGMA-NOT

Wydawnictwo SIGMA-NOT
ul. Ratuszowa 11, 03-450 Warszawa

PATRONAT:
Stowarzyszenie Inżynierów Mechaników i Techników Polskich

Za treść ogłoszeń i artykułów promocyjnych redakcja nie odpowiada
Wersja pierwotna: elektroniczna

WSKAZÓWKI DOTYCZĄCE PRZYGOTOWANIA ARTYKUŁÓW

- Artykuły przeznaczone do opublikowania w kwartalniku „Technologia i Automatyzacja Montażu" powinny mieć oryginalny i naukowo-techniczny charakter i być zgodne z problematyką czasopisma. Redakcja przyjmuje artykuły w jęz. polskim, jęz. angielskim i jęz. rosyjskim.
- Artykuł o maksymalnej objętości 5 stron A4 wraz z ilustracjami powinien być napisany czcionką Times Roman lub Arial 12 pkt, z interlinią 12 pkt. Formatowany tekst nie powinien mieć podziału na kolumny.
- Tytuł artykułu należy podać w jęz. polskim i jęz. angielskim. Tytuł nieprzekraczający 10 słów powinien odzwierciedlać istotne elementy treści artykułu.
- Struktura artykułów naukowo-technicznych prezentujących prace autora(ów) powinna być następująca: wstęp (wprowadzenie); metodyka (badań, analiz, pracy z podaniem ewentualnie materiałów, założeń itp.); wyniki (badań, analiz); omówienie wyników; wnioski; spis literatury.
- Podpisy pod ilustracjami oraz tytuły tablic należy podać w jęz. artykułu i jęz. angielskim.
- Ilustracje należy dołączyć również jako osobne pliki w formacie: .jpg, .tiff, z rozdzielczością co najmniej 300 dpi. Wszystkie zamieszczane ilustracje powinny być własnością autora(ów) lub należy podać źródło pochodzenia rysunków.
- Wzory matematyczne pisane w edytorze równań Microsoft Equation i powinny być oznaczane kolejnym numerem w nawiasie okrągłym. Wszystkie symbole powinny być objaśnione. Należy stosować jednostki układu SI.
- Spis literatury należy podać w kolejności cytowania w tekście, a odnośniki w tekściepo winny być ponumerowane cyframi arabskimi i umieszczone w nawiasach kwadratowych. W przypadku korzystania z Internetu należy podać adres strony i datę odczytu. Liczbę autocytowań należy ograniczyć do niezbędnych.
- Do artykułu należy dołączyć streszczenie w jęz. artykułu i jęz. angielskim, zawierające minimum 200–250 słów.
- Pod streszczeniem należy podać 3–6 słów kluczowych w jęz. artykułu i jęz. angielskim, zwracając uwagę, by nie były one powtórzeniem tytułu pracy.
- Po spisie literatury zaleca się podanie źródła finansowania pracy.
- Na końcu artykułu należy podać: imiona i nazwiska autorów, tytuły naukowe lub zawodowe, telefon, faks, e-mail, miejsce zatrudnienia wraz z adresem do korespondencji.

PROCEDURA RECENZOWANIA

Procedura recenzowania artykułów w czasopiśmie jest zgodna z zaleceniami Ministerstwa Naukii Szkolnictwa Wyższego zawartymi w opracowaniu „Dobre praktyki w procedurach recenzyjnych w nauce", Warszawa 2011.

Wszystkie artykuły naukowo-techniczne publikowane w kwartalniku „Technologia i Automatyzacja Montażu" są recenzowane.

Nadesłane artykuły są poddawane redakcyjnej ocenie formalnej i otrzymują numer redakcyjny, identyfikujący je na dalszych etapach procesu wydawniczego, a redakcja wysyła do autorów informację o przyjęciu artykułu i wysłaniu go do recenzentów. Do oceny każdej publikacji powołuje się co najmniej dwóch niezależnych recenzentów. Redakcja dobiera recenzentów rzetelnych i kompetentnych w danej dziedzinie. Nadesłane artykuły nie są nigdy wysyłane do recenzentów z tej samej placówki, z której pochodzi autor. Prace recenzentów są poufne i anonimowe. Recenzja musi mieć formę pisemną i kończyć się jednoznacznym wnioskiem o dopuszczeniu artykułu do publikacji w czasopiśmie lub jego odrzuceniu. W przypadku pracy w języku obcym, co najmniej jeden z recenzentów jest afiliowany w instytucji zagranicznej innej niż narodowość autora pracy. Autorzy są informowani o wynikach recenzji oraz otrzymują je do wglądu. W sytuacjach spornych redakcja powołuje dodatkowych recenzentów.

Lista recenzentów publikowana jest w ostatnim zeszycie każdego rocznika.

Kwartalnik „Technologia i Automatyzacja Montażu" ukazuje się formie elektronicznej w otwartym dostępnie (Open Access) i jest dostępny na Portalu Informacji Technicznej Wydawnictwa SIGMA-NOT www.sigma-not.pl

CONTENTS / W NUMERZE

MODELLING OF THE DRAW BEAD COEFFICIENT OF FRICTION IN SHEET METAL FORMING

Modelowanie współczynnika tarcia na progu ciągowym w procesie kształtowania blach

Łukasz CHODOŁA ORCID: 0000-0002-9637-4669
Daniel FICEK ORCID: 0000-0002-9978-8939
Ireneusz SZCZĘSNY ORCID: 0000-0002-3712-8548
Tomasz TRZEPIECIŃSKI ORCID: 0000-0002-4366-0135
Łukasz WAŁEK ORCID: 0000-0002-2446-4403

DOI: 10.15199/160.2021.3.1

Abstract: This paper presents the results of determining the value of the coefficient of friction on the drawbead in sheet metal forming. As the research material, steel, brass and aluminium alloy sheets cut at different directions according to the sheet rolling direction were used. Sheet strip specimens were tested under dry friction and lubrication of sheet surfaces using machine oil. Results of experiments were used to study the effect of process parameters on the coefficient of friction using artificial neural networks. Input data was optimized using genetic algorithm, forward stepwise selection and backward stepwise selection. The aim of the research was to determine the effect of the value of the unit penalty on the significance of individual input parameters of the neural network and the value of the error generated by the multilayer perceptron. It was found that in the case of all materials the value of coefficient of friction for specimen orientation 90° was greater than for the specimen orientation 0°. Friction tests also reveal that sheet lubrication reduced the frictional resistance by 12-39%, depending on the grade of sheet material. Among all input parameters that significantly affect the value of the coefficient of friction the most important are the lubrication conditions and the orientation of the sample.

Keywords: artificial neural networks, coefficient of friction, drawbead, friction, sheet metal forming

Streszczenie: W artykule przedstawiono wyniki wyznaczania wartości współczynnika tarcia na progu ciągowym w procesie kształtowania blach. Jako materiał badawczy wykorzystano blachy stalowe, mosiężne i ze stopu aluminium, które zostały wycięte w różnych kierunkach względem kierunku walcowania blachy. Pasy blachy badano w warunkach tarcia suchego oraz smarowania powierzchni blach olejem maszynowym. Wyniki eksperymentów posłużyły do zbadania wpływu parametrów procesu tarcia na wartość współczynnika tarcia za pomocą sztucznych sieci neuronowych. Dane wejściowe zostały zoptymalizowane przy użyciu algorytmu genetycznego, selekcji krokowej postępującej oraz wstecznej. Celem badań było określenie wpływu wartości kary jednostkowej na istotność poszczególnych parametrów wejściowych sieci neuronowej oraz wartość błędu generowanego przez perceptron wielowarstwowy. Stwierdzono, że w przypadku wszystkich materiałów wartość współczynnika tarcia próbek zorientowanych pod kątem 90° była większa niż dla orientacji próbek 0°. Testy tarcia wykazały również, że smarowanie blach zmniejszyło opory tarcia o 12–39% w zależności od gatunku materiału blachy. Spośród wszystkich parametrów wejściowych, które istotnie wpływają na wartość współczynnika tarcia, najważniejsze z nich to warunki smarowania oraz orientacja próbki.

Słowa kluczowe: sztuczne sieci neuronowe, współczynnik tarcia, próg ciągowy, tarcie, kształtowanie blach

Introduction

The friction between the working surface of the tool and the plastically deformed material has a significant impact on the deformation process and the surface roughness of the drawpiece. External friction causes geometric and kinematic limitations in the implementation of plastic working processes [8, 13]. The type of friction (i.e., dry mixed, boundary) significantly affects the damage to the surface of the component. The frictional connections formed on the surface of the tool cause scratches and burrs on the surfaces of the drawpiece. The phenomenon of friction in plastic working processes differs significantly from friction in machine joints due to [11, 15, 18]:

– large deformations,
– continuous change of surface topography of the workpiece,
– high normal pressures greater than the yield point of the workpiece,
– low relative speeds.

Deep drawing is one of the basic operations of plastic working and consists in transforming a flat sheet into a drawpiece with an non-developable surface [14,17]. During deep-drawing in the bottom of the drawpiece and the cylindrical surface dominate tensile stresses [12, 16]. In the flange, apart from tensile stress, compressive stresses also occur. The sheet metal forming process is most often carried out on presses with tools consisting of a punch, die and blankholder. When forming drawpieces with complex shapes, different sliding speeds occur at different locations on the drawpiece [16]. Draw beads (Fig. 1) are used to limit the flow of material around the flange of the drawpiece [5, 10].

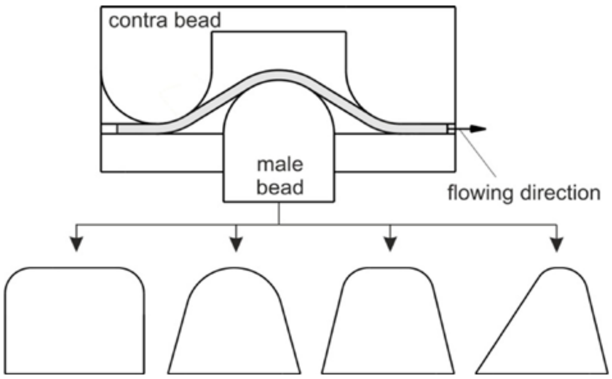

Fig.1. Design of the machined element

Due to the large number of factors influencing a given phenomenon, the development of analytical relationships for determining the response function for given process conditions is practically impossible. This task is successfully performed by artificial neural networks belonging to artificial intelligence methods. The condition for the proper operation of the neural network is the necessity to preselect the input data, which significantly affect the value of the variable explained by the use of the decomposition mechanism. The purpose of data decomposition is to find an answer to the question whether there is a relationship between the input variables and the dependent variable, or whether the relationship is completely random. Data processing systems allow for automatic analysis of a complex set of information and generating answers to the questions asked.

Due to the large number of factors influencing a given phenomenon, it is practically impossible to develop analytical relationships to determine the response function for given conditions of process implementation. This task is successfully performed by artificial neural networks belonging to artificial intelligence methods, whose structure and principle of operation are similar to information processing by living organisms [9]. The condition for the proper operation of the neural network is the necessity to preselect the input data, which significantly affect the value of the output variable by the use of the decomposition mechanism [3, 6]. The purpose of data decomposition is to find an answer to the question whether there is a relationship between the input variables and the dependent variable, or whether the relationship is completely random. Data processing systems allow for automatic analysis of a complex set of information and generating answers to the questions asked [1, 4].

Among the many methods of optimizing the number of training variables, one can mention the Hellwig method, the forward selection method, backward selection, stepwise selection, taboo-search and floating selection. The genetic algorithm searches combinations of features at random. In the next steps of the algorithm, sets of possible solutions (populations) are assessed. The rules governing mutation, crossing and selection ensure that a new population is generated randomly. Nevertheless, in the next steps of the algorithm, better and better individuals are obtained, i.e. sets of features with higher and higher ratings. Simulated annealing algorithm moves sequentially among all possible combinations of features. The rating of a subset of features after the step, i.e. after eliminating one feature, is compared with the rating before the step. There is some probability that the feature will be removed from the subset, even though the resulting subset is judged worse.

In this paper, methods of optimizing the number of input variables of a neural network using three different algorithms based on the results of friction testing. The draw-bead tribological test is used to model the friction phenomenon at the drawbead during sheet metal forming. Three grades of brass, steel and aluminium alloy sheets were tested. The aim of the investigations is to determine the effect of the value of the unit penalty function on (i) the significance of individual input variables of the neural network and (ii) the value of the error generated by the artificial neural network for the training set.

Material and methods

In the tests three grades of brass sheets M63 z4 (1/2 hard), M80 r (soft) and M90 z4 (1/2 hard), three grades of aluminium alloy sheets AA5251 r (recrystallised), AA5251 H14 (strain-hardened – 1/2 hard) and AA5251 H22 (strain-hardened and partially annealed - 1/4 hard), and deed-drawing quality steel sheets DC01, DC03 and DC04 were used. The samples for the friction test were prepared as strips approximately 200 mm long and 20 mm wide. The values of the basic mechanical parameters were determined in the uniaxial tensile test. Tensile tests were carried out using a universal testing machine with a constant crosshead speed of 5 mm/min at ambient temperature. The values of the strain hardening cefficient K and the strain hardening exponent n in the Hollomon equation are determined as follows:

$$\sigma_p = K \cdot \varepsilon^n \tag{1}$$

where σ_p – stress and ε – plastic strain are determined from the logarithmic true stress–true strain plot by linear regression.

The values of the roughness parameters were determined using the Surtronic 3+ Taylor Hobson surface roughness profilometer.

The friction phenomenon arising in the drawbead region of the stamping die have been determined using a drawbead simulator. The model of the simulator is shown in Fig. 2. The device is designed to allow the separation of the deformation resistance of the sheet and the frictional resistance from the total resistance of the sheet metal deformation at the drawbead. Counter-samples in the form of rollers with a diameter of 20 mm and a width of 22 mm were made of cold work tool steel. The surface roughness of rollers was Ra = 0.32

Table. 1. Mechanical properties and roughness parameters of the tested sheets *

Material	Grade	$R_{p0.2}$, MPa	R_m, MPa	A_{50}, %	K, MPa	n	Ra, µm		Rq, µm		Rt, µm	
							0°	90°	0°	90°	0°	90°
Brass	M63 z4	313	397	0.36	589	0.15	0.17	0.2	0.31	0.4	2.5	4.8
	M80 r	120	280	0.48	594	0.37	0.14	0.16	0.18	0.18	1.4	1.9
	M90 z4	346	352	0.12	426	0.04	0.40	0.6	0.58	0.94	6.1	9.9
Aluminium alloys	AA5251 r	68	203	0.18	252	0.28	0.58	0.59	1.14	0.93	6.9	7.0
	AA5251 H14	212	234	0.04	254	0.06	0.22	0.28	0.29	0.35	2.4	2.5
	AA5251 H22	111	201	0.19	370	0.24	0.48	0.49	0.64	0.64	4.1	4.1
Steel	DC01	193	351	0.36	554	0.17	0.23	0.28	0.28	0.41	2.5	4.7
	DC03	196	336	0.42	557	0.19	0.45	0.35	0.62	0.49	3.1	6.4
	DC04	162	310	0.42	54	0.21	0.62	0.51	0.84	0.72	4.1	8.2

* $R_{p0.2}$ – yield stress, Rm – ultimate tensile stress, A_{50} – elongation, K – strain hardening coefficient, n – strain hardening exponent, Ra – average surface roughness, Rq – root mean square deviation of the profile under assessment, Rt – total height of the profile

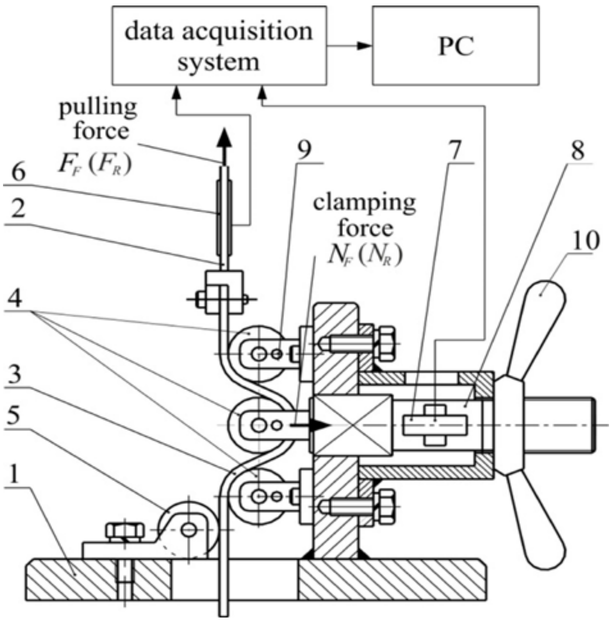

Fig. 2. Cross-section of a drawbead simulator: 1 – frame; 2 – upper tension member; 3 – specimen; 4 – working rollers; 5 – support roller; 6 and 7 – load cells; 8 – horizontal tension member; 9 – pin; 10 – wing nut

µm, measured parallel to the shaft axis. The tests were carried out at the wrap angle of the middle roller equal to 180°. Friction tests were carried out at dry friction and lubrication conditions using LAN 46 machine oil (Orlen Oil, Kraków, Poland). The properties of this oils provided by the manufacturer are listed in Table 2. Prior to testing, both sides of the specimen were oiled by a roller system that permits one to obtain a uniform oil coating between 1.5 and 2 g·m^{-2}, which is comparable with the conditions of the stamping process. Specimens for tests were cut along (0°) and transversely (90°) to the rolling direction of the sheet. The drawing speed of strip specimens was 0.002 m/s.

Table 2. Selected properties of LAN 46 machine oil

Parameter	Value
Kinematic viscosity at 40°C	43.9 mm2/s
Viscosity index	94
Ignition temperature	232°C
Flow temperature	−10°C

The method of determining the coefficient of friction (COF) requires two tests of drawing a sheet metal strip over rotating and fixed rollers. Drawing the specimen over a set of rotating rollers allows one to minimise the frictional resistance. The drawing force in this case is mainly associated with overcoming the deformation resistance of the sheet metal strip. A set of fixed rollers represents the total resistance of drawing the specimen through the drawbead.

The difference in the pulling force for the rotating and fixed rollers can be attributed to the friction process and used to calculate the value of the coefficient of friction according to the relationship:

$$\mu = \frac{1}{\pi}\frac{F_F - F_R}{N_F} \qquad (2)$$

where N_F is the normal force obtained with fixed beads, F_F is the pulling force obtained with fixed rollers and F_R is the pulling force obtained with the freely rotating rollers.

As a result of the experimental friction tests, 36 different training sets (TSs) were obtained (6 grades of sheets × 2 sample orientations × 2 lubrication conditions). On the basis of the received sets of input signals and the corresponding values of the COF, regression models were built using the Statistica program and the impact of the applied methods of optimizing the input signals on the quality of the neural network was assessed. For the analysis, the model of a multilayer perceptron (MLP) was adopted, which, with a properly selected structure, can model any regression problem [2, 7]. From all training pairs (input signals and the corresponding output signal), 10% of cases were randomly selected and included in the validation set (VS). Data from this group was used for independent control of the training algorithm. The remaining number of cases was assigned to the training set.

Data preprocessing

The following set of variables was selected as input parameters in MLP:

– mechanical parameters $R_{p0.2}$, R_m, A_{50}, K and n,
– surface roughness parameters of sheets, Ra, Rq and Rt,
– lubrication conditions,
– sample orientation.

The input data was optimized with a genetic algorithm, forward stepwise selection, and backward stepwise selection. The aim of the genetic algorithm is to find a solution for which the value of the fitness function reaches the maximum. The algorithm worked on the initial population of 300 individuals with the crossing coefficient c_k = 0.5, the mutation rate r_m = 0.1 and different values of the unit penalty ρ = 0.0005, ρ = 0.001, ρ = 0.002, ρ = 0.004, ρ = 0.01, ρ = 0.03. The unit penalty is multiplied by the number of input variables selected in each mask, and then added to the validation error value. The task of the genetic algorithm was to check the quality of the network implementing the generalized regression for a given set of input variables resulting from the reproduction mechanism of the initial population.

Results

• Coefficient of friction

Table 2 presents the values of the friction coefficient of the tested sheets, determined in the conditions of dry friction (μs) and in the conditions of lubricating the sheet surface with oil (μ_o). For the specimen orientation 0°, the values of the coefficient of friction under lubricated conditions were lower by about 22-28% for brass sheets, 19-20% for aluminium alloy sheets and 23-39% for steel sheets. For the specimen orientation 90°, the values of the coefficient of friction under lubricated conditions were lower by about 12-22% for brass sheets, 23-37% for aluminium alloy sheets and 32-37% for steel sheets. In the case of all materials the value of COF for specimen orientation 90° was greater than for the specimen orientation 0°.

Table 2. Values of COFs for tested materials

Specimen orientation	Coefficient of friction					
	μs	μo	μs	μo	μs	μo
Material	**M63 z4**		**M80 r**		**M90 z4**	
0°	0.23	0.17	0.18	0.14	0.25	0.18
90°	0.25	0.22	0.19	0.15	0.27	0.21
Material	**5251 r**		**5251 H14**		**5251 H22**	
0°	0.24	0.19	0.2	0.16	0.21	0.17
90°	0.26	0.2	0.26	0.18	0.29	0.18
Material	**DC01**		**DC03**		**DC04**	
0°	0.24	0.18	0.17	0.13	0.23	0.14
90°	0.27	0.17	0.25	0.16	0.28	0.19

• Artificial neural networks

The results of the optimization analyzes carried out to determine the input signals to the neural network are presented in Tables 3-5. Parameters that significantly affect the value of the coefficient of friction and their removal will worsen the explanation of the value of the coefficient of friction are the lubrication conditions and the orientation of the sample - these variables were selected by each method, regardless of the value of the unit penalty. Among the parameters of sheet surface roughness, the parameters Ra (0°) and Rt (0°) have the most important influence on the value of the friction coefficient.

In terms of the unit penalty values for each of the tested algorithms, the local minimum network error value for the training set is observed. The high error value with a large number of variables can be explained by the noise introduced by the variables, which can be correlated with each other. For further analysis, set of input variables were selected for which the network error value was the smallest, i.e. 0.018 (Table 3).

When assessing the regression model, particular attention should be paid to the ratio of the standard deviation of errors and the standard deviation of the value of the explained variable (S.D. ratio), and the Pearson correlation coefficient R^2. These parameters are determined independently for each of the data sets.

Table 6 shows the regression statistics of the network with input the parameters presented in Table 3 that ensure the lowest value of the network error. Multiple analyzes have been performed with MLPs containing varying numbers of neurons in hidden layer 5-15. The highest value of the Pearson correlation coefficient with the lowest value of S.D. ratio provided a network with a structure of 6:6-11-1:1 (Fig. 3). Selected regression statistics of this network are presented in Table 6. The value of the correlation

Table 3. The influence of the value of the unit penalty on the selection of input variables by genetic algorithm

Variable / Unit penalty	R_{p02}	R_m	A_{50}	C	n	Ra (0°)	Ra (90°)	Rq (0°)	Rq (90°)	Rt (0°)	Rt (90°)	Lubrication conditions	Specimen orientation	ANN error for set TS
0.0005	-	-	-	-	+	+	-	+	-	-	-	+	+	0.0036
0.001	+	+	-	+	-	-	+	+	-	-	-	+	+	0.0028
0.002	+	+	+	+	+	-	-	-	-	-	-	+	+	0.0031
0.004	-	+	+	-	-	-	+	-	-	+	-	+	+	0.0018
0.01	-	-	+	-	+	-	-	-	+	+	-	+	+	0.0029
0.03	-	-	-	-	-	-	-	-	-	-	+	+	+	0.0045

Table 4. The influence of the value of the unit penalty on the selection of input variables by backward stepwise selection

Variable / Unit penalty	R_{p02}	R_m	A_{50}	C	n	Ra (0°)	Ra (90°)	Rq (0°)	Rq (90°)	Rt (0°)	Rt (90°)	Lubrication conditions	Specimen orientation	ANN error for set TS
0.0005	+	-	+	+	-	-	-	-	-	-	-	+	+	0.0033
0.001	-	-	+	+	-	-	+	-	-	-	-	+	+	0.0043
0.002	+	-	+	+	+	-	-	+	-	-	-	+	+	0.0029
0.004	-	+	+	-	+	-	-	-	+	+	-	+	+	0.0041
0.01	-	+	+	-	-	+	-	+	-	+	-	+	+	0.0045
0.03	-	-	-	-	-	+	-	+	-	+	+	+	+	0.0051

Table 5. The influence of the value of the unit penalty on the selection of input variables by forward stepwise selection

Variable / Unit penalty	R_{p02}	R_m	A_{50}	C	n	Ra (0°)	Ra (90°)	Rq (0°)	Rq (90°)	Rt (0°)	Rt (90°)	Lubrication conditions	Specimen orientation	ANN error for set TS
0.0005	+	+	+	-	+	+	-	+	-	-	+	+	+	0.0042
0.001	+	+	-	+	-	+	+	-	-	+	-	+	+	0.0031
0.002	-	-	-	-	-	+	-	-	-	-	-	+	+	0.0023
0.004	-	+	+	-	+	-	+	-	-	-	+	+	+	0.0019
0.01	+	+	+	+	+	+	-	-	-	+	-	+	+	0.0028
0.03	-	+	+	-	-	-	-	-	-	-	-	+	+	0.0061

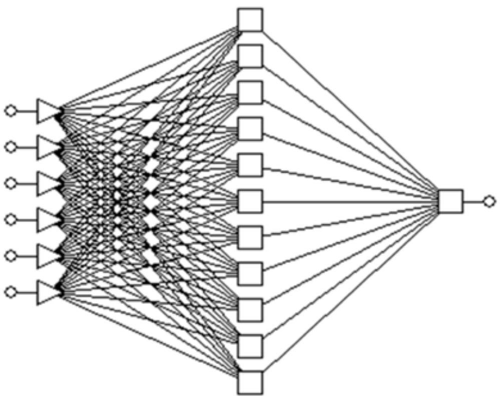

Fig. 3. Structure of MLP 6:6-11-1:1

Table 6. Regression statistics of MLP 6:6-11-1:1

Parameter	TS	VS
Data Mean	0.2117	0.1814
Data S.D.	0.0428	0.0452
Error S.D.	0.0018	0.0106
Abs E. Mean	0.0084	0.0250
S.D. ratio	0.247	0.696
Correlation	0.968	0.795

coefficient for the training set R2 = 0.968 proves a good convergence of the training algorithm. The value of the correlation coefficient for the validation set is much smaller, but it should be emphasized that this set contained only 10% of the training data. With an increasing number of input data in the validation set, the statistics values for that set will approach the corresponding statistics specified for the training set.

As the sample orientation angle changes from 0° to 90°, the value of the friction coefficient increases (Fig. 4). The change of the roughness parameter Ra (90°) in a lesser extent affects the change of the friction coefficient. A different relationship can be observed for the influence of the sample orientation and the roughness parameter Ra (90°) on the value of COF (Fig. 5). When the Rt (0°) parameter increases, the value of the friction coefficient decreases, but only for small values of the sample orientation angle. For the sample orientation of 90°, the value of the friction coefficient depends to a small extent on the value of the Rt (0°) parameter.

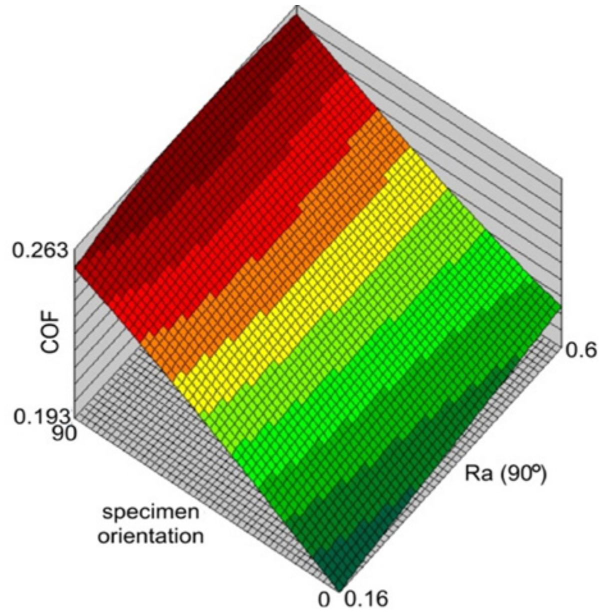

Fig. 3. Structure of MLP 6:6-11-1:1

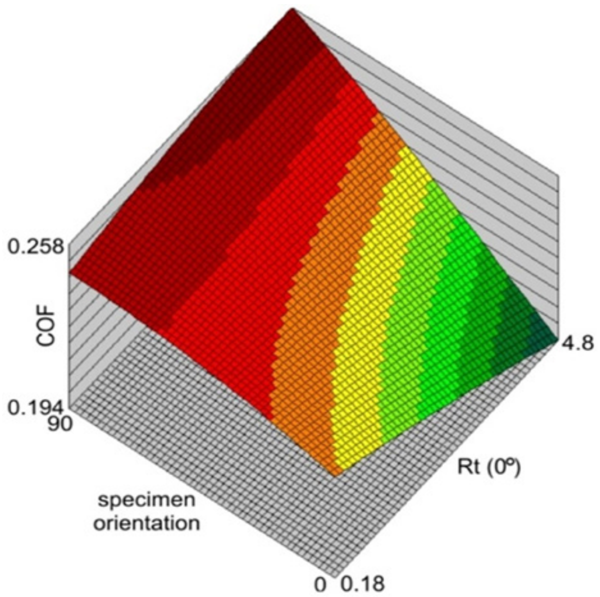

Fig. 3. Structure of MLP 6:6-11-1:1

Conclusions

An approach to integration genetic algorithms and stepwise selection of input variables in the working process of neural networks to calculate the friction coefficient in sheet metal forming is demonstrated in this article. Proper selection of input variables is found to be crucial task to ensure proper quality of the MLPs. This process allows avoiding the time-consuming testing of MLPs with different structure in order to find the optimum network for specific task. The following conclusions are drawn from the research:

– in the case of all materials the value of COF for specimen orientation 90° was greater than for the 0° orientation,
– lubrication reduced the coefficient of friction by 12-39%, depending on the grade of sheet material,
– optimisation of the number of input parameters shown that surface roughness parameters Ra (0°) and Rt (0°) have the most important influence on the value of the COF,
– parameters that significantly affect the value of the COF are the lubrication conditions and the orientation of the sample,
– results of ANN modelling shows that as the sample orientation angle changes from 0° to 90°, the value of the COF increases,
– the change of the roughness parameter Ra (90°) in a small extent affects the change of the COF.

References

[1] Antosz K., Chandima R.R.M. 2019. „Spare parts' criticality assessment and prioritization for enhancing manufacturing systems' availability and reliability". Journal of Manufacturing Systems 50 : 212-225.

[2] Buj-Corral I., Sivatte-Adroer M., Llanas-Parra X. 2020. „Adaptive indirect neural network model for roughness in honing processes". Tribology International 141 : 105891.

[3] Jamli M.R., Farid N.M. 2019. „The sustainability of neural network applications within finite element analysis in sheet metal forming: A review". Measurement 138: 446-460.

[4] Jasiukiewicz-Kaczmarek M., Antosz K., Wyczółkowski R., Mazurkiewicz D., Sun B., Qian C., Ren Y. 2021. „Application of MICMAC, Fuzzy AHP, and Fuzzy TOPSIS for Evaluation of the Maintenance Factors Affecting Sustainable Manufacturing". Energies 14 (5) : 1436.

[5] Ke J., Liu Y., Zhu H., Zhang Z. 2018. „Formability of sheet metal flowing through drawbead–an experimental investigation". Journal of Materials Processing Technology 254 : 283-293.

[6] Kluz R., Antosz K., Trzepieciński T., Bucior M. 2021. „Modelling the Influence of Slide Burnishing Parameters on the Surface Roughness of Shafts Made of 42CrMo4 Heat-Treatable Steel". Materials 14 : 1175.

[7] Liu X., Tian S., Tao F., Yu W. 2021. „A review of artificial neural networks in the constitutive modeling of composite materials". In Press. https://doi.org/10.1016/j.compositesb.2021.109152

[8] Meng F., Gong J., Yang S., Huang L., Zhao H., Tang X. „Study on tribo-dynamic behaviors of rolling bearing-rotor system based on neural network". Tribology International 156 : 106829.

[9] Ramkumar T., Selvakumar M., Chandrasekar P., Mohanraj M., Krishnasharma R. 2021. „Monitoring the neural network modelling of wear behaviour of Ti-6Al-4 V reinforced with nano B4C particle”. Materials Today: Proceedings 41 : 942-950.

[10] Schmid H., Hetz P., Merklein M. 2019. „Failure behaviour of different sheet metal after passing a drawbead”. Procedia Manufacturing 34 : 125-132.

[11] Seshacharyulu K., Bandhavi C., Balu Naik B., Rao S.S., Singh S.K. 2018. „Understanding Friction in sheet metal forming-A review”. Materials Today: Proceedings 5 (9) : 18538-18244.

[12] Shisode M., Hazrati J., Mishra T., de Rooij M., van den Bogaard T. 2021. „Mixed lubrication friction model including surface texture effects for sheet metal forming”. Journal of Materials Processing Technology. 291 : 117035.

[13] Sigvant M., Pilthammar J., Hol J., Wiebenga J.H., Chezan T., Carleer B., van den Boogard T. 2019. „Friction in sheet metal forming: influence of surface roughness and strain rate on sheet metal forming simulation results”. Procedia Manufacturing 29 : 512-519.

[14] Smith L.A., Zhou Y.J., Zhou D.J., Du C., Wanintrudal C. 2009. „A new experimental test apparatus for angle binder draw bead simulations”. Journal of Materials Processing Technology 209 (10) : 4942-4948.

[15] Trzepieciński T., Fejkiel R. 2017. „On the influence of deformation of deep drawing quality steel sheet on surface topography and friction”. Tribology International 115 : 78-88.

[16] Wang W., Zhao Y., Wang Z., Hua M., Wei X. 2016. „A study on variable friction model in sheet metal forming with advanced high strength steels”. Tribology International 93 : 17-28.

[17] Wang Z., Zhang Q., Liu Y., Zhang Z. 2017. „A robust and accurate geometric model for automated design of drawbeads in sheet metal forming”. Computer-Aided Design 92 : 42-57.

[18] Xu Z., Huang J., Mao M., Peng L., Lai X. 2020. „An investigation on the friction in a micro sheet metal roll forming processes considering adhesion and ploughing”. Journal of Materials Processing Technology 285 : 116790.

mgr inż. Łukasz Chodoła – Rzeszow University of Technology, Faculty of Mechanics and Technology, Department of Integrated Design and Tribology Systems, Stalowa Wola, Poland

mgr inż. Daniel Ficek – Rzeszow University of Technology, Faculty of Mechanical Engineering and Aeronautics, Department of Aerospace Engineering, Rzeszów, Poland

mgr inż. Ireneusz Szczęsny – Rzeszow University of Technology, Faculty of Mechanical Engineering and Aeronautics, Department of Aerospace Engineering, Rzeszów, Poland

dr inż. Tomasz Trzepieciński – Rzeszow University of Technology, Faculty of Mechanical Engineering and Aeronautics, Department of Manufacturing and Production Engineering, Rzeszów, Poland
e-mail: tomtrz@prz.edu.pl

mgr inż. Łukasz Wałek – Rzeszow University of Technology, Faculty of Mechanical Engineering and Aeronautics, Avionics and Control Department, Rzeszów, Poland

DESIGN OF AN INNOVATIVE WINDOW-TO-BALCONY BUILDING MODULE

Projekt innowacyjnego modułu budowlanego okno-balkon

Stanisław KOZIOŁ ORCID: 0000-0001-9952-2260
Tomasz SAMBORSKI ORCID: 0000-0001-6914-1678
Andrzej ZBROWSKI ORCID: 0000-0002-6146-3522

DOI: 10.15199/160.2021.3.2

A b s t r a c t: The article presents the concept as well as the geometric and calculation model of an innovative window-to-balcony building module that enables a reversible room rearrangement. The module to be mounted in the building structure changes both the net internal area and the exterior (façade) appearance. The window-to-balcony module provides apartment, office, and hotel room users with a flexible solution that allows for a tightly insulated window to be automatically morphed into an open balcony extension, which makes compact interior more spacious and adds external space to it. Depending on the geometric interdependencies of the ventilation system, the window may be tightly or partly sealed, just like typical tilt and turn windows. Moreover, the window can be titled from the bottom for ventilation purposes or opened fully, in which case it transforms into a balcony.
K e y w o r d s: building, façade, automation, reconfiguration, arrangement

S t r e s z c z e n i e: W artykule przedstawiono koncepcję oraz model geometryczny i obliczeniowy innowacyjnego modułu budowlanego typu okno-balkon, który umożliwia rearanżację pomieszczeń. Moduł montowany w konstrukcji budynku zmienia zarówno wewnętrzną powierzchnię netto, jak i wygląd zewnętrzny (fasadę). Moduł okno-balkon oferuje użytkownikom mieszkań, biur i pokoi hotelowych elastyczne rozwiązanie, które pozwala na automatyczne przekształcenie szczelnie izolowanego okna w otwarte przedłużenie balkonu, co sprawia, że kompaktowe wnętrze staje się bardziej przestronne i dodaje do niego przestrzeń zewnętrzną. W zależności od geometrycznych zależności systemu wentylacyjnego, okno może być szczelne lub częściowo szczelne, tak jak typowe okna uchylno-rozwierane. Ponadto okno może być uchylane od dołu w celu przewietrzenia lub otwierane całkowicie, wówczas przekształca się w balkon.
S ł o w a k l u c z o w e: budynek, elewacja, automatyka, rekonfiguracja, aranżacja

Introduction

The Łukasiewicz Research Network – Institute for Sustainable Technologies is the third biggest research network in Europe. It delivers attractive, comprehensive and competitive technological solutions, also those requested by and tailored to the needs of companies as part of the "challenge us" campaign, where a company's request is analysed by a group of 4,500 scientists within no more than 15 business days and an effective solution that is ready to implement is proposed, all at no costs charged to the company. In doing so, Łukasiewicz engages recognised and highly-qualified researchers and unique scientific equipment, which enables the network to meet companies' needs and expectations. A business owner may choose to contact the network via an on-line form available on https://lukasiewicz.gov.pl/en/for-business/, or visit one of its affiliated institutes or branches in more than 50 locations across Poland, and they may be sure that they will always be provided with the same high-quality product or service, no matter which entity they contact. Łukasiewicz's scientific potential is concentrated in the following research areas: Health, Smart Mobility, Digital Transformation, and Sustainable Economy and Energy. The innovative window-to-balcony solution developed at the Łukasiewicz Research Network – Institute for Sustainable Technologies and described in this article is an example of a solution proposed in response to a request made in the Health and Sustainable Economy areas.

The structures of modern houses more frequently offer reconfiguration, extension and flexible arrangement possibilities, depending on changing user needs [6, 9]. Modular houses are built from several prefabricated segments that are put together. A window-to-balcony component is one of such modular house segments that additionally allows for a reversible room and façade arrangement [15, 16, 17]. The module to be mounted in the building structure changes both the net internal area and the exterior (façade) appearance.

The window-to-balcony module can be widely used in modern multi-storey buildings in which classic balconies that are a fixed architectural element may not be used for stylistic reasons [4, 10]. The window-to-balcony module provides apartment, office, and hotel room users with a flexible solution that allows for a tightly insulated window to be automatically morphed into an open balcony extension, which makes compact interior more spacious and adds external space to it. Depending on the geometric interdependencies of the ventilation system, the window may be tightly or partly sealed, just like typical

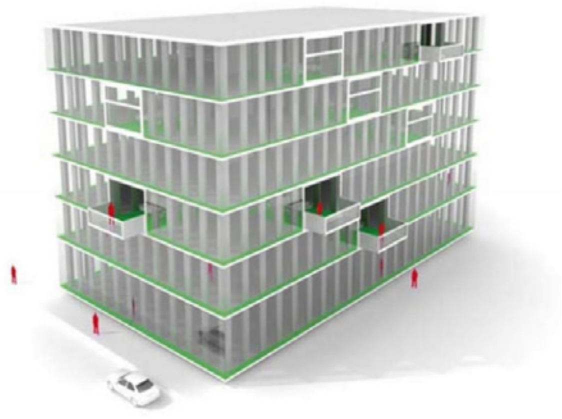

Fig. 1. Residential building with window-to-balcony modules (https://www.treehugger.com/sustainable-product-design/bloomframe-window-transforms-into-balcony.html)

tilt and turn windows. Moreover, the window can be titled from the bottom for ventilation purposes or opened fully, in which case it transforms into a balcony.

Concept of the mechanism

The authors developed a kinematic diagram of the window-to-balcony structure together with its opening and closing mechanisms. The kinematic diagrams in the most characteristic positions of the module are presented in Fig. 2; in Fig. 2.b the individual components of the window-to-balcony mechanism are marked (1–8).

The complete window-to-balcony module is mounted in the opening in the external building (1). The balcony decking (2) and the balustrade (3) are glazed frames that in the closed position (Fig. 2.a) constitute window frames, and in the open position (Fig. 2.d) become structural elements of the balcony extension. The decking (2), balustrade (3) and balustrade handrail (4) are connected using a joint and they form a rhomboid that – as a result of a changed angle between the sides (Figs. 2.a, 2.b, 2.c, and 2.d) – transforms smoothly from a closed to open position, or vice versa.

To change the rhomboid shape, i.e. to either open or close the window-to-balcony module, a mechanism powered by an electric motor that employs a flexible cable (6) that changes its length and thus modifies the angular position of the decking (2) between its two (vertical and horizontal) positions, is used. The flexible cable is rewound using the passive roller (7) to prevent collision with other components of the mechanism and to ensure that the angle at which the decking (2) is pulled up or down is proper. When the decking (2) is in the horizontal position, the window-to-balcony module plays a role of a balcony extension and it needs to transfer high load of, for example, persons standing on it [11, 12]. Such loads are transferred in particular by the articulated rigid rod (8) of a proper length in the fully extended position (Fig. 2.d). The rod (8) also secures the structure against

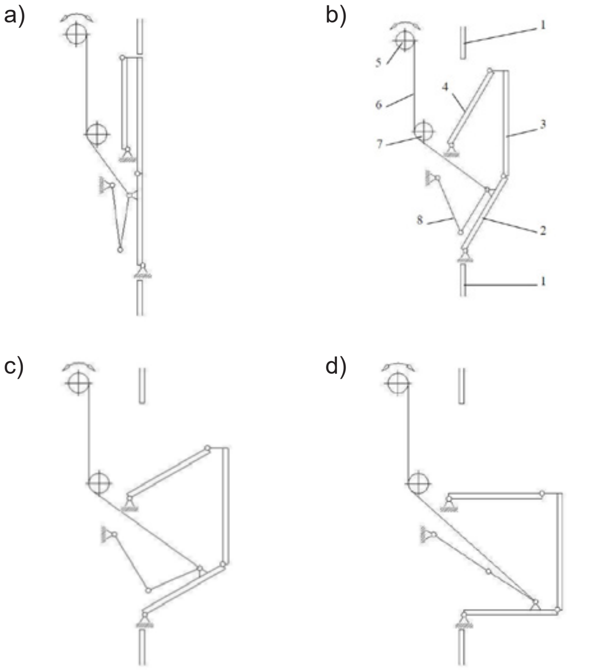

Fig. 2. Kinematic diagram of the window-to-balcony module: a – closed position (window); b – tilted position 1 (30°); c – tilted position 2 (60°); d – open position (balcony); 1 – external wall of a building; 2 – balcony decking; 3 – balustrade; 4 – balustrade handrail; 5 – flexible cable drive system; 6 – flexible cable; 7 – passive roller; 8 – articulated rigid rod

uncontrolled deformation in the event the drive system (5) failure. The mechanism, whose draft is presented in Fig. 3 is composed of two symmetrical systems located at both ends of the structure, the length of which is determined by the transverse dimensions of the decking (2) and the balustrade (3) that decide on the module's net surface. The drive shaft (5) used by the two systems, at the ends of which chain sprockets that cooperate with the cable chains (6) are mounted, ensures synchronous operation of the system in question.

Complying with applicable construction laws [1, 3, 4, 5, 10,], the authors made the following technical assumptions:

Total dimensions (HxWxD)	2,400 x 1,700 x 300 mm
Balcony dimensions (HxWxD)	1,100 x 1,300 x 900 mm
Permitted load	2.5 kN/m^2

3D model

The 3D model of the balcony extension module was developed in accordance with the above-described concept of the opening/closing mechanism and in compliance with applicable construction laws [7]. The model covers the complete window-to-balcony module ready

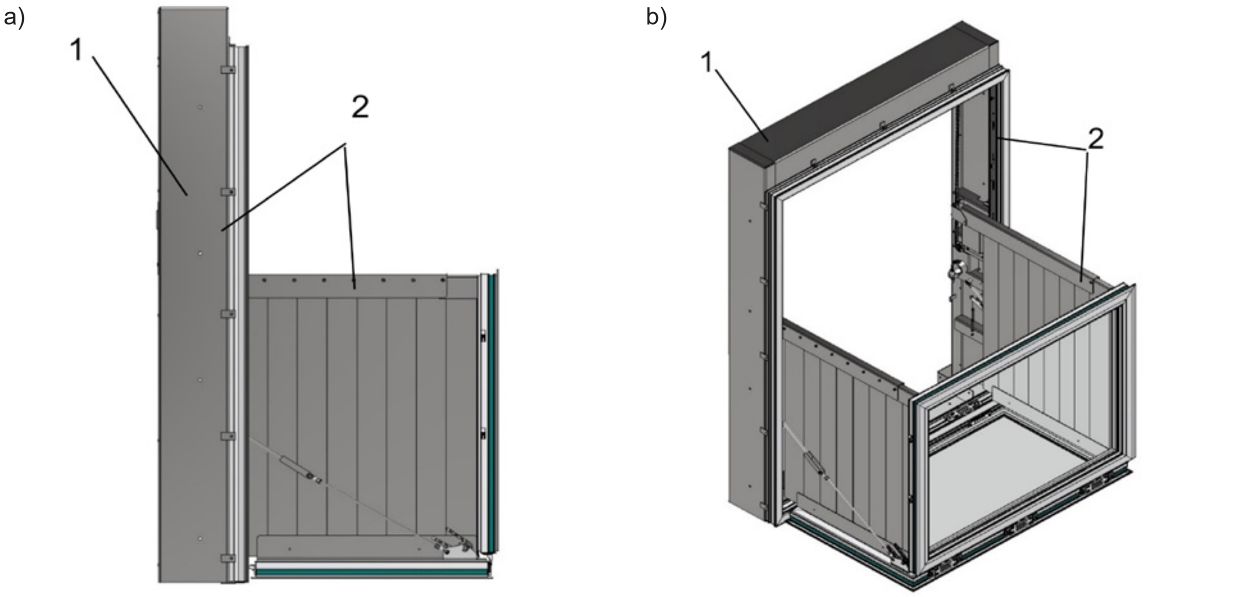

Fig. 3. Complete window-to-balcony module ready to mount in the building wall: a) 2D side view; b) 3D view; 1 – complete case; 2 – window-to-balcony – functional part

to mount in a properly prepared opening in the external building wall.

The complete window-to-balcony module ready to mount in the building wall (Fig. 3) is composed of the following two main units:

- a case mounted in the wall;
- a moveable functional part with a jamb that is mounted in the case and—depending on the position—plays the role of a window or balcony extension.

The case (Fig. 3) is to be installed in the building wall using fasteners fitted in holes with the diameter of 12 mm, and it has the form of a frame welded from bent steel profiles (Fig. 4) in which individual mechanisms and control systems responsible for the operation of the window-to--balcony module are placed.

In the frame there are elements, holes, and threaded holes for the installation of the following mechanisms and systems:

- a moveable functional part with a jamb that plays the role of a window or balcony extension and is mounted using screw fasteners and anchor bolts welded in the frame;
- a chain opening and closing mechanism including an electric drive, gearbox, two synchronous chain gears, and an emergency power supply battery;
- mechanisms supporting the opening of the window--to-balcony module in the initial movement phase;
- collapsible rods transmitting loads in the ‘balcony’ position;
- proximity sensors identifying characteristic positions of the moveable functional part;
- a control panel with which the user operates the window-to-balcony module; and
- inside frame and mechanism covers.

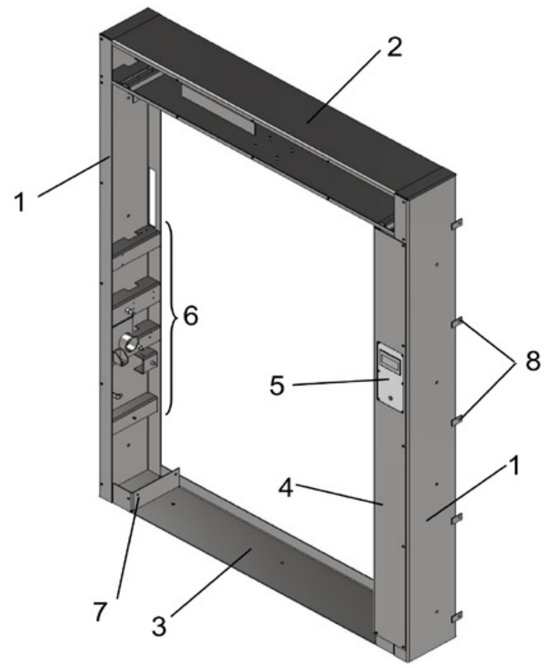

Fig. 4. Frame of the window-to-balcony case welded from bent steel profiles: 1 – vertical profiles (columns); 2 – top profile with a drive system case; 3 – bottom profile; 4 – cover mounted on the case; 5 – control panel; 6 – supports with mechanism assembly elements; 7 – cover mounting bracket; 8 – anchor bolts for the assembly of the window-to-balcony usable part

The moveable functional part of the window-to-balcony module (Fig. 5) is a window structure made of aluminium profiles with good thermal insulation properties (Ponzio) [2, 13] that is composed of a jamb and two sashes connected with high-load capacity hinges, and equipped with dedicated, collapsible side balustrades. The jamb is mounted on the frame of the window-to-balcony module case using 17 screw fasteners screwed on to welded anchor bolts (Fig. 4). The sides of the jamb are connected in each corner with special shape fasteners with strength higher than in the case of typical window or door solutions.

The synchronous movement of both sashes is ensured, as assumed during the concept phase, by the top handrails of the side balustrades that constitute one of the rhomboid's sides. The side balustrade (Fig. 5) is composed of a grip mounted to the top window frame, a guide mounted to the bottom window frame, a top panel (handrail) connecting the top edge of the top sash with the case frame, and the balustrade infill made of overlapping segments that, when closed, fold similarly to blind laths or folding fan leaves.

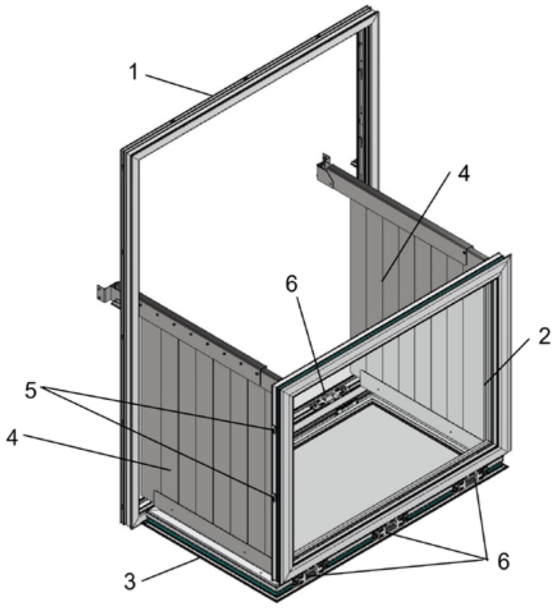

Fig. 5. Moveable functional part of the window-to-balcony module: 1 – jamb made of PONZIO profiles; 2 – top sash playing the role of the front railing; 3 – bottom sash playing the role of the balcony's floor; 4 – side balustrades; 5 – window lock catches; 6 – high-load capacity hinges

The window-to-balcony module is opened and closed by an electric drive system that includes a direct current electric drive, a two-stage worm gearbox and an emergency power supply battery (Fig. 6). The rotational motion is transmitted by a long shaft with chain sprockets located at the ends of the top profile of the window-to-balcony case.

Top chain sprockets put cable chains wrapped around chain sprockets located in the bottom sash into synchronous motion (Fig. 7). The passive end of the cable chain is fixed to the frame of the window-to-balcony case. The drive system lengthens or shortens the cable chain, which results in the opening and closing of the window-to-balcony module respectively.

When fully closed (the 'window' position) the sashes are locked with the use of a locking mechanism

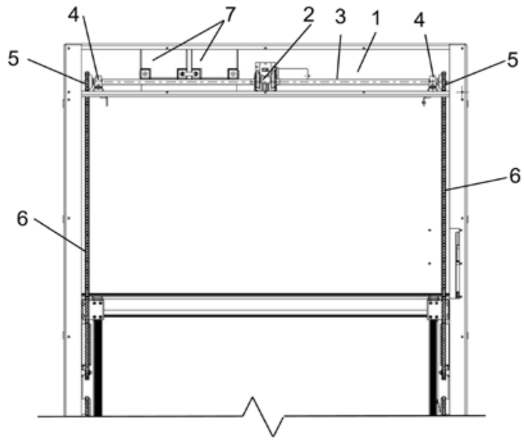

Fig. 6. Drive of the closing/opening mechanism: 1 – top case profile; 2 – gear motor with a direct current electric drive; 3 – drive shaft; 4 – bearing support; 5 – chain sprockets; 6 – cable chains; 7 – emergency power supply batteries

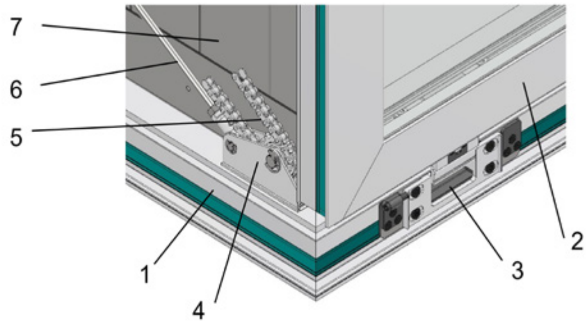

Fig. 7. Cable chain and rod grip in the bottom sash: 1 – bottom sash; 2 – top sash; 3 – hinge; 4 – cable chain and rod grip; 5 – cable chain (fragment); 6 – articulated rigid rod; 7 – balustrade infill

consisting of roller latches located symmetrically at the opposite sides of the jamb, the roller bolts of which move into mortices in strike plates fitted in window frames. The latch is closed automatically by electric actuators fitted in the frame of the case and hid in the mortices in the jamb. When the module is locked in the 'window' position, the load resulting from the wind pressure [8, 9] or pressure difference is transferred onto the locking mechanism; the mechanism also ensures that the window is tightly sealed. In such a position, the tension of the active cable chain can be released.

Strength calculations

The authors calculated the strength of elements and structural nodes of the window-to-balcony module carrying the heaviest load. In calculations the loads resulting from the weight of the designed structure and the balcony decking load capacity complying with applicable construction laws were used [11, 12]. Mechanism strength calculations [8, 14] were made in Mathcad, and modelled complex element calculations – in Autodesk Inventor Professional, using the MES method [7]. Strength calculations concerned in particular: the latch mechanism

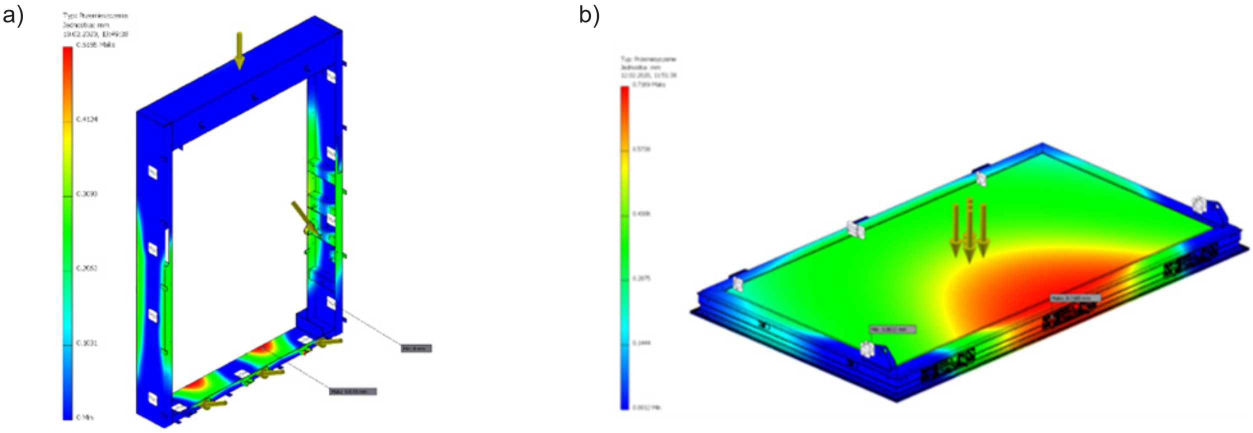

Fig. 8. Shift distribution maps for a) the case frame and b) the floor of the window-to-balcony module under maximum load obtained during the MES analysis

with an articulated rigid rod and catches; hinges; and the opening/closing mechanism with a cable chain. The MES analysis was performed on the frame of the window-to--balcony module case, front and side balustrades, and the balcony floor (decking). Sample maps of the window-to-balcony module case and floor shift distribution under maximum load obtained during the MES analysis are presented in Fig. 8.

Summary

The developed structural design enables the implementation of a reconfigurable module in modern buildings with changeable net internal area and the façade arrangement. The proposed structure of the module is an alternative to traditional building design in which fixed structural elements are used. The module design includes mechatronic components with automatic diagnostics and safety systems. Future work will focus on the construction of a prototype and verification tests that will enable all required permits and certificates to be issued and the product to be marketed.

References

[1] Appendix no. 1 to the Ordinance of the Minister of Infrastructure of 12 April 2002: List of Polish norms referred to in the Ordinance.

[2] Appendix no. 2 to the Ordinance of the Minister of Infrastructure of 12 April 2002: Thermal insulation requirements and other energy efficiency-related requirements.

[3] Appendix no. 3 to the Ordinance of the Minister of Infrastructure of 12 April 2002: Terms relating to flammability and fire propagation as used in the Ordinance and corresponding reaction to fire and roof fire resistance classes.

[4] Construction Law of 7 January 1994 (consolidated text, Journal of Laws of 2019, Item 1186, as amended: Journal of Laws of 2018, Item 2245 and of 2019, Items 1309, 1524, 1696, 1712, 1815, and 2170)

[5] Construction Products Act of 16 April 2004 (consolidated text, Journal of Laws of 2019, Item 266, as amended: Journal of Laws of 2019, Item 730).

[6] Dymkowski R. 2015. Okna dachowe - inne niż inne. Fachowy Dekarz & Cieśla. 03.2015. http://fachowydekarz.pl/okna-dachowe-inne-niz-inne/

[7] http://www.autodesk.pl/products/inventor/features/simulation-visualization

[8] Jastrzębski P., Mutermilch J., Orłoś W. 1985. Wytrzymałość materiałów. Warszawa: Arkady.

[9] Konstantinos-Alketas Oungrinis. 2013. “Implementation of Kinetic Systems in Architecture: A Classification of Techniques and Mechanisms Appropriate for Discreet Building Parts”. Conference: International Conference on Adaptation and Movement in Architecture (ICAMA2013), Toronto Canada. Volume: Proceeding of International Conference on Adaptation and Movement in Architecture.

[10] Ordinance of the Minister of Infrastructure of 12 April 2002 regarding technical conditions to be met by buildings and locations in which they are erected (consolidated text, Journal of Laws of 2019, Item 1065).

[11] PN-EN 1990 Eurocode: Basis of Structural Design.

[12] PN-EN 1991 Eurocode 1: Actions on Structures.

[13] PN-EN ISO 10077-1:2007 Thermal performance of windows, doors and shutters — Calculation of thermal transmittance — Part 1: General.

[14] Podstawy konstrukcji maszyn. 1995.Vol. 1, ed. M. Dietricha, Kraków: WNT,.

[15] Rider N. 2017. “Australian first: window-meets-balcony system to be used for Brisbane tower”. Architecture & Design 3.

[16] Rogers S. A.: Bloomframe: Window Morphs Into a Balcony in Seconds. https://weburbanist.com/2016/01/29/bloomframe-window-morphs-into-a-balcony-in-seconds/

[17] Smisek P.: The Window that Transforms into a Balcony. https://www.theb1m.com/video/bloomframe-the-window-that-transforms-into-a-balcony. 02.2018.

dr inż. Stanisław Kozioł – Łukasiewicz Research Network – Institute for Sustainable Technologies,
ul. K. Pułaskiego 6/10, 26-600 Radom,
e-mail: stanislaw.koziol@itee.radom.pl

dr inż. Tomasz Samborski – Łukasiewicz Research Network – Institute for Sustainable Technologies,
ul. K. Pułaskiego 6/10, 26-600 Radom,
e-mail: tomasz.samborski@itee.radom.pl

dr hab. inż. Andrzej Zbrowski, prof. Ł-ITeE-PIB Łukasiewicz Research Network – Institute for Sustainable Technologies,
ul. K. Pułaskiego 6/10, 26- 600 Radom,
e-mail: andrzej.zbrowski@itee.radom.pl

THE INFLUENCE OF NATURAL SEASONING ON THE LOAD CAPACITY OF CYLINDRICAL ADHESIVE JOINTS

Wpływ sezonowania naturalnego na nośność połączeń klejowych czopowych walcowych

Władysław ZIELECKI ORCID: 0000-0002-7864-5525
Ewelina GUŹLA ORCID: 0000-0002-7359-6007
Przemysław BIELENDA

DOI: 10.15199/160.2021.3.3

A b s t r a c t: The aim of the work was to investigate the influence of natural seasoning on the load capacity of cylindrical adhesive joints subjected to and not subjected to additional heat treatment. The adhesive joints ware made of ENAC-AlSi7Mg0.3 aluminum alloy (sleeve) and glass-epoxy composite (pivot). The elements were joined together using the Araldite 2014 adhesive composition. The adhesive joins were subjected to an axial shear test. The research was carried out for several variants of seasoning: seasoning for 6 months in the summer period, seasoning for 6 months in the winter period, seasoning for one year and two years. The test results show that the seasoning of samples not subjected to additional heat treatment increased the load capacity of the adhesive joints by 0.1-21.3%. On the other hand, in the case of samples subjected to additional heat treatment, seasoning contributed to the reduction of the load capacity of the joints by 0.6-24%. The analysis of significant differences (Student's t-test) showed that in the adopted range of variability of the input factors, the seasoning conditions did not have a significant impact on the load capacity of the adhesive connections. Only in the case of samples with additional heat treatment, seasoned for 2 years, the load capacity shows statistically significant differences compared to other variants (pv=0.23%). The results of correlation and regression analysis indicate that in the case of samples subjected to additional heat treatment, the load capacity of the adhesive joints decreases with the increasing duration of seasoning (r=-0.835). In the case of samples that have not been subjected to additional heat treatment, the load capacity of the joints increases with the increasing duration of seasoning (r=0.841).
K e y w o r d s: natural seasoning, cylindrical adhesive joints, heat treatment, EN AC-AlSi7-Mg0.3 aluminum alloy, glass-epoxy composite EP405-GE

S t r e s z c z e n i e: Celem pracy była ocena wpływu sezonowania naturalnego na nośność połączeń klejowych czopowych walcowych poddanych i niepoddanych dodatkowej obróbce cieplnej (dotwardzaniu cieplnemu). Złącza klejowe wykonano ze stopu aluminium EN AC-AlSi7Mg0,3 (tuleja) oraz kompozytu szklano-epoksydowego (czop). Elementy połączono ze sobą za pomocą kompozycji klejowej Araldite 2014. Połączenia klejowe poddano próbie ścinania osiowego. Badania przeprowadzono dla kilku wariantów sezonowania: sezonowania przez 6 miesięcy w okresie letnim, sezonowania przez 6 miesięcy w okresie zimowym, sezonowania przez jeden rok oraz przez dwa lata. Wyniki badań wskazują, że sezonowanie próbek niepoddanych dodatkowej obróbce cieplnej spowodowało zwiększenie nośności połączeń klejowych o 0,1-21,3%. Natomiast w przypadku próbek poddanych dodatkowej obróbce cieplnej sezonowanie przyczyniło się do zmniejszenia nośności złączy o 0,6-24%. Analiza istotnych różnic (test t-Studenta) wykazała, że w przyjętym zakresie zmienności czynników wejściowych warunki sezonowania nie miały istotnego wpływu na nośność połączeń klejowych. Jedynie nośność próbek z dodatkową obróbką cieplną sezonowanych przez okres 2 lat wykazuje istotne statystycznie różnice w porównaniu do pozostałych wariantów (pv=0,23%). Wyniki analizy korelacji i regresji wskazują, że w przypadku próbek poddanych dodatkowej obróbce cieplnej nośność połączeń klejowych maleje wraz ze wzrostem czasu sezonowania (r=-0,835). W przypadku próbek, które nie zostały poddane dodatkowej obróbce cieplnej, nośność złączy zwiększa się wraz ze wzrostem czasu sezonowania (r=0,841).
S ł o w a k l u c z o w e: sezonowanie naturalne, połączenie klejowe czopowe walcowe, obróbka cieplna, stop aluminium EN AC-AlSi7-Mg0.3, kompozyt szkło-epoksydowy EP405-GE

Introduction

Adhesive joints are widely used in various industries and in many cases they successfully replace mechanical joints. Compared to conventional mechanical joints, adhesive joints provide a more even stress distribution along the joint area, can be used to join various materials with different thermal expansion coefficients, are more resistant to corrosion and have good damping and sealing properties [10].

Due to the shape and mutual positioning of the joined elements, the adhesive joints can be divided into cylindrical and non-cylindrical connections. Among the cylindrical joints, there are non-tapered and tapered joints. The non-cylindrical joints are divided into flat (frontal and lap) and angular (T-shaped and corner) connections [17].

The most popular adhesive joints are lap joints, which are characterized by a very simple structure [12, 17].

Cylindrical joints can be used, for example, as an alternative to interference fits connections [17]. One of the applications of cylindrical joints is joining composite pipes used for pipeline transport [22]. Another example of the use of this type of adhesive joints is hollow insulator. There are four types of such insulators: ceramic, glass, polymer (composite and resin) and hybrid [5]. Ceramics and glass are traditional materials used in the construction of insulators. These materials are characterized by durability, good mechanical properties and resistance to environmental factors. Their disadvantages are brittleness and low resistance to dirt [7]. In recent years, composite insulators have been gaining more and more popularity. The advantages of composite insulators are good mechanical properties, resistance to dirt, flexibility, low weight (compared to ceramic insulators), ease of transportation and installation. Due to the relatively short service life, and thus relatively small operating experience, composite insulators are still not fully tested in terms of long-term service life [8, 23]. Composite insulators are made of a glass-epoxy tube or a rod with metal fittings attached to the ends of it, and an insulating sheath made of silicone rubber. The element transmitting mechanical loads is a glass-epoxy composite tube. In the exemplary composite insulator (Fig. 1), metal fittings are attached to the pipe with epoxy adhesive. The insulating sheath protects the core against environmental influences. The shape of insulating sheath determines the electrical properties of the insulator. The insulating sheath may be formed by injection molding. Composite insulators, depending on the manufacturer, may differ in dimensions, the method of making the insulation sheath, material and execution of fittings, etc. [7, 8].

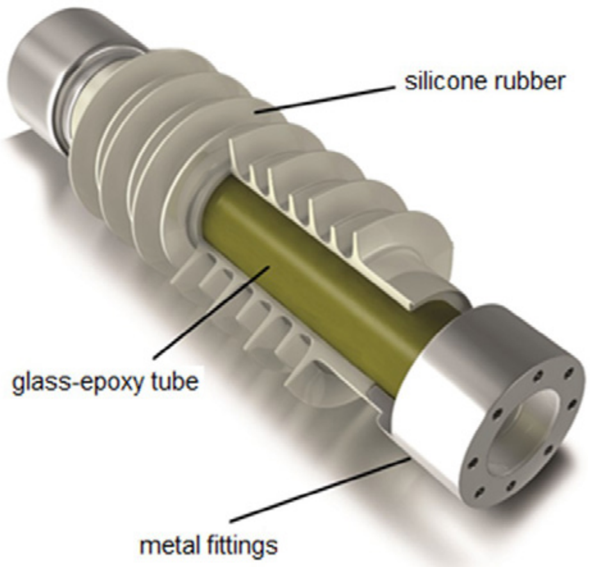

Fig. 1. The composite insulator [8]

Adhesive connections in composite insulators are exposed to environmental factors, such as cyclical temperature and air humidity changes. In the currently available literature, there are no results of research on the influence of natural seasoning in the Polish climatic zone on the strength of adhesive cylindrical joints used in composite insulators. Nevertheless, existing similar analyzes of the influence of temperature or aging time on the behavior of adhesive joints may be helpful in the design of adhesive joints in composite insulators.

The main components of adhesives are polymers. Therefore, the thermal properties of polymers largely determine the behavior of the adhesive joint at high, low or changing temperatures [9]. In the case of polymers (as well as adhesives), long-term exposure to elevated temperature leads to the so-called thermal degradation. As a result of degradation, macromolecules break down into smaller fragments. Additional cross-linking of the material structure in the first phase of degradation may contribute to the improvement of adhesive properties, including the increase of mechanical strength [18]. Nevertheless, further degradation can lead to a reduction in molecular weight or an excessive cross-linking of the structure, ultimately leading to deterioration of the strength properties. In the work [24], studies were carried out on the effect of additional heat treatment on a butt joint static strength at ambient temperature and elevated temperature. It has been shown that as a result of the heat treatment, the static strength of the joints tested at ambient temperature can be increased. However, in the case of joints created using compositions with an excess of hardener, which are additionally exposed to high temperatures, additional heat treatment may weaken such joints. Therefore, additional heat treatment cannot be treated as a universal method of increasing the strength of adhesive joints.

The process of structural changes occurring during degradation may be caused not only by long-term exposure to high temperature, but also by other external factors such as oxygen, ozone, high-energy radiation, light radiation, UV radiation, chemicals (including steam and water) and mechanical stress (in particular, cyclically changing dynamic stresses) [18].

In the case of long-term exploitation of adhesive joints, the adhesive bonds may be weakened as a result of moisture diffusion processes taking place at the interface between the adherent element and the adhesive joint. The method of protection the joints in this case may be coating the joints with special agents resistant to moisture adsorption [19].

Adhesives, as macromolecular materials with a spatially cross-linked structure, exhibit the characteristics of a viscoelastic body under long-term exploitation under load (they have both sticky and elastic properties). In the case of viscoelastic systems, the values or velocities of deformation depend on both the stresses and the duration of the load. As a result of viscoelastic properties the deformations change under the influence of constant stress, even when the stress is very small [19].

Another property that may affect the strength of adhesive joints is the value of the coefficients of thermal expansion of the joined elements. If the difference between the coefficients is large, then significant stresses may be constituted within the joint [9].

The influence of seasoning conditions or temperature on the strength of adhesive joints was analyzed in various studies [4, 6, 11, 13-15, 20, 21]. The paper [10] presents the results of research on the influence of the curing and seasoning time on the strength of single-lap 1H18N9T stainless steel adhesive joints. The joints were made with three different compositions consisting of Epidian 53 epoxy resin and PAC, Z1 or TFF hardener. Curing was carried out in cold conditions, in one stage for 7 days at the temperature of 22±2° C and the humidity of 32%. After curing, the samples were seasoned for 14 or 28 days. It was shown that in the case of joints made with Epidian 53 + Z1 composition, the seasoning resulted in a reduction of the shear strength of the connections.

The subject of work [20] was the analysis of the influence of temperature and aging time on selected mechanical properties of four different adhesive compositions. The following variants of seasoning were used: seasoning for one month, two months, five months and eight months at a temperature of 24±2°C, seasoning for one month at a temperature of -10±2°C, and seasoning for five months first at negative temperature and then at a temperature of 24±2˚C. Cylindrical samples, made of adhesive mass, were subjected to compressive strength tests. It was found that in the case of seasoning at the temperature of 24±2°C, the compressive strength of the samples increased with the increase of the seasoning time. The samples were especially sensitive to the effects of negative temperature. The negative temperature made the epoxy compounds brittle. Variable seasoning conditions had a slight effect on the compressive strength of the samples.

The paper [14] presents the results of research on the effect of thermal shocks on the strength of lap and butt joints made of steel and aluminum alloy. Two types of adhesives were used in the research - one of them was characterized by stiffness and the other by increased flexibility. The tests were carried out for 500 cycles of temperature changes. The minimum temperature was -20˚C and the maximum 38˚C. It was observed that the strength of butt and lap joints slightly increased in the initial stage of aging and then began to decline.

The subject of the work [4] was the analysis of the influence of temperature on the shear strength of lap joints made of aluminum alloy. The glass transition temperature (Tg) of the tested adhesive composition was 155°C. According to the test results, the samples tested at a temperature slightly lower than the Tg were characterized by a higher shear strength than the joints tested at room temperature. According to the authors of the study, the higher strength of joints at elevated temperatures resulted from the increase in the plasticity of the adhesive and the reduction of maximum stresses at the ends of the overlap. However, at temperatures above Tg, the adhesive behaved like rubber and the shear strength dropped drastically.

The work [6] searched for methods to increase the strength of adhesive joints at elevated temperatures. The authors of the study showed that nanofillers in the form of nanosilica have a positive effect on the strength of joints exposed to high temperature.

The authors of the paper [11] looked for a method to increase the strength of joints exposed to both low and high temperatures. The solution proposed by the researchers was to make the connection using two types of adhesive compositions - brittle in the middle of the joint (transferring loads at high temperatures) and plastic at the ends of the joint (transferring loads at low temperatures).

To sum up, the problem of the influence of natural seasoning on the load capacity of adhesive joints is very important when designing adhesive structures. A method that can be used to improve mechanical properties of adhesive joints is additional heat treatment. In the literature, there are analyzes of the influence of additional heat treatment or seasoning conditions on adhesive joints. However most of the analyzes, are carried out for lap joints and concern relatively short seasoning times. Therefore, it is justified to carry out further research on the influence of the seasoning conditions and additional heat treatment on the load capacity of the cylindrical adhesive joints used, among others, in composite insulators. Accordingly, the aim of the research presented in the article is to assess the effect of natural seasoning on the load capacity of the cylindrical adhesive joints made of EN AC--AlSi7-Mg0.3 aluminum alloy and glass-epoxy composite EP405-GE subjected and not subjected to additional heat treatment.

Methodology

The analysis was carried out for cylindrical adhesive joints. The sleeves were made of EN AC-AlSi7-Mg0.3 aluminum alloy (Table 1), while the pivots were made of glass-epoxy composite EP405-GE (manufacturer: KUVAG ISOLA Composites GmbH).

The adhesive joints were made using the two-component composition Araldite 2014 (manufacturer – Huntsman). Araldite 2014 is an epoxy-based construction adhesive. This adhesive is resistant to temperatures up to 120˚C (248˚F). It withstands exposure to water and different chemicals. It is suitable for bonding metals, ceramics, GRP, electronic components and other parts which may be exposed to aggressive environments or elevated temperatures [2].

The surfaces of the sleeves and pivots were mechanically treated in order to develop the appropriate geometrical structure and, as a result, to increase the strength of adhesive bonds. The sleeves were turned using the LZ-360 universal lathe (Fabryka Maszyn Tarnów, Poland). The surfaces of the pivots were ground. Grinding was

Table 1. Chemical composition of ENAC-AlSi7Mg0.3 aluminium alloy [1]

Fe	Si	Mn	Ti	Cu	Mg	Zn	Others	
max 0.19	6.5 - 7.5	Max 0.1	Max 0.25	Max 0.05	0.25 - 0.45	Max 0.07	each 0.03; total 0.1	Al - balance

performed using a RUP-280 roller grinder (Fabryka Maszyn Tarnów, Poland) with an MVBE 45 grinding wheel with dimensions of 400x50x107 mm.

The next step was to measure the surface roughness of the sleeves and pivots. The surface roughness measurements were carried out using the Talysurf CCI Lite optical profilometer (manufacturer: Hobson) which scans surfaces and allows to perform measurements in 2D and 3D. Table 2 presents the results of surface roughness measurements.

Table 2. Results of surface roughness measurements

SLEEVE (turned)								
2D parameters								
Rp	Rv	Rz	Rc	Rt	Ra	Rq	Rsk	Rku
11.8 µm	7.51 µm	19.4 µm	17.7 µm	20.9 µm	4.64 µm	5.46 µm	0.579	2.00

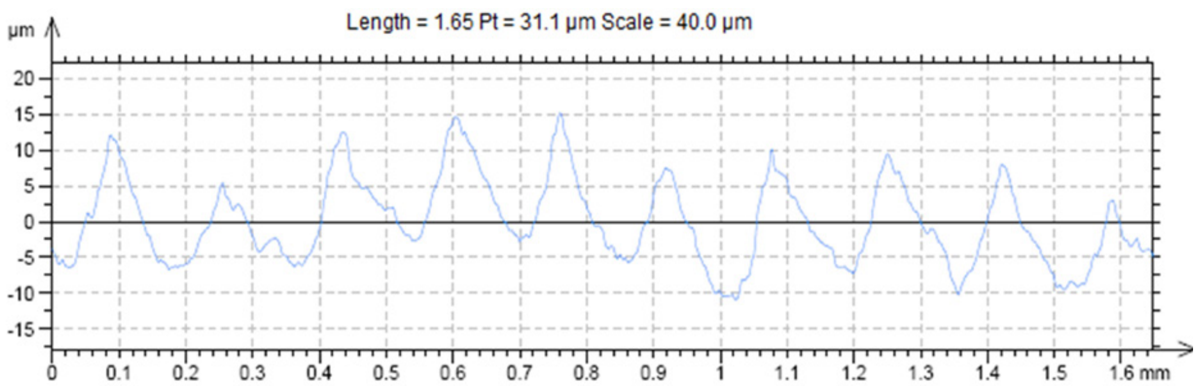

3D parameters						
Sq	Ssk	Sku	Sp	Sv	Sz	Sa
16.1 µm	0.853	3.10	63.1 µm	26.3 µm	89.5 µm	13.0 µm

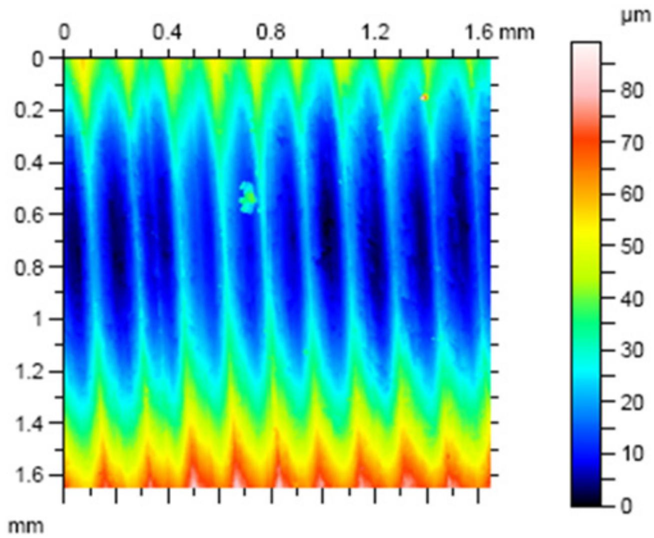

PIVOT (ground)								
2D parameters								
Rp	Rv	Rz	Rc	Rt	Ra	Rq	Rsk	Rku
9.88 µm	8.75 µm	18.6 µm	4.16 µm	18.6 µm	0.599 µm	1.14 µm	0.635	29.4

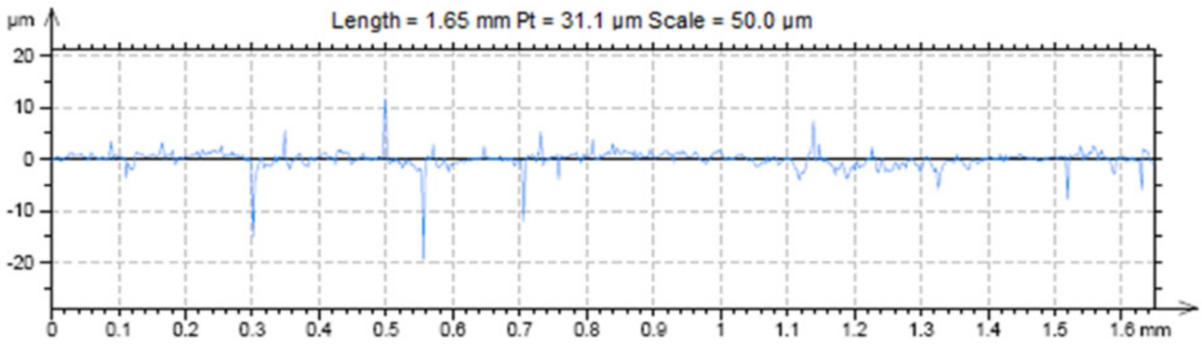

3D parameters						
Sq	Ssk	Sku	Sp	Sv	Sz	Sa
12.6 µm	-0.597	2.21	36.2 µm	40.8 µm	77.0 µm	10.8 µm

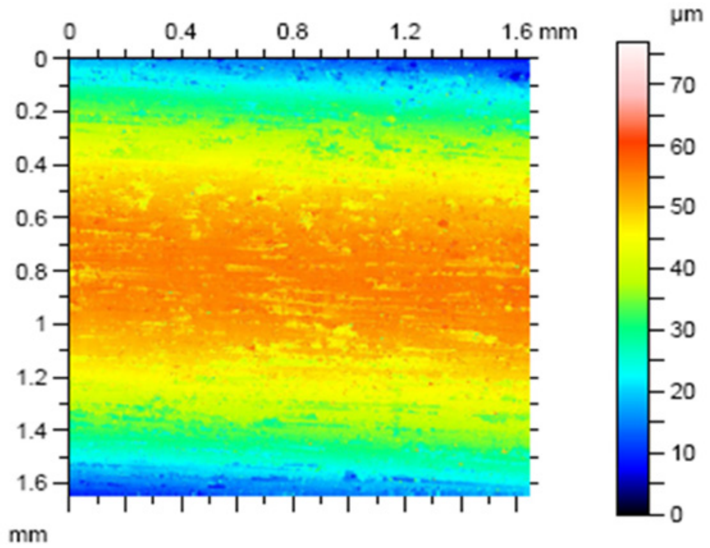

Subsequently, the surfaces of the sleeves and pivots were degreased in order to remove fatty impurities and machining residues. Degreasing was carried out in an EMMI-40HC ultrasonic cleaner (manufacturer: EMAG, Poland) filled with acetone. The degreased elements were placed in the washer for 5 minutes. After this time, the elements were removed from the washer and allowed to dry. Degreased and dried elements were joined using Araldite 2014 composition. The scheme of the cylindrical adhesive joints created in this way is shown in Figure 2.

The adhesive was applied to the inside surface of the sleeve and the center surface of the pivot with a spatula. The pivots were then placed in the sleeve in such a way that the sleeve was in the middle of the pivot. The thickness of the adhesive layer was 1 mm. After removing the adhesive flashes, the samples were placed in a special device (jigging fixture). As a result, the desired position of

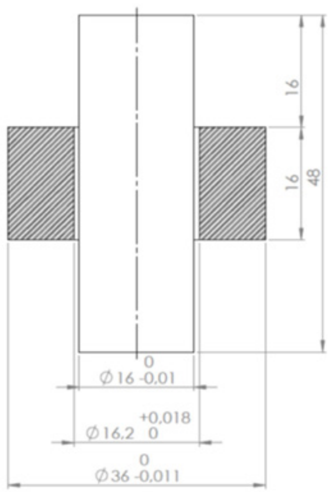

Fig. 2. Dimensions and shape of the cylindrical adhesive joints

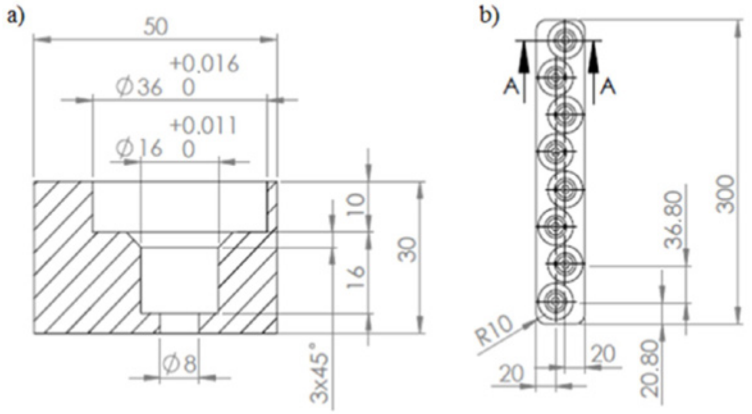

Fig. 3. Scheme of the device

Table 3. Seasoning variants

Variant description	Variant – without heat treatment	Variant – with heat treatment
Without seasoning	**0M**	**0M-HT**
6 months of seasoning started in the summer period (01.07.2013 – 31.01.2014)	6MS	6MS-HT
6 months of seasoning started in the winter period (10.01.2014 –10.07.2014)	6MW	6MW-HT
1 year of seasoning (01.07.2013 – 30.06.2014)	12M	12M-HT
2 years of seasoning (01.07.2013 – 30.06.2015)	24M	24M-HT

the connection elements was maintained (including the central position of the pivot in the sleeve, which ensures the same thickness of the adhesive layer throughout the cross-section). The cross-linking time of the samples in the device was 48 h, and the temperature was 21±1˚C. The scheme of the device is shown in Figure 3.

Then, half of the prepared cylindrical adhesive joints were subjected to additional heat treatment. The samples were heated in a chamber furnace (Polish producer Kepka Group) at 120˚C for 60 minutes. After removal from the furnace the samples were cooled at room temperature.

The next stage was the natural seasoning of the adhesive joints. The seasoning was carried out in several variants, differing in the length of the seasoning and the period in which it was carried out. Each variant consisted of 5 heat treated and 5 non-heat treated samples. The seasoning variants are shown in Table 3.

The samples were seasoned in Rzeszow (Podkarpackie Voivodeship, Poland) in urban conditions and were exposed to the sun and other weather conditions (rainfall, snow). The temperature and relative humidity distribution during the 24 months of seasoning shown in Figure 3 was taken from the weather archive [25–26].

a) b)

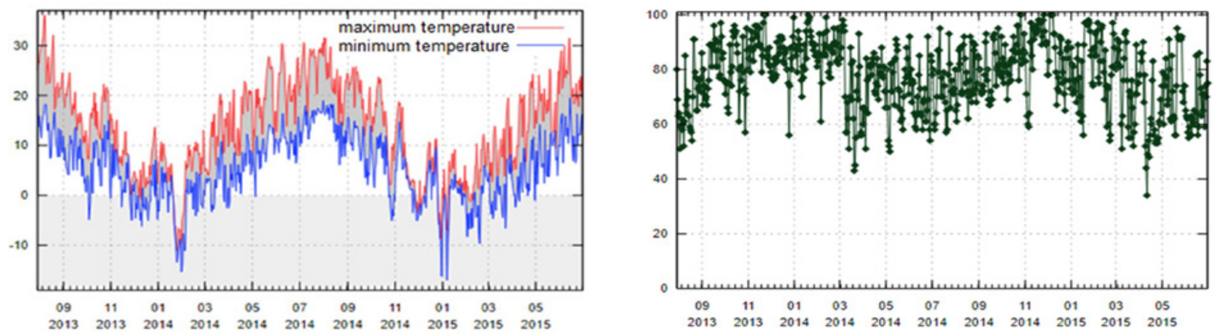

Fig. 4. Graphs showing the distribution of temperature (4a) and relative humidity (4b) during the 24 months of seasoning (01.07.2013 – 30.06.2015) [25–26]

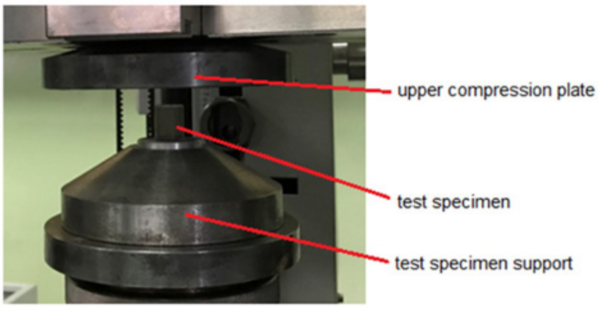

Fig. 5. The sample placed in the handle of the machine

The last step was testing the strength of the cylindrical adhesive joints. For this purpose, the samples were subjected to an axial shear test on a Zwick/Roell Z100 testing machine (manufacturer: Zwick Roell GmbH & Co. KG, Germany). Figure 5 shows a sample placed in the handle of the machine.

The test was performed in accordance with the standard PN-EN ISO 10123:2019-07 (Adhesives - Determination of shear strength of anaerobic adhesives using pin-and-collar specimens) [16].The pin-and-collar test is applied to compare the shear strength of adhesives. This test can be used for quality control purposes and not for joint design. The sample consists of two elements glued together: a cylindrical pin and a slip collar. The sample is placed in the test machine in such a way that the collar is supported on the ring on a compression plate. A compressive load is applied to the top end of the pin and forces the pin through the collar. The force required to shear the adhesive joint is used to calculate the shear strength of the adhesive [3, 16].

During the shear test, an initial force of 50 N, a test speed of 5 mm min and a maximum deformation of 15 mm were assumed. The testXpert software from Zwick/Roell was used for the tests.

Results and discussion

Table 4 and Figure 6 show the results of strength tests for cylindrical adhesive joints differing in the seasoning variant and the presence of additional heat treatment.

Fig. 6. Average values of the load capacity of cylindrical adhesive joints and standard deviation values

Based on Table 4 and Figure 6, it can be concluded that in the case of joints that were not subjected to additional heat treatment, the six-month seasoning started in summer (variant 6MS) contributed to an increase in the load capacity of the joints. High summer temperatures could have increased the cross-linking and stiffness of the joint. The joint may have strengthened naturally under the influence of the sun. The six-month seasoning started in winter (variant 6MW) did not increase the load capacity of the connections. The lower winter temperatures did not allow the connections to strengthen. After one-year seasoning (12M variant), the strengthening effect has stabilized. The two-year seasoning (variant 24M) contributed to the highest strengthening of the joints. To sum up, the test results show that in the accepted range of

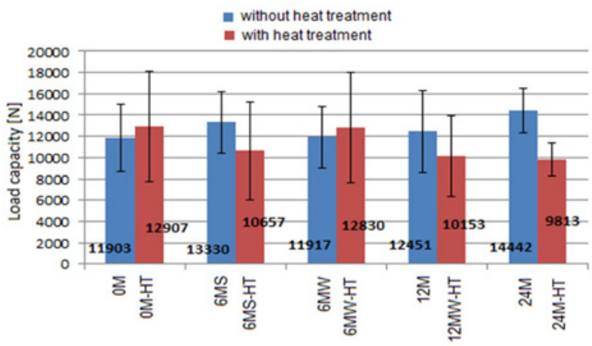

Fig. 6. Average values of the load capacity of cylindrical adhesive joints and standard deviation values

Table 4. The results of strength tests

Wariant	Load capacity – sample no 1	Load capacity – sample no 2	Load capacity – sample no 3	Load capacity – sample no 4	Load capacity – sample no 5	Load capacity – average	Change in load capacity	Standard deviation	Range $R=P_{max}-P_{min}$	Percentage error $(0.5\cdot R):P_{śr}$
	P_1 [N]	P_2 [N]	P_3 [N]	P_4 [N]	P_5 [N]	$P_{śr}$ [N]	ΔP [%]	σ [N]	R [N]	B [%]
0M	14760	15383	10073	11412	7886	11903	---	3162	7497	31
0M-HT	9284	12230	9526	21886	11609	12907	---	5180	12602	49
6MS	10236	11931	16890	15933	11661	13330	12.0	2905	6654	25
6MS-HT	6061	17771	11651	10589	7213	10657	-17.4	4599	11709	55
6MW	7917	13748	10573	15412	11937	11917	0.1	2889	7495	31
6MW-HT	10668	11731	10523	21914	9315	12830	-0.6	5150	12599	49
12M	8595	11702	17161	9096	15701	12451	4.6	3855	8566	34
12M-HT	14332	10043	12432	9631	4328	10153	-21.3	3771	10004	49
24M	16746	11457	14367	15912	13726	14441	21.3	2055	5288	18
24M-HT	10742	10126	10175	7084	10937	9813	-24.0	1565	3853	20

input factors variability, the seasoning of joints that were not subjected to additional heat treatment resulted in an increase in the load capacity of the connections.

In the case of joints that were subjected to additional heat treatment, the six-month seasoning started in July (variant 6MS-HT) resulted in a decrease in the load capacity of the connections. The probable cause of the reduction in load capacity was excessive degradation which could result in a reduction in molecular weight or excessive cross-linking of the structure. The six-month seasoning started in winter (variant 6MW-HT) contributed to the decrease in the load capacity of the connections to a lesser extent. The one-year (12M-HT variant) and two-year (24M-HT variant) seasoning also resulted in a decrease in the load capacity of the connections. The difference in the load capacity of the connections between the one-year and two-year variants was small. Summarizing, it can be concluded that the seasoning of adhesive joints subjected to additional heat treatment resulted in a decrease in the load capacity of the joints. This decrease is the highest in the case of 12-month seasoning (12M-HT variant) and the lowest in the case of 6-month seasoning started in winter (6MW-HT). Moreover, by comparing the obtained values of the load capacity of the joints, it can be stated that higher values of the standard deviation were obtained in the case of samples subjected to additional heat treatment (variants 12M-HT and 24M-HT are the exception).

The results of the research on the load capacity of cylindrical adhesive joints were statistically analyzed using the Student's t-test. Statistical significance $\alpha=0.05$ was assumed for the analyzes. In the first step, the Student's t-test was used to analyze the significant differences between the load capacity of connections subjected or not been subjected to additional heat treatment (Table 5).

Table 5. The results of the analysis of significant differences between the load capacity of joints subjected and not subjected to additional heat treatment

Compared variants		Pv [%]
0M	0M-HT	36.15
6MS	6MS-HT	15.47
6MW	6MW-HT	37.39
12M	12-HT	18.43
24M	24M-HT	0.23

Based on Table 5, it can be concluded that the pv probability values are in most cases higher than 5%. This means that in the assumed range of variability of input factors, the load capacities of joints subjected and not subjected to heat treatment do not differ significantly. A statistically significant difference is revealed only in the case of two-year seasoning (pv = 0.23%). Therefore, only in this case the additional heat treatment has a significant impact on the load capacity of the adhesive joints.

Student's t-test was also used to analyze significant differences between the load capacities of connections seasoned in different time periods. These analyzes were carried out for joints that were not subjected to heat treatment (Table 6) and for joints that were subjected to heat treatment (Table 7).

Table 6. The results of the analysis of significant differences between the load capacities of adhesive joints not subjected to heat treatment and seasoned in different time periods

Pv [%]	0M	6MS	6MW	12M	24M
0M	X	23.94	50.00	40.61	8.84
6MS		X	23.94	34.77	23.35
6MW			X	40.61	8.84
12M				X	17.35
24M					X

Table 7. The results of the analysis of significant differences between the load capacities of adhesive joints subjected to heat treatment and seasoned in different time periods

Pv [%]	0M-HT	6MS-HT	6MW-HT	12M-HT	24M-HT
0M-HT	X	24.43	48.94	18.36	13.01
6MS-HT		X	23.35	42.73	35.69
6MW-HT			X	19.21	13.75
12M-HT				X	42.94
24M-HT					X

Based on tables 6 and 7, it can be concluded that all probability pv values are greater than 5%. Therefore, in the adopted range of variability of input factors, the seasoning conditions (seasoning variant) do not have a significant impact on the load capacity of the adhesive joints.

The test results were subjected to regression and correlation analysis. The input factor was the duration of seasoning (SL): 0 months, 6 months (summer period), 12 months and 24 months. The resulting factor was the load capacity (P[N]) of adhesive joints. The analyzes were carried out for joints subjected to and not subjected to additional heat treatment. Regression equations showed a relationship between the seasoning time and the load capacity of adhesive joints. The calculated values of the Pearson correlation coefficient determined the degree of linear dependence between the studied variables. The results of the regression and correlation analysis are presented in Table 8.

According to the results presented in Table 8, it can be stated that in the case of samples subjected to additional heat treatment, the load capacity of the adhesive joints decreases with the increasing duration of seasoning. Moreover, there is a strong negative linear correlation of –0.835 between the load capacity of the joints

Table 8. The results of correlation and regression analysis

Variant	Linear regression equation	Pearson correlation coefficient r	Determination coefficient R^2 [%]	p-value
Adhesive joints subjected to heat treatment	$y_P = 12075 - 114\ x_{SL}$	-0.835	70.8	0.165
Adhesive joints not subjected to heat treatment	$y_P = 12075 + 91\ x_{SL}$	0.841	69.8	0.159

subjected to heat treatment and the seasoning duration. In the case of samples that have not been subjected to additional heat treatment, the load capacity of the joints increases with the increasing duration of seasoning. The obtained value of the Pearson correlation coefficient in this case also indicates a strong linear correlation (r = 0.841) between the seasoning duration and the load capacity of the connections.

Conclusion

1. Seasoning of samples not subjected to additional heat treatment, started in the summer period, resulted in an increase in the load capacity of the adhesive joints. The load capacity of connections seasoned for 6 months increased by 12.0%, while the load capacity of connections seasoned for 24 months increased by 21.3%. The increase in load capacity of joints that were not subjected to additional heat treatment can be explained by the fact that high summer temperatures may have increased the cross-linking of the adhesive-bonded joint. Under the influence of solar radiation, the adhesive-bonded joint may have naturally post-hardened and the connection may have strengthened.
2. Additional heat treatment of the cylindrical adhesive joints increased their load capacity by 8.4% in comparison to the samples not subjected to heat treatment. The increase in load capacity was caused by the increase in cross-linking of the adhesive-bonded joint. Seasoning of the joints subjected to additional heat treatment, commenced in the summer period, resulted in a decrease in their load capacity by 17.4% after 6 months, by 21.3% after 12 months and by 24.0% after 24 months of seasoning. On the other hand, the 6-month seasoning started in the winter period resulted in the reduction of the load capacity by only 0.6%. The obtained test results indicate that more cross-linked adhesive-bonded joints of connections subjected to additional heat treatment are more sensitive to changes in stresses caused by deformations of the joined elements at higher temperatures.
3. The analysis of significant differences between the load capacity of adhesive joints subjected to and not subjected to additional heat treatment showed that within the adopted range of variability of input factors, only in the case of two-year seasoning, additional heat treatment had a significant impact on the load capacity of the adhesive joints. In the case of two-year seasoning, the load capacity of joints not subjected to additional heat treatment was 32% higher than the load capacity of connections subjected to heat treatment.
4. The analysis of significant differences between the load capacity of joints seasoned in different periods and lengths of time has shown that, within the adopted range of variability of input factors, the seasoning variant did not have a significant impact on the load capacity of adhesive joints (both for joints subjected to and not subjected to additional heat treatment).
5. The regression and correlation analysis showed that there is a strong linear relationship between the duration of the seasoning and the load capacity of the tested adhesive joints. In the case of joints not subjected to additional heat treatment, the load capacity increased with the increase in the duration of the seasoning and the linear correlation coefficient was 0.841. In the case of samples subjected to additional heat treatment, the extension of the seasoning time reduced the load capacity of the adhesive joints and the linear correlation coefficient was –0.835.
6. The obtained results of tests of the cylindrical adhesive joints made of EN AC-AlSi7-Mg0.3 aluminum alloy and glass-epoxy composite EP405-GE bonded with Araldite 2014 adhesive showed that natural aging over a period of 24 months does not cause statistically significant changes in their strength properties, therefore the adhesive technology can be successfully used in the production of composite overhead insulators.

References

[1] Aluminium alloy EN AC-AlSi7Mg0.3 technical data, [access May 2021], http://www.steelnumber.com/en/steel_alloy_composition_eu.php?name_id=1225 [2] [2] Araldite 2014 technical data, [access May 2021], http://www.adhesive-help.com/productdatasheets/huntsman-a2014.pdf

[3] ASTM D 4562–0. Standard Test Method for Shear Strength of Adhesives Using Pin-and-Collar Specimen. ASTM Standards Volume 15.06.

[4] Banea M.D., da Silva L.F.M., Campilho R.D.S.G. 2014. “Effect of temperature on the shear strength of aluminium single lap bonded joints for high temperature applications”. Journal of Adhesion Science and Technology 28: 1367-1381.

[5] Bielecki J., Wańkowicz J. 2014. “Nieznormalizowane wymagania i kryteria oceny kompozytowych wsporczych izolatorów stacyjnych do sieci 110 kV i 220 kV”. Przegląd Elektrotechniczny 10: 106-109.

[6] Biruk-Urban K., Kuczmaszewski J. 2013. „Modyfikacja klejów epoksydowych w aspekcie ich właściwości cieplnych”. Technologia i Automatyzacja Montażu 2: 31-34.

[7] Bretuj W., Wieczorek K. 2016. „Zachowanie się układu hybrydowego izolatorów kompozytowego i ceramicznego w warunkach eksploatacyjnych”. Przegląd Elektrotechniczny 10: 171-174.

[8] Composite hollow insulators technical data, [access May 2021], https://www.izolatory.pl/en/produkty/composite-hollow-insulators/composite-hollow-insulators

[9] Comyn J. 2018. Thermal Properties of Adhesives. In da Silva L. F. M., Öchsner A., Adams R. D. (ed.) Handbook of Adhesion Technology, 459-487. Springer International Publishing AG.

[10] da Silva L. F. M., Öchsner A., Adams R. D. 2018. “Introduction to Adhesive Bonding Technology”. In da Silva L. F. M., Öchsner A., Adams R. D. (ed.) Handbook of Adhesion Technology, 1-7. Springer International Publishing AG.

[11] da Silva L. F.M., Adams R.D. 2007. „Joint strength predictions for adhesive joints to be used over a wide temperature range”. International Journal of Adhesion & Adhesives 27: 362-379.

[12] Her S. C., Chan C. F. 2019. “Interfacial Stress Analysis of Adhesively Bonded Lap Joint”. Materials 12: 2403.

[13] Kłonica M. 2017. “Wpływ zmiennych obciążeń cieplnych na bezpieczeństwo klejonych konstrukcji lotniczych”. In Bielawski R., Grenda B. (ed.) Bezpieczeństwo lotnicze w aspekcie rozwoju technologicznego. Warszawa: Wydawnictwo Akademii Sztuki Wojennej.

[14] Kuczmaszewski J. 2006. Fundamentals of metal-metal adhesive joint design. Lublin: Lublin University of Technology, Polish Academy of Sciences, Lublin Branch.

[15] Mirski Z., Wróblewski R., Gołembiewski A. 2015. „Resistance of adhesive joints to impact high temperaturę”. Przegląd spawalnictwa 10: 108–114.

[16] PN-EN ISO 10123:2019-07. Adhesives - Determination of shear strength of anaerobic adhesives using pin-and-collar specimens. Warsaw: Polish Committee for Standardization.

[17] Porębska M. 2013. Połączenia spójnościowe. Warszawa: Wydawnictwo Naukowe PWN.

[18] Rojek M. 2011. Metodologia badań diagnostycznych warstwowych materiałów kompozytowych o osnowie polimerowej. Open Access Library.

[19] Rośkowicz M. 2008. „Statyczna trwałość czasowa połączeń klejowych”. Przegląd Spawalnictwa 8: 31–37.

[20] Rudawska A. 2019. “The Impact of the Seasoning Conditions on Mechanical Properties of Modified and Unmodified Epoxy Adhesive Compounds”. Polymers 11: 804.

[21] Rudawska A., Celejewski F., Miturska I., Kowalska B. 2016. „Wytrzymałość połączeń klejowych po różnym czasie sezonowania”. Przetwórstwo Tworzyw 3: 126-131.

[22] Selahi E. 2018. “Elasticity solutions of adhesive tubular joints in laminated composites with axial symmetry”. Archives of Mechanical Engineering 3: 441-456.

[23] Strużewska E. 2010. „Długotrwała wytrzymałość konstrukcji kompozytowych izolatorów liniowych”. Elektroenergetyka: Współczesność i Rozwój 1: 75-79.

[24] Szabelski J., Domińczuk J., Kuczmaszewski J. 2019. Wpływ ciepła na właściwości połączeń klejowych. Lublin: Wydawnictwo Politechniki Lubelskiej.

[25] Weather condition data – temperature, [access May 2021], https://www.weatheronline.pl/weather/maps/city?LANG=pl&WMO=12580&ART=MXMN&CONT=plpl&R=150&LEVEL=150&REGION=0001&LAND=__&NOREGION=0&MOD=&TMX=&TMN=&SON=&PRE=&MONAT=&OFFS=&SORT=&MM=06&YY=2015&WEEK=100

[26] Weather conditio data - relative humidity, [acces May 2021], https://www.weatheronline.pl/weather/maps/city?LANG=pl&WMO=12580&ART=RLF&CONT=plpl&R=150&LEVEL=150&REGION=0001&LAND=__&NOREGION=0&MOD=&TMX=&TMN=&SON=&PRE=&MONAT=&OFFS=&SORT=&MM=06&YY=2015&WEEK=100.

dr hab. inż. Władysław Zielecki, prof. PRz - Wydział Budowy Maszyn i Lotnictwa Politechniki Rzeszowskiej, Katedra Technologii Maszyn i Inżynierii Produkcji, al. Powstańców Warszawy 8, 35-959 Rzeszów, e-mail: wzktmiop@prz.edu.pl

mgr inż. Ewelina Guźla – Wydział Budowy Maszyn i Lotnictwa, Katedra Technologii Maszyn i Inżynierii Produkcji, al. Powstańców Warszawy 8, 35-959 Rzeszów, e-mail: e.guzla@prz.edu.pl

mgr inż. Przemysław Bielenda - Wydział Budowy Maszyn i Lotnictwa, Katedra Technologii Maszyn i Inżynierii Produkcji, al. Powstańców Warszawy 8, 35-959 Rzeszów

SIMILARITIES AND DIFFERENCES IN THE PROCESS OF AUTOMATING THE ASSEMBLY OF RIGID BODIES AND ELASTIC ELEMENTS OF PNEUMATIC TIRES

Podobieństwa i różnice w procesie automatyzacji montażu brył sztywnych oraz elementów plastycznych opon pneumatycznych

Paweł KNAST ORCID: 0000-0001-7430-9914

DOI: 10.15199/160.2021.3.4

A b s t r a c t: The paper presents the classification of tyre elements intended for automatic and robotic assembly into rigid bodies (material points within the geometric part of the element cannot move against each other) and plastic elements (subject to irreversible deformation under the influence of external forces, temperature, gravity, which act on the unvulcanised tyre elements). The assembly process has been divided into 7 closed-loop areas of the automation and robotisation process of industry 4.0 factories in order to demonstrate the similarities and differences that affect the degree of automation and robotisation of assembly. Characteristic features of rigid bodies and plastic elements are also described. Plastic elements of the tyre prior to vulcanization are characterized by internal friction due to shifting of its individual layers in relation to one another. The placement of layers has a major impact on the selection of technology, machines and instrumentation necessary for the automation and robotisation of production processes in modern factories and logistics centres. The author presents several examples of physical and geometric features facilitating the automation of rigid bodies and plastic elements assembly, as well as their positioning on the machine in the process of multi-layer tyre production. The multi-layer nature of pneumatic tyres determines the process of designing automatic and robotic assembly stations, which is only possible after the completion of the tyre design.
K e y w o r d s: assembly, rigid body, plastic element, tyre, automation

S t r e s z c z e n i e: W pracy przedstawiono klasyfikację elementów przeznaczonych do montażu automatycznego i zrobotyzowanego na bryły sztywne i elementy plastyczne. Proces montażu podzielono na *7 obszarów stanowiących pętlę zamkniętą procesu automatyzacji i robotyzacji fabryk przemysłu 4.0. Opisano cechy charakterystyczne brył* sztywnych i elementów plastycznych oraz *lepkich*, które mają główny wpływ na dobór technologii, maszyn i oprzyrządowania niezbędnego do automatyzacji oraz robotyzacji procesów produkcyjnych w nowoczesnych fabrykach i centrach logistycznych. Przedstawiono kilka przykładów cech fizycznych i geometrycznych ułatwiających automatyzację brył sztywnych i zasady pozycjonowania elementów plastycznych oraz lepkich. Następnie, opisano zagadnienia wielowarstwowość opon pneumatycznych i uwarunkowania wpływające na proces projektowania automatycznych i zrobotyzowanych stanowisk montażu, który poparto przykładami przedstawionymi na rysunkach. Kolejny etap pracy przedstawia właściwości fizyczne elementów opon, które ułatwiają automatyzację i robotyzację procesów technologicznych montażu. W podsumowaniu zdefiniowano proces technologiczny montażu elementów opon.
S ł o w a k l u c z o w e: montaż, bryła sztywna, element plastyczny, opona, automatyzacja

Introduction

The automation of production and logistics processes has been developing over the past 20 years, as evidenced in the report *Opportunities and challenges for the Polish Industry 4.0* [1]. Based on the information published on the website of the Ministry of Development, Labour and Technology in the article *Tax relief for robotisation - new support measures from 1 January 2021* [2] it can be assumed that automation and robotization will continue to develop dynamically.

Automatic assembly processes are optimised in terms of work organisation, logistics and technological equipment. Numerous researchers are dealing with assembly technology and automation, including, in particular: Jerzy Łunarski, Jan Żurek, Jerzy Honczarenko, Olaf Ciszak, and others, who in their works address issues such as innovative design technologies, as well as implementation and use of automated and robotic workstations. According to the author of the paper, the classification of literature on the subject of assembly technology and automation can be divided into 5 basic topics:

1. selection of the assembly sequence variant for machine parts and assemblies [3],
2. balancing assembly lines to shorten the assembly time, consideration of its various organisational variants, and subsequent selection of the optimal process depending on the established criteria [4, 5, 6, 7],
3. designing for manufacturability, ensuring the positioning of the assembled elements in the shortest possible time, while maintaining the required technological and structural parameters [8],

4. development of machines and tools used in assembly automation processes [9, 10, 11, 12]
5. mathematical description of assembly processes, technologies and automation [13].

Progress in the field of automation and robotisation is possible thanks to the development of machine vision technologies and contactless measurement sensors, as well as the use of physical and geometrical characteristics of elements that can be grasped and moved from place to place without their deformation.

Characteristic features of rigid bodies and plastic elements of tyres which have an impact on the automation and robotisation of production processes in Industry 4.0 factories and warehouses

In the automation of many industrial technological processes, the physical and geometric properties of rigid bodies are used [14, 15], which retain their physical properties when exposed to various forces during transport, positioning or assembly, and even if some deformations occur, they do not affect the quality of the final product. Progress in the field of assembly automation and robotisation was initiated in the automotive and home appliances industry due to the high volume of production. Currently, an increasing degree of automation is also observed in the food, pharmaceutical and logistics industries.

The author of this paper has divided the automation and robotisation process into 7 closed-loop areas of the technological process of industry 4.0 factories, which can be applied to the assembly of tyre elements:

1. **warehouse logistics I** (receipt of raw materials at the warehouse):
   a. identification of the needs of individual departments,
   b. automation of the order schedule,
   c. transport of raw materials to the production plant,
   d. designation of an area in the warehouse,
   e. unloading deliveries and receipt of raw materials and parts at the warehouse (e.g. via mobile robots, automated cranes and other specialised logistics equipment),
   f. segregation and storage (with the use of specialised logistics equipment),
   g. preparation of raw materials and parts for technological processes (rotation of raw materials in the warehouse in order to maintain the correct order of their release for production and to prevent the accumulation of outdated raw materials in the warehouse),
2. **process logistics I** (ensuring continuity of supplies for production workstations):
   a. identification of the needs of individual workstations,
   b. automation of the information flow from the workstations to the warehouse,
   c. automatic retrieval of the required items from the warehouse,
   d. delivery to workstations (e.g. via feeders, specialised tables and containers transported by mobile robots and other specialised logistics equipment),
   e. transport of parts and assemblies between workstations, where they are assembled into subassemblies and assemblies (e.g. with the use of specialised pallets, carriages, feeders),
3. **positioning of elements to be joined I** (making use of the specific shape and position of the centre of gravity of the manipulated element, e.g. for gravitational movement of elements stopped on buffers)
   a. unambiguous orientation of parts (workstations equipped with sensor systems),
   b. preparation of the part for gripping, movement and operation,
4. **technological process of assembly** (mutual alignment of parts and fixing their position by screwing, thermal clamping, soldering, welding, sealing, gluing and stitching for rigid bodies; in the case of plastic elements of tyres, adhesion is used for joining and minimum pressure is applied so as not to cause their permanent deformation):
   a. orientation in space and measurements before the technological operation,
   b. execution of the technological operation in accordance with the planned operational procedures,
   c. orientation in space and measurements to verify the quality of the joint,
   d. sending notification to the process control system about the completion of the process and its results
5. **positioning of joined elements II** (making use of the specific shape and centre of gravity of the manipulated element, alignment to the buffers or other orientation of the product in space)
   a. unambiguous orientation of the product to prepare it for removal from the assembly zone,
   b. gripping and moving the product to the designated place after completion of the technological operation,
   c. measurement of the geometry and weight of the product,
   d. sending information to the production process control system,
   e. assignment of an appropriate identification code,
   f. transfer and placement of the finished product in the designated area, pallet, etc.
6. **process logistics II** (transfer of subassemblies and assemblies between individual workstations; delivery of the assembled elements to the warehouse after completion of the assembly process, e.g. using feeders, conveyors, containers, robots and similar equipment)
   a. identification of the product,
   b. sending information to the process control system,
   c. determination of the subsequent storage location (for work in progress),

   d. transport of parts and assemblies between workstations to the clearly specified place,
   e. delivery of assembled products to a clearly specified place in the warehouse (e.g. with the use of feeders, specialised containers, carriages, mobile robots and similar equipment),
7. **warehouse logistics II** (issuing products) - receiving the finished product into the warehouse, storage, issuing the assembled product and repeating the cycle.
   a. identification of the recipients' needs,
   b. automation of the shipping schedule (taking into account the rotation of products in the warehouse),
   c. optimisation of transport to customers (optimal placement of the goods in a truck or freight car),
   d. searching for and identification of products in the warehouse,
   e. transfer of the finished product to the loading area of vehicles or railway cars,
   f. validation of conformity of the shipped goods with the order,
   g. loading (e.g. by means of mobile robots, automated cranes and other specialised logistics equipment).

This process is identical for the assembly of many popular devices and is shown graphically in Figure 1.

Warehouse logistics I and II (Fig. 2) and process logistics I and II (Fig. 3) are mentioned twice in the above-mentioned classification. These are, in principle, the same processes (the diagrams in Figures 1, 2 and 3 are universal for different industries) and are listed twice since the assembly technology uses different feeders, racks, pallets and tooling for the assembly components before and after assembly. After the completion of the assembly technological process, different dimensions, mass and functionalities are obtained (hence, a different type of tooling must be used than before). When designing an automated and robotic technological process, the designer cannot assume that auxiliary tooling will be used for the same components before and after assembly. The parameters of overall dimensions, individual dimensions, shape and mass characterising the technological assembly processes of tyre components can be defined as follows:

1. **overall dimensions** – the outline of the component with maximum external dimensions,
2. **dimension** – the physical distance between points that mark individual surfaces of a component or assembly,
3. **shape** – the measurable relationship between all surfaces of a component that can be described with dimensions and tolerances of straightness, flatness, circularity, cylindricity, line and surface profiles, which can be used to characterise a component or an assembly,
4. **mass** – the parameter defining inertia and gravitational interaction of components or assemblies of the assembled product.

Changes in the mass and shape of a component have an impact on the position of its centre of gravity and the value of the moment of inertia, which is decisive when designing drives and selecting parameters of the drive system. The tyre industry uses very heavy and large machinery that must ensure stability of the assembly process and high productivity. Tyre assembly in most

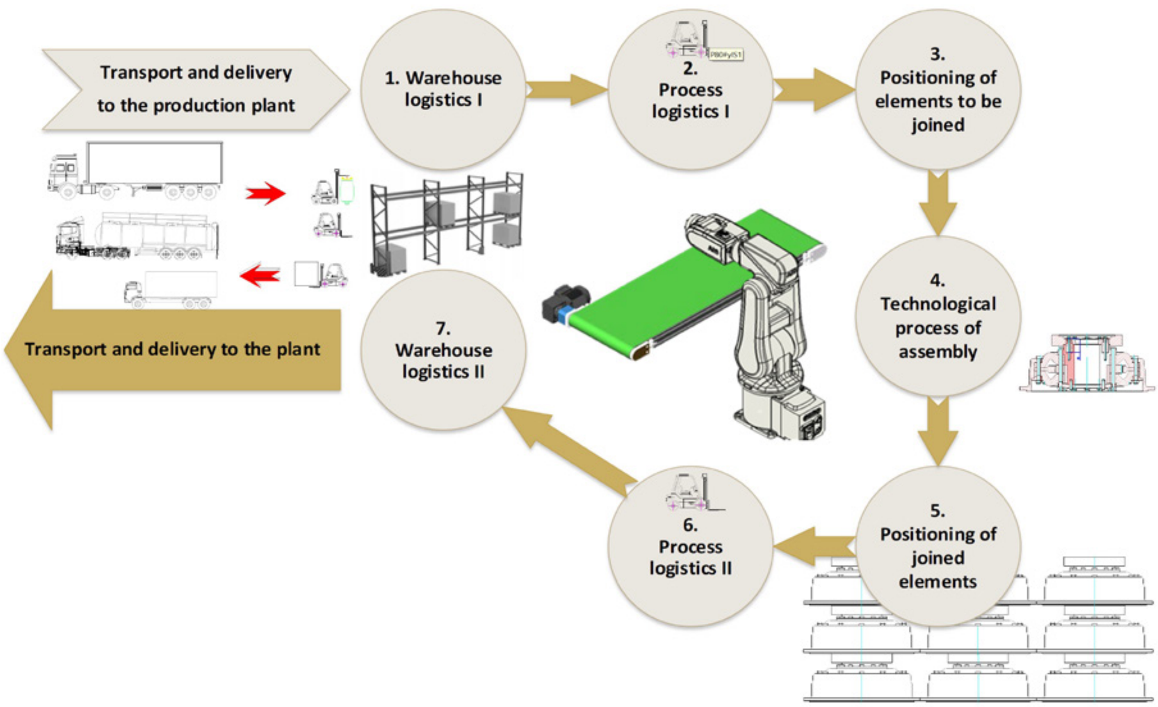

Fig. 1. Closed loop of the automation and robotisation process of Industry 4.0 factories [own elaboration]

plants is a serial production process. Disregarding the moment of inertia in calculations can lead to serious accidents in the workplace (as a result of changes in the weight and size of the product during the tyre assembly process due to the winding of successive tyre layers). For example, in the Bridgestone production plant in Poznań which manufactures passenger car tyres, there were as many as 36 accidents and 20 incidents at work in 2019 alone [16]. Fatal accidents in tyre factories are not uncommon, either (e.g. the accidents in Olsztyn in 2006 and 2011) [17, 18].

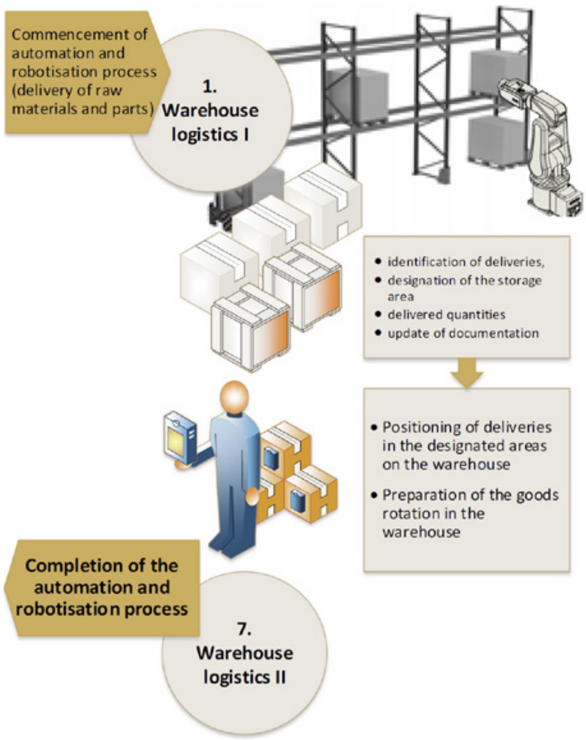

Fig. 2. Warehouse logistics I is the first stage of the automation and robotisation process of Industry 4.0 factories enabling the continuity of production [own elaboration] Fig. 4. View of the Appendix sheet for assembling the bus engine [2]

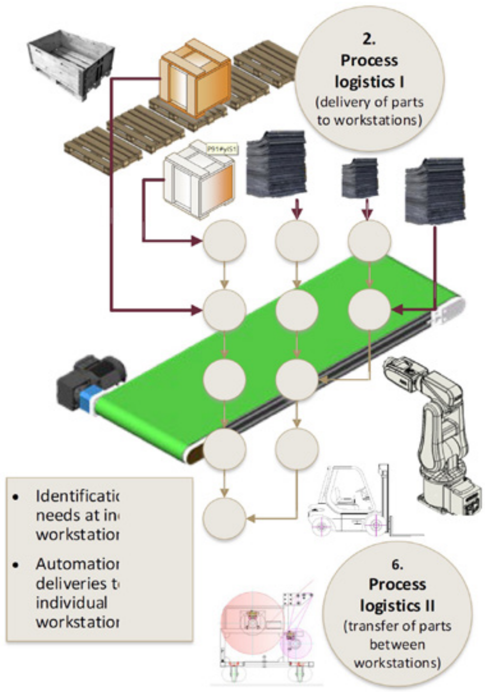

Fig. 3. Process logistics I and II are the stages of production in Industry 4.0 factories enabling automation and robotisation of processes between workstations [own elaboration]

According to the author of this paper, when it comes to the assembly technology, the maximisation of the use of the physical and geometric features of the joined components should be ensured. Works conducted in the industry in the period 1998-2020, including projects presented in the technology database of the Agencja Rozwoju Przemysłu S.A. [19, 20, 21, 22, 23, 24, 25, 26] and patented works [27, 28, 29, 30, 31, 32] allow to conclude that designing the technological processes of automatic tyre assembly can be facilitated by:

1. **defining the minimum stiffness** (no deformation of tyre components due to external and thermal stresses) - required for the selection of equipment for storage and positioning of tyre components (Fig. 4); if the tensile strength is exceeded during the assembly process the tyre component is damaged (Fig. 5),
2. **determining the mass of the components and the range of their inertia and unwinding speed, as well as the torsional torque and the clamping force** – required for the selection of operating parameters of the system elements necessary for the orientation and positioning of the components in space (Fig. 6),
3. **identification of dimensions and shapes** – specific dimensions are taken into account to select the required workspace and confirm the quality and correctness of the selected components (Fig. 7),
4. **using the moment of inertia and other physical relationships** – required for the positioning of rigid body type parts and setting unwinding parameters for plastic parts (Fig. 8 and 9
5. **concentration of raw materials and parts processing in pre-assembly processes**, as well as minimisation of the number of product components and simplification of their shapes (Fig. 10),
6. **using colours and codes for identification of components in the assembly process** (optical sensors and thermal imaging cameras for process supervision (Fig. 11).

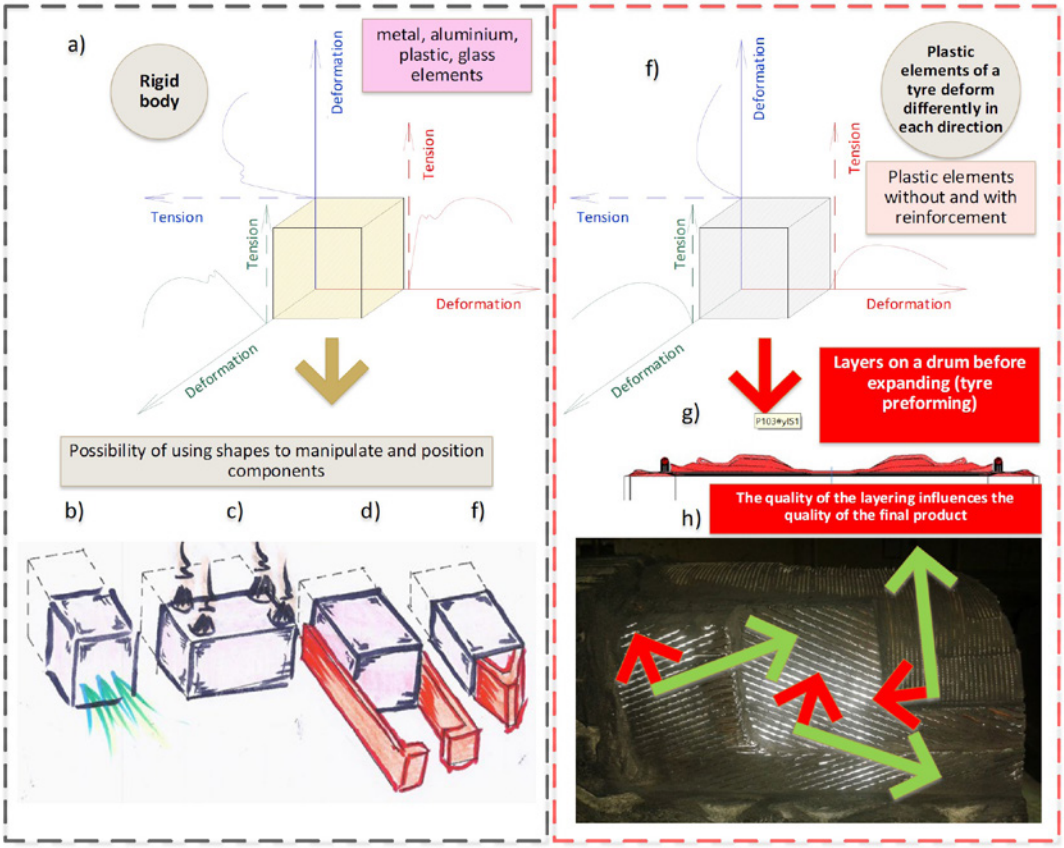

Fig. 4. Defining the minimum stiffness and dimensional stability of components to determine the parameters of grippers, bumpers and similar solutions in different configurations. 2.a) Minimum stiffness and dimensional stability to allow the use of grippers, bumpers, regular and specialised containers. The manipulated component may have different strengths in different planes and directions of forces. The weakest contact point and pressure exerted by the handling system are assumed. The force exerted must not exceed the tensile or compressive strength. 2.b) Displacement of parts with compressed air blast (e.g. blowing off incorrectly manufactured parts). 2.c) Transport by a vacuum system with vacuum suction nozzles and ejector pumps (e.g. gripping of parts which are very difficult to transport such as car windows). 2.d) Handling and free manipulation of any component by means of grippers exerting friction between the gripper surface and the handled component (e.g. pneumatic or hydraulic grippers, etc.) 2e) Pushers, locking devices of various shapes and drives (electric, pneumatic, hydraulic, spring) for sliding, positioning and other functions depending on the industrial application, 2f) Tyre elements are subject to substantial deformation at low stresses of 0.5 - 3.5 MPa. 2g) Layers on the drum of a tyre manufacturing machine. 2h) Example of tyre layering and different tensile strength of individual layers in each direction [own elaboration].

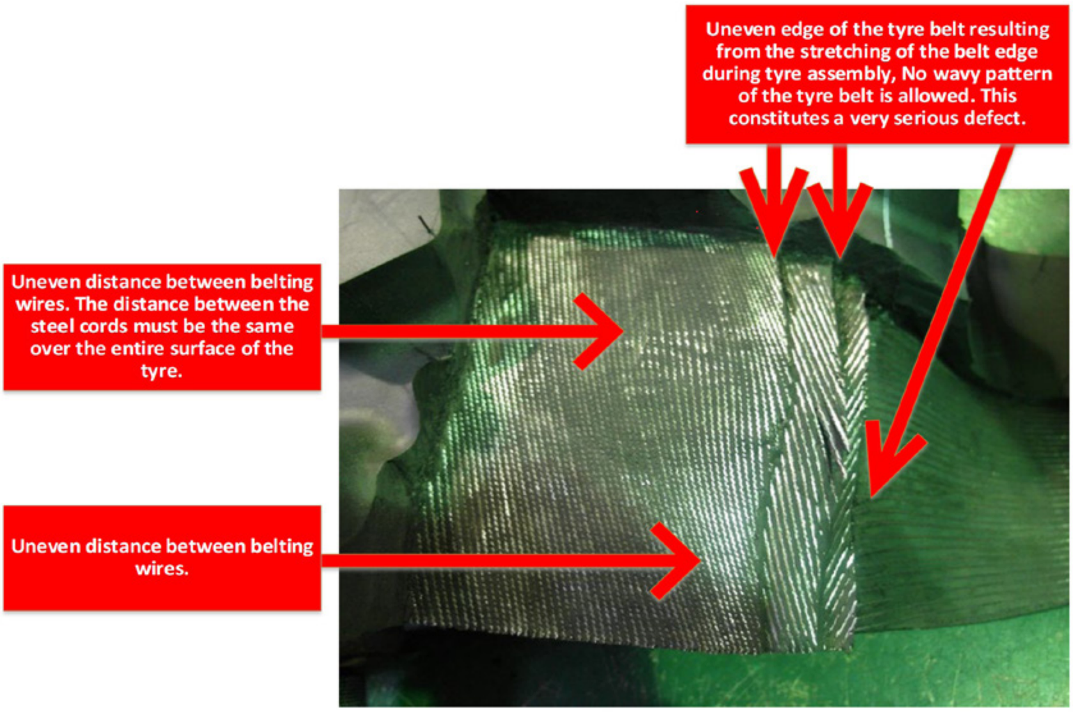

Fig. 5. Example of exceeding the tensile strength limit during the assembly of tyre belt elements [own elaboration]

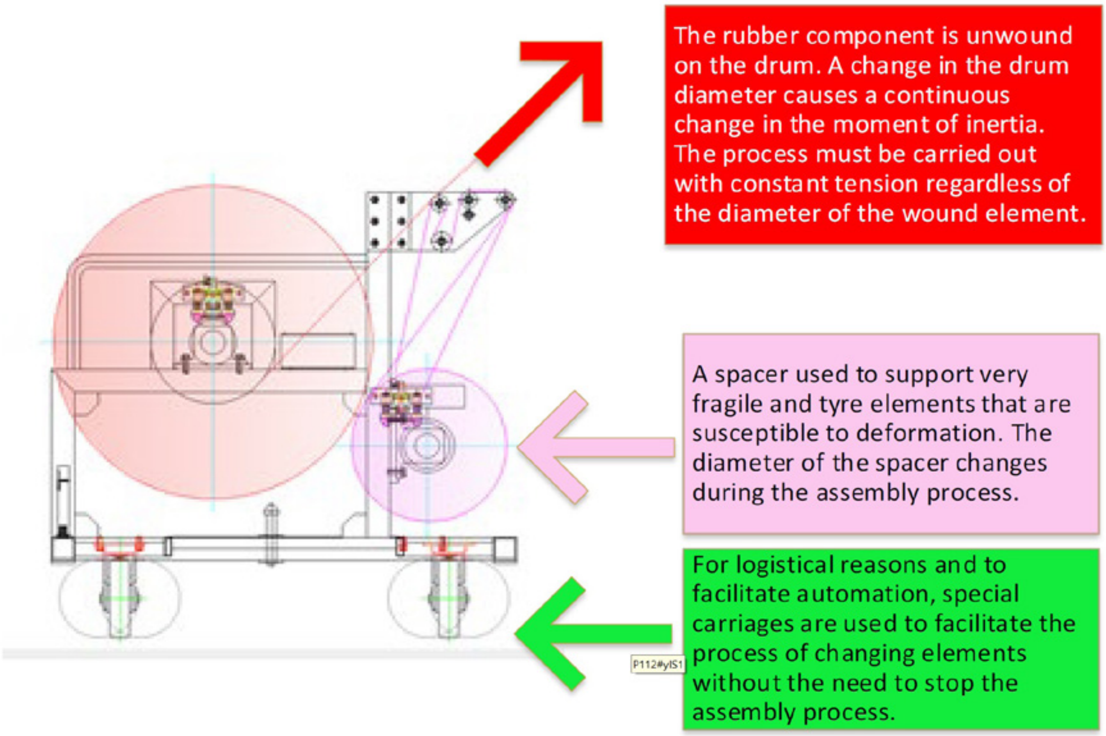

Fig. 6. During the process of tyre elements assembly, the mass of the wound elements and their inertia, as well as the unwinding speed are constantly changing. For this reason, the drive must be equipped with the measurement systems of the unwinding force, the diameter of the wound tyre element and the the diameter of the spacer [own elaboration].

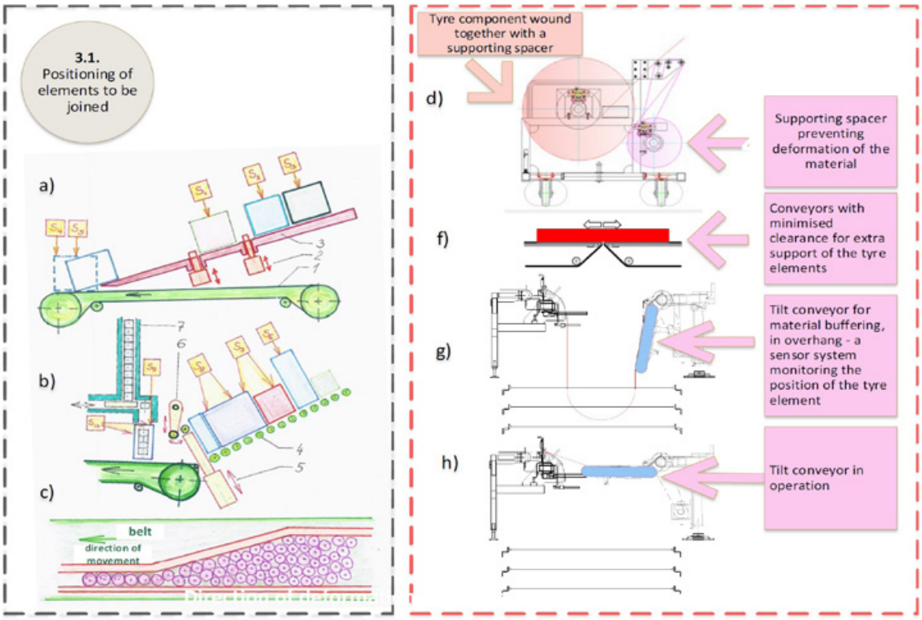

Fig. 7. Gravitational and friction forces facilitating transport and handling of components, as well as their orientation in space. 3.a) Example of the use of a belt conveyor 1, which the elements waiting on the gravity conveyor 3 are fed on after inserting a pin 2, which can be driven electrically, pneumatically or by a hydraulic actuator. The sensor system S1÷S5 can recognise colours, positions, bar codes and letters. 3.b) Elements of various shapes, sizes and weights may be placed on the gravitational conveyor 4 to shield the buffers 5 and 6. Shifting the position of the buffers moves the element onto the conveyor which transports it in order to insert an appropriate number of parts stored in the feeder 7 cooperating with the pusher. The pusher is activated after an appropriate positioning of the elements on the conveyor by means of the sensors S9÷S10 (e.g. optical sensors detecting the edges of the elements and counting the number of inserted elements from the feeder 7). 3.c) The principle of buffering and positioning multiple rotating elements, the movement of the conveyor and the possibility of exerting friction and rotation causes the elements to line up individually. 3.d) A carriage with wound tyre elements and a spacer to prevent deformation and sticking of the wound coils of material. 3.e) Transfer of elements by means of conveyors positioned with a minimum gap so as to prevent damage of the transported element. 3.g) Buffering tyre elements by means of a tilt conveyor and a system of sensors measuring the maximum overhang of the material to prevent it from damage due to gravitational forces (the greater the mass of the material, the greater its weight and the risk of stretching along the length, causing narrowing in width). 3.h) After the completion of buffering, the conveyor is lifted so that the material is not exposed to deformation [own elaboration]

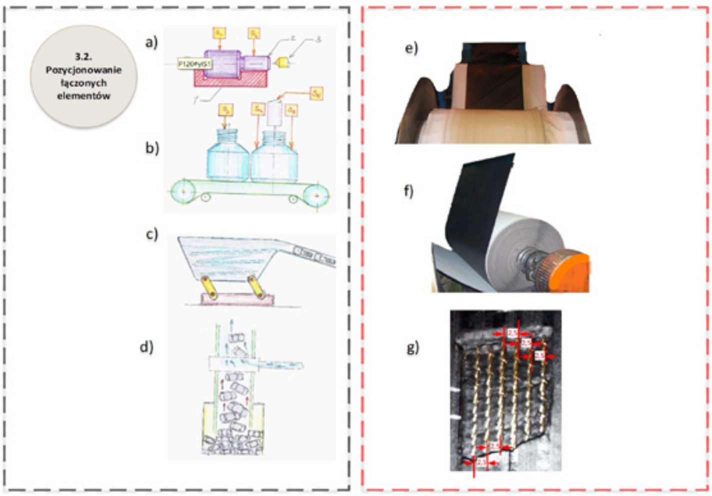

Fig. 8. Identification of shapes. 8.a) Elements 2 can be placed on the feeder 1, and their position is verified by the sensor system S1÷S2; an element positioned in such a way can be gripped, for instance by centre holes. 8.b) Bottles may be placed on the conveyor, the quality of which is verified by sensor S3 immediately prior to their filling (e.g. by an optical sensor with stored pattern of correct thread quality), the correct position for pouring is measured by sensors S4 and S5, then the bottle is filled and the amount of dispensed liquid is controlled by sensor S6. 8.c) Possibility of using vibrating systems. 8.d) Vacuum or pneumatic conveying and feeding systems. 8.e) Systems for supporting tyre elements on spacers (fabric or plastic spacer with anti-adhesive properties and sufficient rigidity to support the plastic elements). 8.f) and 8.g) Separation of the spacer from a plastic element reinforced in one direction with a steel cord, where individual steel elements are aligned at the same intervals across its width [own elaboration]

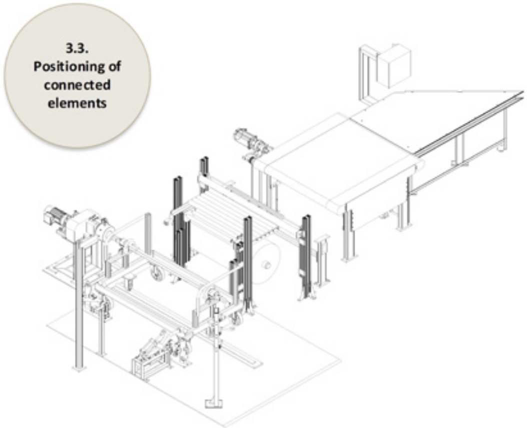

Fig. 9. An example of a winder for plastic elements of the tyre, in which the above-mentioned components are used [own elaboration].

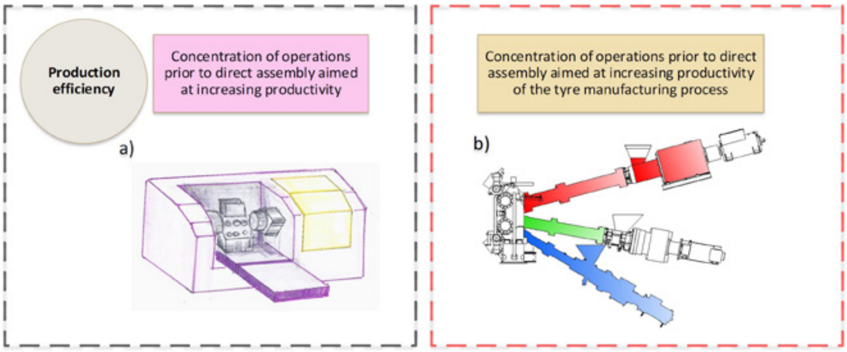

Fig. 10. Concentration of raw materials processing in pre-assembly processes, as well as minimisation of the number of product components and simplification of their shapes. Fig. 10.a Multi-axis machine tools, rotary tables, possibility of turning, milling and drilling, interchangeable machine tables, wide doors to the machine interior enabling the use of an overhead crane or a robot to insert and remove elements, multi-tool magazines, as well as direct measurement of processed elements and tools used in the process. Fig. 10.b In the tyre production process, concentration mainly consists in making as many joined elements as possible on the extruder systems so that joining of the elements takes place directly in the extruder head [own elaboration]

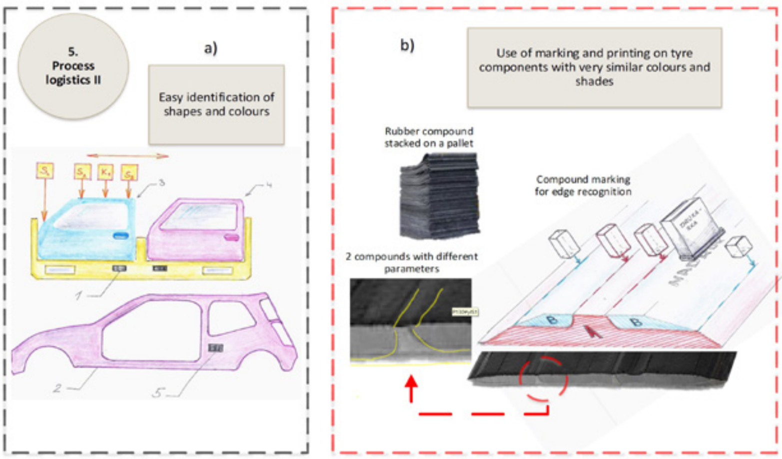

Fig. 11. The use of element colours and bar codes to automate the process of searching for goods in a warehouse. Fig. 11.a The camera K1 allows to find the right colour of an element (e.g. a door of the colour 3 or 4) positioned on the pallet 1. After finding the right pallet based on the bar code (comparison with the code on the body 5), the element is grasped by the manipulator positioned on the basis of measurements taken by sensors S1÷S3 and the camera K1. Fig. 11.b The use of the colours of the elements, sensors and thermal imaging cameras to supervise the processes. The compounds are very similar in colour, dimensions and mass. In order to identify the products on the tyre manufacturing machine, colour printers can be used at the component manufacturing stage to mark the boundary lines of the individual material layers and print the component codes. The use of optical sensors on the machine allows for error-free identification of components and their centring. The letters A and B mark compounds with different parameters. [own elaboration]

The assembly technology used for rigid body type components cannot be directly applied for plastic elements, including unvulcanised rubber compounds, as well as textile and steel components joined during the tyre assembly process. Unvulcanised tyre components are very susceptible to deformation. Only after the **vulcanisation** process, the product takes on its final shape and the required strength. For the purpose of this paper, vulcanisation can be defined as *a process of high-pressure heat treatment of the assembled tyre components, after which the product is cooled and dimensional stability of the product is ensured to achieve the required fatigue limit*.

The main strength parameter of tyre components during the assembly process is their tensile strength, which ranges between 0.5 and 3.5 MPa. These values are very low compared to steel, cardboard, glass and plastic components, and makes plastic components very susceptible to damage. For example, general purpose carbon steel of ordinary quality in accordance with EN 10027-2, marked as 1.0035 (also known in the industry as St0S or S185) reaches a tensile strength of 314 [MPa], alloy steel for quenching and tempering marked as 45HNMF reaches 1470 [MPa], while the value for tool steel 65S2WA can be as high as 1860 MPa. Modern cardboard packaging is much less plastic, with very rigid structure in one or several selected directions (e.g. Cardboard boxes for storing raw materials and vegetables, packages arranged in several layers on one pallet). The parameters of packaging are defined by the index of corrugated board resistance to edge crushing, marked by the abbreviation ECT [33]. Depending on the packaging design, it ranges from 2 to 10 kN/m. The strength of cardboard packaging increases if the products placed inside the box can be used to reinforce it (e.g. cans or containers filled with liquid). Another parameter, less commonly used in the packaging industry, is the flat crush resistance of the packaging wall (FCT), expressed in N. In the case of plastic elements used for the manufacturing of tyres, such a parameter is practically non-existent in industrial practice. The processes of packaging, handling of cardboard boxes, their positioning on transport pallets and stacking into layers are increasingly widely automated. Handling of cardboard boxes in the process of automation and robotisation is subject to the principles of rigid bodies handling, provided appropriate humidity parameters are ensured, as excessive humidity can lead to the deterioration of ECT and FCT parameters. For this reason, even the automation of the assembly and transport of cardboard boxes is much easier to achieve as compared to tyre components.

In the case of products made of rubber compounds, such as tyres, the rigid body handling principles can be applied only after the completion of the vulcanisation process and ensuring the dimensional stability of tyres. Tyres take on their final shapes after they are removed from the mould and cooled to ambient temperature. After the completion of the entire production process, the components made of rubber compounds reach a tensile strength of 5 up to 25 MPa. From this point, tyres can be positioned, gripped and stacked like regular rigid bodies.

An important parameter of super plastic components is their hardness. For the purpose of this paper, plastic elements have been divided into *6 hardness categories that determine the way of automation and robotisation of the technological process of tyre assembly*:

1. very soft from 5 to 50 on the shore Shore 00 hardness scale :
   a. difficult to automate,
   b. requires the use of spacers
2. soft from 10 to 30 on the Shore A scale,
   a. difficult to automate,
   b. requires the use of spacers
3. medium hard from 40 to 60 on the Shore A scale,
   a. possible to automate,
   b. requires the use of spacers
4. slightly hard from 60 to 80 on the Shore A scale,
   a. possible to automate on a rigid body basis,
   b. does not require the use of spacers
5. hard from 80 to 100 on the Shore A scale,
   a. easy to automate - the component behaves like a rigid body.
   b. does not require the use of spacers
6. very hard from 60 to 100 on the Shore D scale,
   a. very easy to automate - the component behaves like a rigid body.
   b. does not require the use of spacers

Plastic element (rubber compound before vulcanisation) becomes easily deformed and in contact with any fixes, immovable part, it sticks to it. Removal of compacted and jammed rubber compound from the machine's workspace and spaces between the machine parts is complicated and poses a risk of a serious accident. Rubber compound processing is a very dangerous process for operators, and, for this reason, modern Industry 4.0 factories use sensors and safety systems to protect staff from accidents. These measures will be described in detail by the author in another publication.

An additional difficulty in the process of tyre assembly is the fact that the hardness of the compound depends on temperature, as evidenced by the research conducted by H. J. Q. K. Joyce and M. C. Boyce, who describe a simulation of hardness tests and elastomer behaviour between tension and deformation [34]. According to the researchers, the predictive ability of the simulation (predicting statistical characteristics of random phenomena) is verified by comparing the calculated Shore A and D values with the conversion table presented in ASTM D2240. The simulation results are then used to determine the relationship between the neo-Hookean model [35] (based on statistical thermodynamics of cross-linked polymer chains, useful for plastics and rubber-like substances) and the Shore A and D hardness values. Transport-related issues, including heat transfer, dimensional analysis of polymer flow, convective momentum, energy and mass transfer, as well as transport in dual-phase systems have been described by R. B. Byron Bird, W. E. Stewart and E. N. Lightfoot [36]. In turn, the issues of polymer fluid dynamics are presented in a scientific publication by R. B. Bird, R. C. Armstrong and O. Hassager *Dynamics of Polymeric Liquids* [37]. Hardness is a frequently used parameter in the tyre industry and in order to standardise nomenclature nomenclature and testing methods, the industry uses standards. The standard described in ASTM D1415 – 18 [38] concerns hardness measurements in the regular elasticity range, and does not apply to materials with high stress relaxation factors or strain hysteresis - in which case it is recommended to use the hardness testing method described in ASTM D2240 – 15e1 [39] and ASTM D1415 – 06 [40]. Measurement readings for rubber compounds may differ when performing the test due to irregular specimen shapes. Elastomers undergo locally large deformations during hardness testing and simulations are performed to limit elastomer stretching during measurement. The standard practice for testing rubber compounds in the automotive industry is based on ASTM D1349 – 14 [41] and ASTM D4483 – 20 [42]. ASTM D1646 – 19a [43] defines other standard test methods for rubber compounds including - measurements of viscosity, stress relief and pre-vulcanisation characteristics - determined with a Mooney viscometer.

The implementation of the above-mentioned principles and procedures for positioning pre-vulcanised rubber components precludes the application of solutions used for positioning components classified as rigid bodies. This is due to the fact that, depending on the temperature and storage time of the raw material, the parameters and properties of rubber compounds change, which hinders conventional automation and robotisation of the assembly process of plastic tyre components. Table 1 presented below lists the properties of the assembled elements which have an impact on the selection of technological settings in operations and procedures of the automated and robotised production process, including the assembly of plastic tyre components.

Table 1. Plasticity and hardness of components influencing the process of assembly automation and robotisation (selection of equipment and technological process settings)

Possibility of automation and robotisation				
Unvulcanised compound	**Vulcanised compound**	**Corrugated cardboard packaging**	**Plastics**	**Steel**
Tensile strength 0,5 ÷ 3,5 [MPa]	Tensile strength 5 ÷ 25 [MPa]	Tensile strength 12 ÷ 19 [MPa]	Tensile strength 33 ÷ 650 [MPa]	Tensile strength 314 ÷ 1860 [MPa]
5 ÷ 50 Shore 00 scale	30 ÷ 80 Shore A scale	2 ÷ 10 ETC [kN/m]	50 ÷ 400 ball indentation hardness [MPa]	180 ÷ 460 HB hardness
Elements very sensitive to shape changes	Elements not sensitive to shape changes	Elements not sensitive to shape changes in selected directions	Elements not sensitive to shape changes	Elements not sensitive to shape changes
Implementation of automation and robotisation process very difficult	Implementation of automation and robotisation process easy	Implementation of automation and robotisation process easy	Implementation of automation and robotisation process easy	Implementation of automation and robotisation process very easy compared to tyre components
For the purposes of automation and robotisation of processes, spacers are used to prevent damage to the joined elements; all drives must gently accelerate and decelerate; tyre components are stored on carriages or special pallets in stable temperature and humidity.	After the vulcanisation process, products can be positioned using bumpers and automated conveyor systems, and moved using robots.	Possibility of using conveyors, bumpers, robots - positioning and gripping of elements by their surfaces and edges reinforcing the cardboard.	Possibility of using conveyors, bumpers, robots - positioning and gripping of elements by reinforced edges of the element structure.	Possibility of using conveyors, bumpers, robots.

Multi-layer pneumatic tyres and conditions determining the process of automation and robotisation of tyre assembly

Tyres are made up of numerous components, as evidenced by patents of such companies as: Michelin [44], Bridgestone [45], Goodyear [46], Continental [47], Yokohama [48]. In industrial practice, vulcanised rubber compound which is not adhesive, has higher tensile strength in MPa, lower elongation in % and hardness described in the Shore scale in accordance to the PN-ISO 868 standard, is used [49].

Based on years of observational studies and the author's design work mentioned at the beginning of the article - tyres can be defined as - *a pressure vessel made of multilayer composites with different strength parameters in different points of its cross-section, which are characterised by fatigue resistance and good vibration damping*.

Tyres should not be treated as a monolithic structure, as its multilayer structure provides resistance to the constantly exerted variable external and internal forces that cause material fatigue. Contemporary tyres must be resistant to material cracking caused by cyclically varying fatigue stress and vibrations of variable amplitude, caused by such overlapping factors as the roughness of asphalt surfaces, wind force, lateral wind gusts, the condition of the vehicle and its load. The more technologically advanced the tyre construction, the more complex the structure of its cross-section. Monolithic tyres are more likely to quickly get damaged, which is why tyres used, for example, in fork lift trucks, have varying strength properties at different points of their cross-section. The multi-layer structure of the tyre ensures a smooth transmission of tensile and compressive stresses. Textile and steel elements serve as reinforcement for the rubber compounds. Cord strands are stronger than single wires. This is due to the favourable ratio of cross-section to the number of fibres or wires in the cord. In addition, such a solution provides the necessary flexibility, which single threads or wires cannot ensure. The multilayer solutions used in contemporary tyres guarantee high quality and safety for users. In order to achieve consistent quality of tyres, great precision during the positioning of their components is required. Precise positioning of elements and durable bonding of individual layers after the vulcanisation process are presented in patent descriptions [50, 51, 52, 53]. An example of tyre structure is shown in Fig. 12 published in patent application P.411809. "*Under the base (2) of the tread (1) there are at least four layers (3) of rubberised steel cord; between the mentioned layers (3) and the bottom sealing layer (4) of the tyre there is an intermediate reinforcement layer (5). Both outer ends of at least three layers (3) of the rubberised steel cord are surrounded by protective wraps (6) and are equipped with positioning rubber wedges (7). In addition, in the tyre shoulder, between the reinforcing intermediate layer (5) and the carcass layer (8), there is a positioning rubber insert (9) in the shape of an elongated C letter. The tyre bead contains a three-part wing (10) surrounded along with the wire (11), by two rubberised steel cords (12) and a rubberised textile cord (13). Both ends of the rubberised steel cords of the bead are protected by wraps (6), while the outer parts of the bead are equipped with reinforcing wedges (14) located between the side wall (15) of the tyre and the protective wraps (6) of the steel cords (12) of the bead.*" [53].

Depending on their dimensions and use, tyres have different structures and performance characteristics (maximum speed, load capacity, nominal pressure, rolling radius, tread height and shape, circumference, rolling resistance, noise and braking distance on wet surfaces). More information on tyre structures can be found in patent publications of tyre manufacturers which have been developed in an empirical way over years. These patents constitute very valuable and legally protected knowledge. The difficulty in the access to scientific publications hampers the development of companies with more limited intellectual potential, which experience difficulties in the acquisition of knowledge and implementation of new structural and technological solutions that would not infringe the intellectual property rights of their competitors.

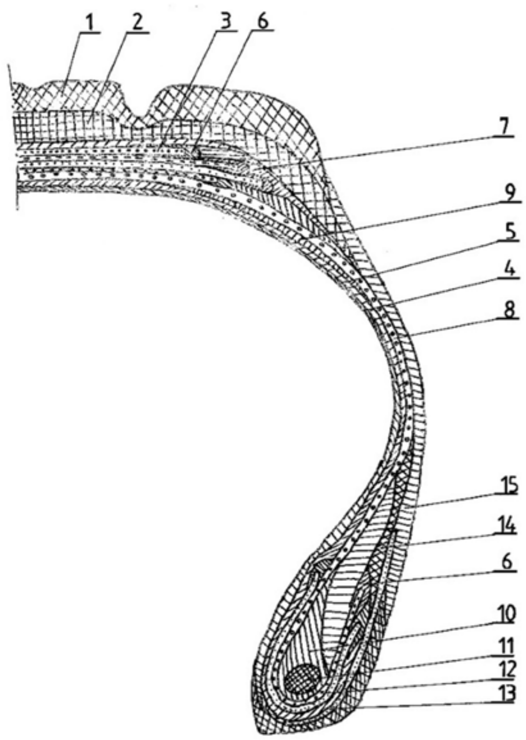

Fig. 12. Example of tyre structure described in the text [53].

The structure, number of layers and equipment determines the design of the assembly process. Tyre manufacturing machines have multiple stations for unwinding materials, positioning and cutting parts immediately prior to their assembly on the drum, which ensures the required accuracy of the process. The length of such machines ranges from a few to a dozen or so metres, and is due to the need for gentle centring of and protection of tyre elements.

Assembly of plastic components of tyres

Measures that facilitate automation and robotisation of technological processes of tyre assembly include:

1. defining the minimum stiffness and dimensional stability of the components in order to determine the parameters required to avoid deformation of the tyre components, e.g. by eliminating all factors that may cause deformation of the thin tyre components – as shown in Fig. 13,
2. concentration of raw material processing operations in pre-assembly processes, as well as using such parameters as mass, shape, temperature and pressure to control the processes of joining of the individual components, e.g. example in Fig. 14,
3. making use of the position of material support rollers to correct the position of the rubberised cords, as well as magnetic field to position the rubberised metal components of the tyre – Fig. 15,
4. making use of colours of the components, sensors and thermal imaging cameras to supervise processes and automate component identification – Fig. 11.

The tyre assembly process can be presented in the form of a diagram shown in Fig. 16, which summarises the main technological operations involved. The issue of tyre assembly process optimisation is extremely important from the point of view of road users. It is a very complicated process, since the individual layers at the stage of their assembly are very susceptible to permanent deformation, which entails a deterioration in the final product quality, as shown in Fig. 5.

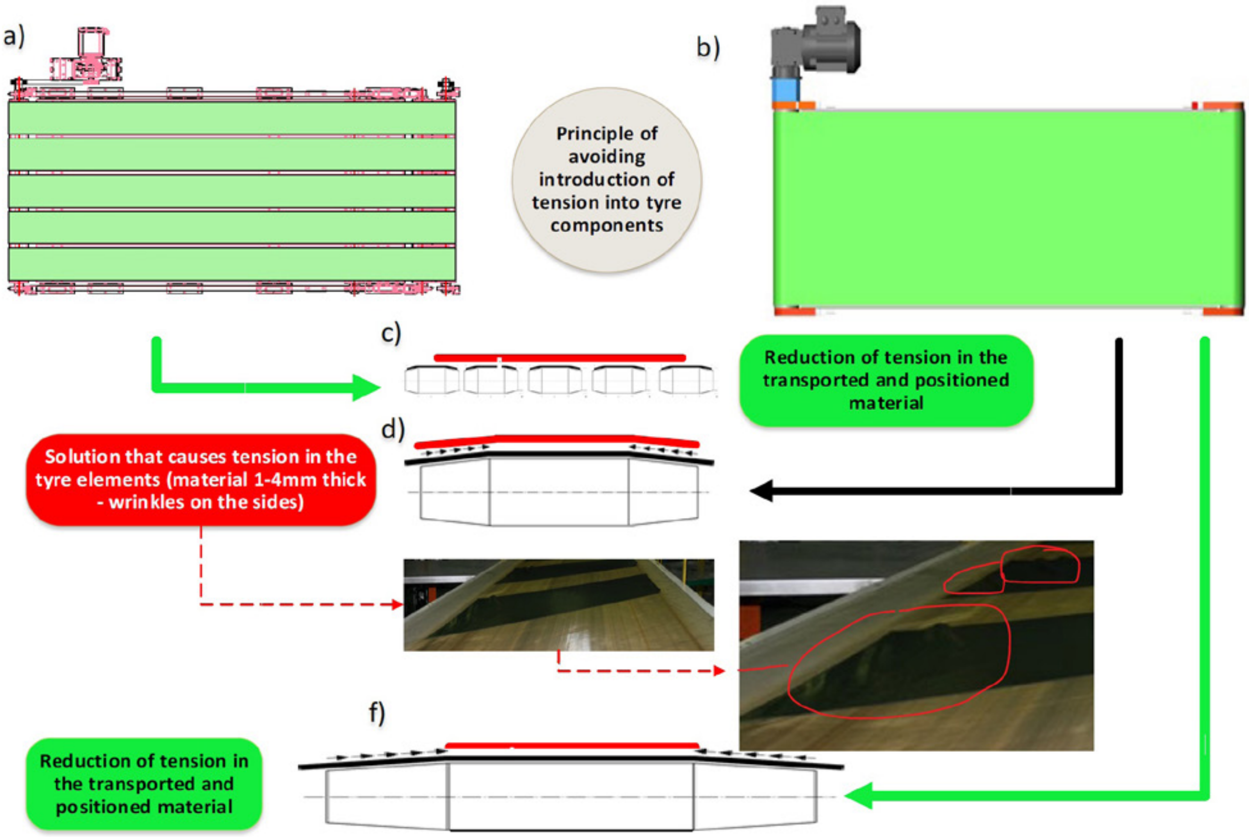

Fig. 13. Defining the minimum stiffness and dimensional stability of the components in order to determine the parameters required to avoid deformation of the tyre components. 11.a) Plastic and viscous components must be transported in the centre of a much wider conveyor belt. No deformation of the plastic component as a result of changes in the conveyor belt tension is allowed. For very fragile components, a steel belt and a thermal chamber with automatic ambient temperature control are used to keep the external environment constant; the tension is monitored by strain gauge measurements of the belt and the torsional moments measured on the rollers. 11.b) A system of several conveyor belts with rotational speed synchronisation and torque measurement reduces the adverse impact on the transported elements. The described solution improves the feeding precision and reduces the deformation of the plastic element caused by the tension of the monolithic belt. The presented solutions can be used interchangeably [own elaboration]

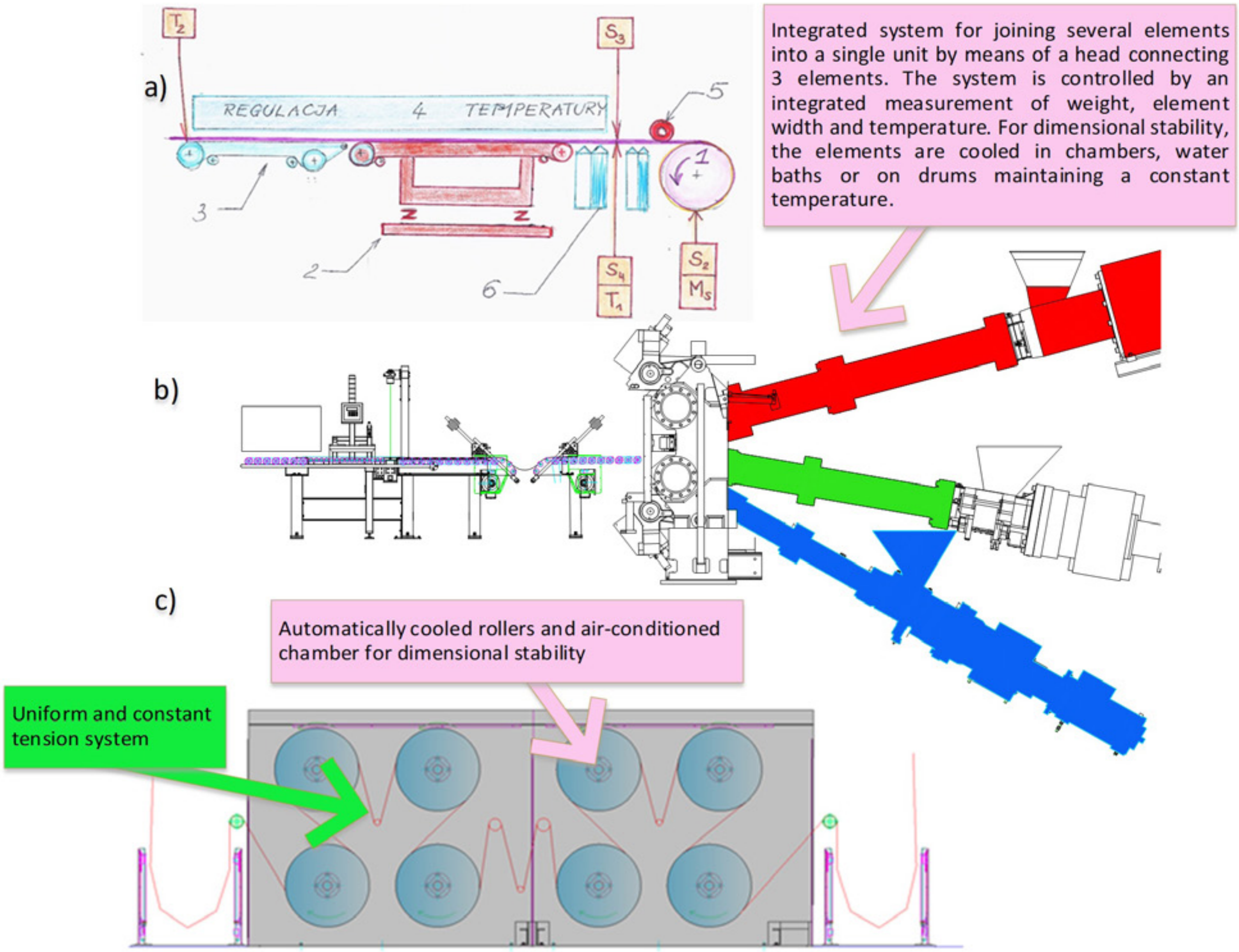

Fig. 14. The use of the parameters of mass, shape, temperature and pressure to automate process control. During the tyre assembly process, many components are wound and unwound. 14.a) As the diameter of the wound material on roll 1 changes (measured with sensor S2), the unwinding speed must change accordingly. In order to automate such processes, drive systems which allow for precise measurement of the torsional moment Ms should be used. Another important parameter in the process of automation of such operations is the ongoing measurement of the material weight 2. Reduction of the weight of the material indicates stretching of the element, while its increase signifies material pile-up. Based on this data, the unwinding speed and linear speed of the conveyor belt 2 and 3 can be controlled and verified. In order to keep the conditions constant, this process should take place under constant temperature conditions (e.g. under a thermally insulated cover 4). Temperature sensors T1 and T2 make it possible to correct the air exchange settings inside the transport space 4. In order to avoid slippage between the tyre components and the belt - encoders 5 are used to measure the speed of the transported element, which is compared with the measurement of the linear speed of the conveyor belts. Slippage of tyre elements in relation to the belt is an undesirable phenomenon as it introduces tension between the layers of tyre components. The transported element should have as many support points as possible, which is why conveyors (3) with a small radius of rollers are used or systems of air nozzles supporting the rubber element from below and reducing the electrostatic charge (6). 14.b) Example of a head design: 3 tyre components controlled by a scale measuring 1 metre of extruded length, a shape sensor, a pressure sensor set inside the extrusion head and a temperature sensor. All these parameters are interrelated and influence the speed of extrusion and compound extraction from the pallet. 14.c) Extruded and calendered components made of rubber compound are subjected to thermal stabilisation on rotating drums in air-conditioned chambers, on conveyors in cooled chambers or in a water bath in the case of thicker sections [own elaboration]

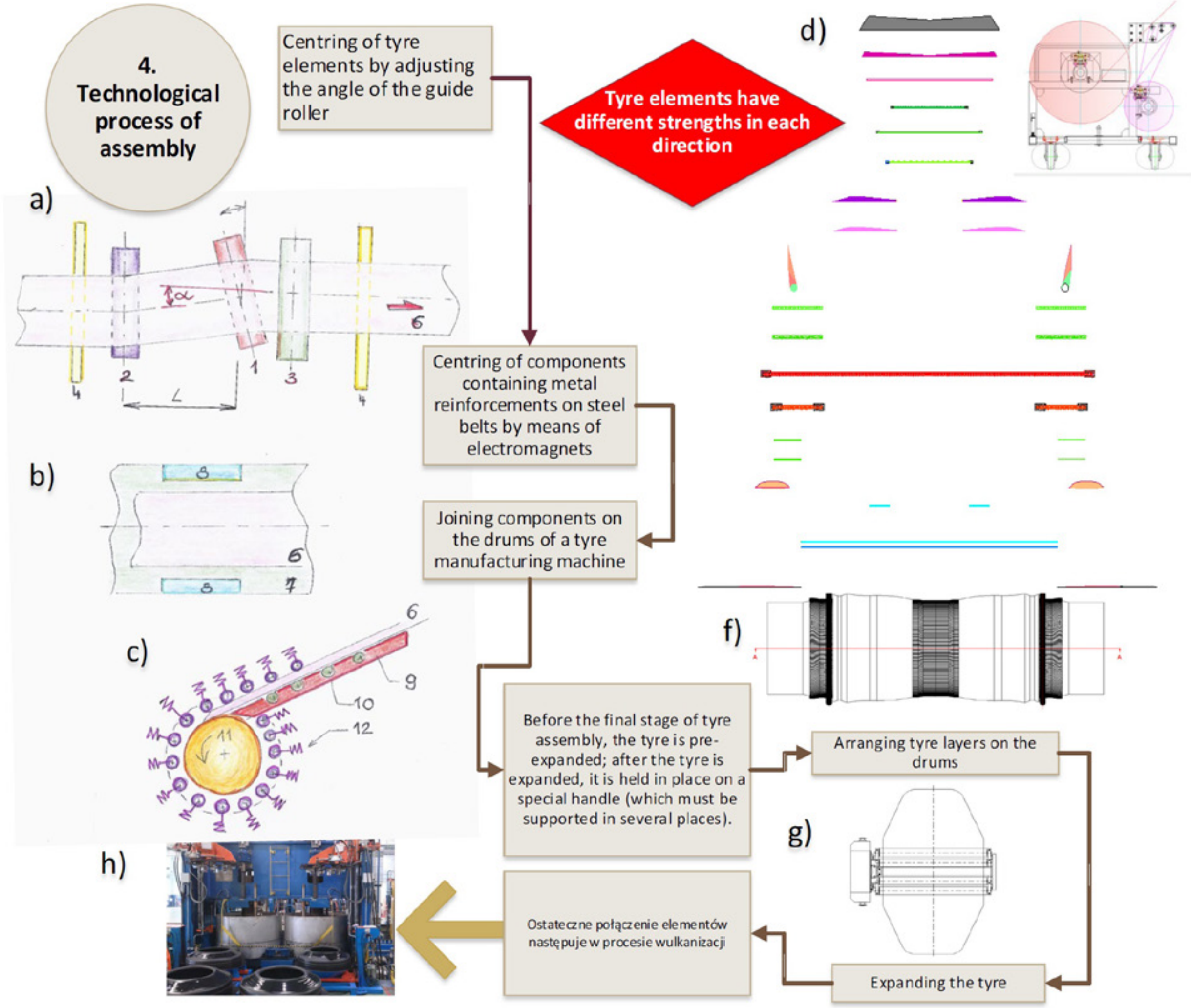

Fig. 15. Use of geometrical alignment of rollers and magnetic field for positioning of metal elements. 15.a) Steel and textile tyre components have high strength in one direction specified by the constructor; in other directions the components, even after reinforcement, still have relatively low tensile strength. Compounds covering steel and textile cords are characterised by high viscosity. For this reason, they cannot be directed to the bumpers in the same way as rigid bodies. In order to properly position cord-reinforced tape, it is necessary to use a roller or a set of rollers 1÷3. Setting the proper position of the roller 1. Two sensors 4 are used to constantly measure the position of the tyre component and correct the settings of the roller 1 in such a way so that the central axis of the tyre component measured by the second sensor 4 coincides with the central axis measured by sensor 4. The greater the distance L, the smaller displacement of roller 1 is required. 15.b) A tyre component reinforced with a steel cord can be positioned by means of elements 8, which generate a magnetic field to centre the tyre component 6 on the perforated belt 7. 15.c) The tyre component 6 slides due to gravitational force down the roller conveyor 10 and rests on the drum 11 of the tyre manufacturing machine, which can be held and pressed by means of pressure rollers 12 of a spring mechanism or pneumatic actuators. The element 9 may provide additional support to the component by means of a vacuum system or, in the case of steel elements, an electromagnetic system. 15.d) Example of a tyre made up of 31 units wound on carriages (this example shows the complexity of the assembly system). 15.f) The layers are placed on drums and the machine design is always adapted to the assembly technology. If more components are combined prior to the direct assembly process, the latter becomes simpler. 15.g) Example of tyre shape after expanding. The tyre must be supported in several places and is usually placed on racks, which should support the largest possible surface of the tyre. 15.h) The layers of the tyre are finally joined together in the vulcanisation press [own elaboration]

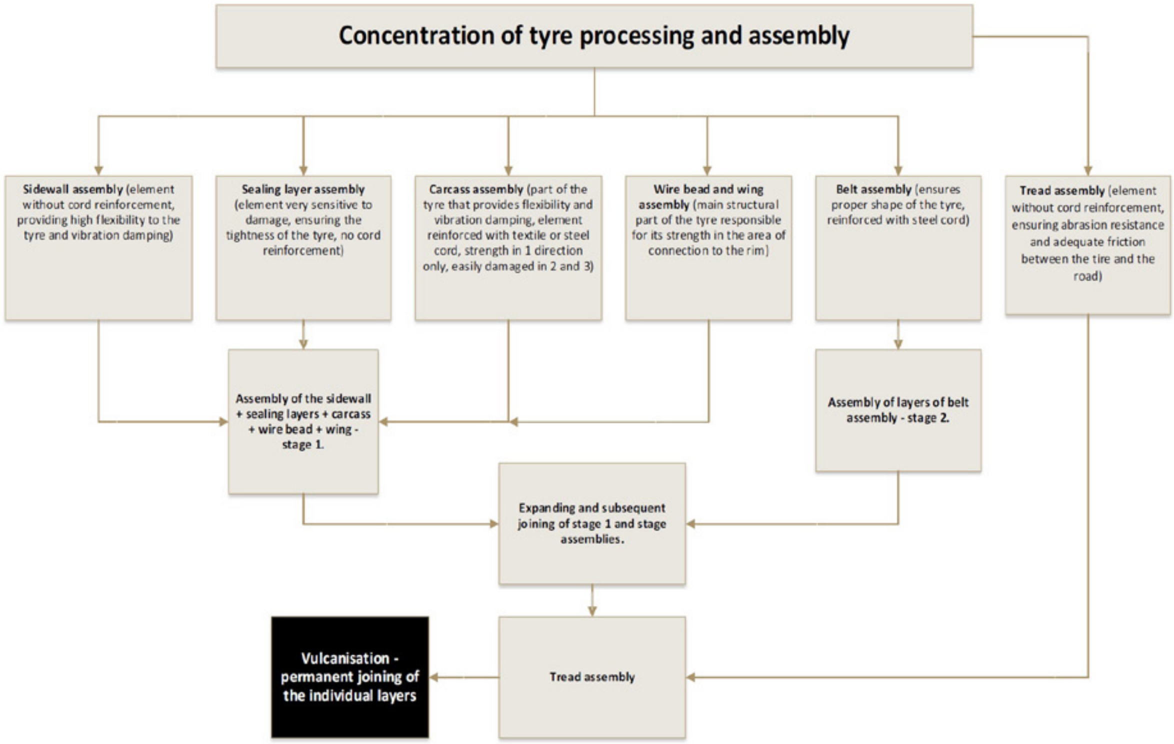

Fig. 16. Concentration of raw material processing operations in pre-assembly processes [own elaboration]

Conclusions

Automation and robotisation is the key to business success for companies manufacturing products with various levels of complexity. Automation and robotisation of processes guarantees repeatability of operations and their stable quality in the long term. The technology of rigid bodies assembly cannot be directly applied to the assembly of tyre components. According to the author of the paper, ***the technological process of tyre assembly*** *consists of identifying the physical and geometric features of the joined elements in order to determine assembly parameters and to select specialist tooling different from the conventional tools used in classical mechanical engineering assembly technology*. The presented paper allows us to identify the differences between the processes of conventional assembly and automatic assembly of tyres.

References

[1] Michałowski B., Jarzynowski M., Pacek P., Integracja rynku robotyki i automatyki przemysłowej z rynkiem teleinformatyki, Szanse i wyzwania polskiego przemysłu 4.0, Agencja Rozwoju Przemysłu S.A., https://www.arp.pl/__data/assets/pdf_file/0008/89918/_Raport_ARP_druk_po_stronie_calosc.pdf [dostęp 25.03.2021]

[2] Ministerstwo Rozwoju, Pracy i Technologii, Ulga na robotyzację – nowe ułatwienie od 1 stycznia 2021 roku, https://www.gov.pl/web/rozwoj-praca-technologia/ulga-na-robotyzacje--nowe-ulatwienie-od--1-stycznia-2021-roku [dostęp 25.04.2021]

[3] Żurek J., Ciszak O. 2000. „Wybór wariantu kolejności montażu części i zespołów maszyn z wykorzystaniem metody Yagera, Choosing the optimal assembly sequence variant of machine parts and sets using the Yager method", Archiwum Technologii Maszyn i Automatyzacji 20(2): 145-153..

[4] Żurek J., Ciszak O., Rose W. 2001. „Balancing of a car assembly line by means of heurestic algorithm, Balansowanie linii montażu samochodu za pomocą algorytmu heurystycznego". Archiwum Technologii Maszyn i Automatyzacji 21(2): 223-230, WPP, Poznań, , ISSN 1233-9709.

[5] Żurek J., Ciszak O., Staniek R.2006. „Application of Genetic Algorithms for balancing assembly lines, Zastosowanie algorytmów genetycznych do zadania wyrównoważenia linii montażowych" Proceedings of the 5th International Conference on Engineering Computational Technology-ECT'06, 12-15.09.2006 r., Las Palmas de Grain Canaria-Spain, Abstract 49, s. 109-110, Civil-Comp Press, 2006, full paper on CD, ISBN 13 978-1-905088-11-9.

[6] Żurek J., Ciszak O., Sibilski A., Analysis of balancing a personal car assembly line, Analiza wyrównoważenia linii montażowej samochodu osobowego, Archiwum Technologii Maszyn i Automatyzacji, kwartalnik, KBM PAN o. Poznań, vol. 23, nr 2, s. 201-208, WPP, Poznań, 2003, ISSN 1233-9709.

[7] Żurek J., Ciszak O., Balancing of vertical milling centre final assembly line, Wyrównoważenie linii montażu finalnego pionowego centrum obróbkowego,

Archiwum Technologii Maszyn i Automatyzacji, kwartalnik, KBM PAN o. Poznań, vol. 26, nr 2, s. 239-245, Poznań, 2006, ISSN 1233-9709.
[8] Żurek J., Ciszak O., Designing a technological assembly process utilizing a CAD system, Projektowanie procesu technologicznego montażu z wykorzystaniem systemu CAD, Archiwum Technologii Maszyn i Automatyzacji, kwartalnik, KBM PAN o. Poznań, vol. 22, nr 2, s. 221-228, WPP, Poznań, 2002, ISSN 1233-9709.
[9] Knast P., Ciszak O., Żurek J., Sposoby szacowania kosztów montażu specjalistycznych maszyn w produkcji jednostkowej, A method to estimate the assembly costs of discrete items, Technologia i Automatyzacja Montażu, nr 1, 2005, s. 12-13, ISSN 1230-7661.
[10] Łunarski J. 2016. Innowacje technologiczne w przedsiębiorstwach – projektowanie, wdrażanie i użytkowanie. Warszawa: Wyd. IMBIGS.
[11] Honczarenko J. 2007. Roboty przemysłowe. Warszawa: WNT.
[12] Honczarenko J., Berliński A. 2011. „Modelowanie energochłonności procesów transportowych w zautomatyzowanych systemach montażowych". Technologia i Automatyzacja Montażu 4.
[13] Honczarenko J. 2021. Elastyczna automatyzacja wytwarzania. Warszawa: PWN..
[14] Kenneth J. Waldron, G. L. Kinzel. 2003. Kinematics, Dynamics, and Design of Machinery, 2nd Edition.
[15] Goldstein H. 1980. Classical Mechanics, 2nd ed. Boston: Addison-Wesley.
[16] Marciniak P. 2020. „Solidne Wiadomości". Informator Bridgestone 19:. 2. https://www.solidarnosc.bspz.pl/Solidne_wiadomosci/solidne_wiadomosci_nr19.pdf [dostęp 31.07.2021]
[17] Magda _515167, Śmierć pracownika w fabryce opon, 2006-05-22, źródło https://www.olsztyn.com.pl/artykul,smierc-pracownika-w-fabryce-opon,1434.html [dostęp 31.07.2021]
[18] Starczewska I., Śmiertelny wypadek w olsztyńskiej fabryce opon, 2011-05-26, https://www.olsztyn.com.pl/artykul,smierteleny-wypadek-w-olsztynskiej-fabryce-opon,7581.html [dostęp 31.07.2021]
[19] Ośrodek Badawczo-Rozwojowy Przemysłu Oponiarskiego Stomil Sp. z o.o, Technologia produkcji bieżnikowanych opon do pojazdów ciężarowych, dostawczych, osobowych i rolniczych, https://ptt.arp.pl/bazy/technologia-produkcji-bie%C5%BCnikowanych-opon-do-pojazd%C3%B3w-ci%C4%99%C5%BCarowych-dostawczych-osobowych-i-rolniczych/ [dostęp 31/07.2021]
[20] Ośrodek Badawczo-Rozwojowy Przemysłu Oponiarskiego Stomil Sp. z o.o, Technologia produkcji barier energochłonnych, https://ptt.arp.pl/bazy/technologia-produkcji-barier-energoch%C5%82onnych/ [dostęp 31.07.2021]
[21] Ośrodek Badawczo-Rozwojowy Przemysłu Oponiarskiego Stomil Sp. z o.o., Technologia produkcji butów strażackich i podeszw obuwia o podwyższonej odporności ogniowej, https://ptt.arp.pl/bazy/technologia-produkcji-but%C3%B3w-stra%C5%BCackich-i-podeszw-obuwia-o-podwy%C5%BCszonej-odporno%C5%9Bci-ogniowej/ [dostęp 31.07.2021]
[22] Ośrodek Badawczo-Rozwojowy Przemysłu Oponiarskiego Stomil Sp. z o.o., Technologia produkcji gąsienic do specjalistycznych pojazdów, https://ptt.arp.pl/bazy/technologia-produkcji-g%C4%85sienic-do-specjalistycznych-pojazd%C3%B3w/ [dostęp 31.07.2021]
[23] Ośrodek Badawczo-Rozwojowy Przemysłu Oponiarskiego Stomil Sp. z o.o., Technologia produkcji odbojnic portowych, https://ptt.arp.pl/bazy/technologia-produkcji-odbojnic-portowych/ [dostęp 31.07.2021]
[24] Ośrodek Badawczo-Rozwojowy Przemysłu Oponiarskiego Stomil Sp. z o.o., Technologia wymiany opon – projekt warsztatu wymiany opon, https://ptt.arp.pl/bazy/technologia-wymiany-opon-projekt-warsztatu-wymiany-opon/ [dostęp 31.07.2021]
[25] Ośrodek Badawczo-Rozwojowy Przemysłu Oponiarskiego Stomil Sp. z o.o., Technologia wytwarzania drzwi drewnianych o podwyższonej odporności ogniowej, https://ptt.arp.pl/bazy/technologia-wytwarzania-drzwi-drewnianych-o-podwy%C5%BCszonej-odporno%C5%9Bci-ogniowej/ [dostęp 31.07.2021]
[26] Ośrodek Badawczo-Rozwojowy Przemysłu Oponiarskiego Stomil Sp. z o.o., Technologia zabezpieczenia PPOŻ zabytkowych konstrukcji drewnianych, https://ptt.arp.pl/bazy/technologia-zabezpieczenia-p-po%C5%BC-zabytkowych-konstrukcji-drewnianych/, dostęp [31.07.2021]
[27] Knast P., nr zgłoszenia 370788 (wynalazek), patent polski, Urządzenie do pakowania opon, data zgłoszenia 2004-10-19, numer prawa wyłącznego 205296, https://ewyszukiwarka.pue.uprp.gov.pl/search/pwp-details/P.370788 [dostęp 31.07.2021]
[28] Hermach M., Knast P., nr zgłoszenia 40748 (wynalazek), patent polski, Sposób bieżnikowania opon, zwłaszcza opon wielkogabarytowych, data zgłoszenia 2014-03-11, numer prawa wyłącznego 226133, https://ewyszukiwarka.pue.uprp.gov.pl/search/pwp-details/P.407483 [dostęp 31.07.2021]
[29] Hermach M., Knast P., nr zgłoszenia 409148 (wynalazek), patent polski, Bariera energochłonna, data zgłoszenia 2014-08-11, numer prawa wyłącznego 226356, https://ewyszukiwarka.pue.uprp.gov.pl/search/pwp-details/P.409148, [dostęp 31.07.2021]
[30] Hermach M., Knast P., nr zgłoszenia 410998 (wynalazek), patent polski, „Wieloczęściowa wkładka zabezpieczająca z mieszanki gumowej niepalnej", data zgłoszenia 2015-01-19, numer prawa wyłącznego 260945, https://ewyszukiwarka.pue.uprp.gov.pl/search/pwp-details/P.410998, [dostęp 31.07.2021]
[31] Hermach M., Knast P., nr zgłoszenia 410946 (wynalazek), patent polski, „Mieszanka gumowa niepalna", data zgłoszenia 2015-01-15, numer prawa wyłącznego 229522, o udzieleniu patentu ogłoszono 31.07.2018 WUP07/18 (Patent dla Ośrodka Badawczo Rozwojowego Przemysłu Oponiarskiego Stomil Sp. z o.o.), https://ewyszukiwarka.pue.uprp.gov.pl/search/pwp-details/P.410946, [dostęp 31.07.2021]
[32] Hermach M., Knast P., nr zgłoszenia 417076 (wynalazek), patent polski, „Maszyna do dynamicznego badania przecięcia opony", data zgłoszenia 2016-05-02, numer prawa wyłącznego 229616, o udzieleniu patentu ogłoszono 31.08.2018 WUP 08/18 (Patent dla Ośrodka Badawczo Rozwojowego Przemysłu Oponiarskiego Stomil Sp. z o.o.), https://ewyszukiwarka.pue.uprp.gov.pl/search/pwp-details/P.410946, [dostęp 31.07.2021]
[33] PN-EN ISO 3037:2013-12, Tektura falista – Oznaczanie odporności na zgniatanie krawędziowe (metoda nieparafinowanej krawędzi).

[34] Joyce H. J. Qi. K., Boyce M. C. 2003. „Durometer Hardness and the Stress-Strain Behavior of Elastomeric Materials", Rubber Chemistry and Technology 76 (2): 419-435.doi.org/10.5254/1.3547752

[35] Ogden R. W. 2013. Non-Linear Elastic Deformations. Dover Publications Incorporated.

[36] Bird R. B., Stewart W. E., Lightfoot E.N., Klingenberg D.J. 2015. Introductory Transport Phenomena. Wiley

[37] Bird R.B., Armstrong R.C., Hassager O. 1987. Dynamics of Polymeric Liquids, Volume 1: Fluid Mechanics. Dynamics of Polymeric Liquids. Wiley, ISBN 978-0-471-80245-7.

[38] ASTM D1415 – 18, Standard Test Method for Rubber Property-International Hardness.

[39] ASTM D2240 – 15e1, Standard Test Method for Rubber Property-Durometer Hardness.

[40] ASTM D1415 – 06, Standard Test Method for Rubber Property-International Hardness.

[41] ASTM D1349 – 14, Standard Practice for Rubber-Standard Conditions for Testing.

[42] ASTM D4483 – 20, Standard Practice for Evaluating Precision for Test Method Standards in the Rubber and Carbon Black Manufacturing Industries.

[43] ASTM D1646 – 19a, Standard Test Methods for Rubber – Viscosity, Stress Relaxation, and Pre-Vulcanization Characteristics (Mooney Viscometer).

[44] Arnaud J. C., Corsi P., Departure E., Lamoureux C., PAT – P.319658, Drut ze stali nierdzewnej do wzmocnienia wierzchołka opony pneumatycznej, Michelin & CIE, Clermont-Ferrand Cédex, FR 1995.

[45] Yasutoshi A., EP0536742A2, Unvulcanized tread material for pneumatic tire and method of manufacturing pneumatic tire, JP 1992.

[46] Vannan F. F. JR., Cappelli M. R., Goldstein A. A., Tubb G. E., P.335689, Trasa osnowy, utrzymywana przez podwulkanizowane wypełnienie, The Goodyear Tire & Rubber Company, Akron, US 1997.

[47] Fenck M., Roppitsch W., DE 1013867, Tire with a belt bandage, Continental Aktiengesellschaft, Hannover, DE 2002.

[48] Hideki H., Kanagawa H., Koshi I., Kotoku, Koichi, WO 2014/010353, Luftreifen, The Yokohama Rubber Co., Ltd., Tokyo, JP 2012.

[49] PN-EN ISO 868:2005, Tworzywa sztuczne i ebonit – Oznaczanie twardości metodą wciskania z zastosowaniem twardościomierza (twardość metodą Shore'a).

[50] Forbes JR. F.V., Matthew R. C., Goldstein A. A., Tubb G. E., Trasa osnowy, utrzymywana przez podwulkanizowane wypełnienie, The Goodyear Tire & Rubber Company z siedzibą główną w Akron USA, P.335689, data zgłoszenia 1997-04-03, https://ewyszukiwarka.pue.uprp.gov.pl/search/pwp-details/P.335689 [dostęp 04.08.2021]

[51] Hata H., Ishii H., Pneumatic Tire, Pub. No.: US 2017 / 0259626 A1, Sep. 14, 2017, The Yokohama Rubber Co., Ltd., Tokyo, JP, Jun. 23, 2016. https://patentimages.storage.googleapis.com/a8/ea/46/a29c455718e996/US20170259626A1.pdf [dostęp 26.04.2021]

[52] Yasutoshi A., Unvulcanized tread material for pneumatic tire and method of manufacturing pneumatic tire, Publication number: 0 536 742 A2, European Patent Office, 08.10.92, Bridgestone Corporation, https://patentimages.storage.googleapis.com/f6/f8/22/e4a04e30651e73/EP0536742A2.pdf [dostęp 26.04.2021]

[53] Hermach M., Knast P., Opona radialna, nr zgłoszenia P.411809, patent polski, data zgłoszenia 2015-03-30, klasyfikacja MKP B60C 9/12 i B60C 9/18, zgłaszający Ośrodek Badawczo Rozwojowego Przemysłu Oponiarskiego Stomil Sp. z o.o., https://ewyszukiwarka.pue.uprp.gov.pl/search/pwp-details/P.411809 [dostęp 04.08.2021].

Paweł Knast, PhD, Eng., Assistant Professor – Department of Mechanics and Mechanical Engineering, Polytechnic Faculty, President Stanislaw Wojciechowski Calisia University, ul. Nowy Świat 4, 62-800 Kalisz, Poland
e-mail: pawel@knast.pl

ANALYTIC OPTIMIZATION FRAMEWORK FOR RESILIENT MANUFACTURING PRODUCTION AND SUPPLY PLANNING IN INDUSTRY 4.0 CONTEXT-BUFFER STOCK ALLOCATION – CASE STUDY

Optymalizacja planowania produkcji oraz zakupów w środowisku analitycznym dla elastycznej i odpornej organizacji produkcyjnej w kontekście Industry 4.0 – studium alokacji buforów

Maria LACIUGA ORCID: 0000-0003-4472-2710

Jarosław SĘP ORCID: 0000-0003-2544-2211

DOI: 10.15199/160.2021.3.5

A b s t r a c t: Advanced components assembly planning and related manufacturing production planning and scheduling (PPS) and supply planningare key elements responsible for deliveries and cost aspects as a resources workload and inventory driver. Industry 4.0 systems broaden science for improving system performance and decision making.Industry site environment because of material flow network, interrelated multi-variable, multilevel production becomes very complex what is challenged by a strong focus on operational excellence. Demand uncertainty requires additional attention and integration with Supply Chain. This paper presents an extended framework for analytics solutions in assembly, production and supply planning for manufacturing company. Risk related to violable customers demand is mitigated by buffer management. Buffer levels relay on a prediction from simulation model using computational methods based on machine learning algorithm using Neutral Networks to guarantee on-time deliveries and rational costs. Actual challenges and requirements for new use cases in data-driven intelligence are presented. The proposed models and the actual state will be comparably discussed with results analyses.

K e y w o r d s: Manufacturing Data analytics, Resilient manufacturing, Production planning, Buffer management

S t r e s z c z e n i e: Planowanie montażu zespołów i wynikające z niego planowanie i harmonogramowanie produkcji (PPS) oraz planowanie zakupu surowców są kluczowymi elementami odpowiedzialnymi za dostawy na czas oraz aspekt kosztowy poprzez odpowiednie obciążenie zasobów oraz nośnik zapasów. Systemy klasy Industry 4.0 poszerzają wiedzę i możliwości dla podniesienia wydajności systemu oraz usprawniają podejmowanie decyzji. Środowisko produkcyjne z uwagi na sieć strumieni wartości, mnogość zmiennych, wielopoziomowe struktury materiałowe staje się bardzo złożone co jest dodatkowo wzmacniane przez nacisk na doskonałość operacyjną. Niepewność zapotrzebowań wymaga dodatkowej atencji oraz integracji z łańcuchem dostaw. W pracy zaprezentowano rozbudowane środowisko dla rozwiązań analitycznych wspierających narzędzia planowania montażu, produkcji oraz zakupów. Ryzyko związane z zmiennymi planami klienta oraz zmiennością dostawców jest ograniczane poprzez zarzadzanie buforami. Poziom bufora zależy od predykcji na bazie modelu symulacyjnego opartego na mechanizmach uczenia maszynowego z wykorzystaniem sieci neuronowych w celu zagwarantowania dostaw na czas oraz w oczekiwanym koszcie. Aktualne wyzwania i oczekiwania w obszarze inteligencji opartej na danych zostały zaprezentowane. Rezultaty zaproponowanego modelu zostały szczegółowo porównane ze stanem obecnym.

S ł o w a k l u c z o w e: Analityka produkcji, Elastyczna i odporna produkcja, Planowanie produkcji, Zarządzanie buforami

Introduction

Assembly planning in industry environments is influenced by volatile markets, the high complexity of products and dynamic production conditions. Companies offer discrete products while maintaining low costs and reducing lead time to remain competitive. [7] Carvajal Soto, J. A., Tavakolizadeh, F. and Gyulai, D. Actual situation show that ability to become more vulnerable to disruptions is a key to run manufacturing organizations successfully. In this uncertain environment quick what-if answers, optimization and data modelling are a powerful tools for learning insights and improving decision making. [14] Daniyan, Muvunzi, Khumbulani. Various sources of data generated in a massive amount, include a huge potential and causes the need for further analysis and predictions. This involves the construction and training of a machine learning model that without experts knowledge is very challenging. Multiple data are coming from Industry 4.0 Systems into Company's databases. Those acquired data are the next characteristics that can better describe the nature and needs of the organization and finally help to find the best data- driven intelligence for decision making. These data can be used to make strategic planning, process control and monitoring. It will also help in long-term problem solving. Multiple optimized algorithms are included in Industry 4.0 systems. [20] Nagorny, Lima, Monteiro. By using data from multiple sources a new optimized possibilities are provided and more accurate recommendations can be set for better decision making. Information on the process outputs at each stage can be useful in improving performance and helping better understand current state. Machine Learning (ML) powered systems are a very promising way of achieving process monitoring which can lead to significant improvement in whole production and supply planning. Optimized safety stock levels have increasing research attention in last decade. Cost of material shortage can be significant when considering the cost of resources waiting (employees performance, lack of machines utilization), material flow dropdowns, customers delivery delays. Dolgui, A. and Prodhon [9] show that different types of buffers may be employed to improve performance but they should only be used when the contribution of a buffer is greater than the cost of it. Management of buffers is an important part of manufacturing planning and controlling (MPC) in order to stay competitive. Dolgui, A. and Prodhon [9] defined a framework for MPC that reflects the significance of buffers. To support the balancing of supply with demand they identified four management perspectives. Buffer management is defined based on the intersection of four management perspectives related to the transformation flow: the resources employed in the flow, the risk involved in the flow, the decision making. In volatilised and uncertified environment buffer strategy also has to have the ability to change quickly because it may lead to redundant inventory levels. The aim of that research is to present the use of ML to enhance the performance of a value stream from assembly to production line and supply as a case study by providing a recommendation for buffer location and safety stock levels. The proposed framework can be used for further research and designing algorithms for data mining.

This paper is constructed in six sections. The second section focuses on the state of research. The third section introduces the used analysis framework. The next fourth section describes methodology and modelling. The fifth section examines and analyses the results of the research. The last sixth section presents the conclusion and further research perspectives.

State of research

We are surrounded by digital environments continuously generating more data and with connections to devices and software. Such an evolution happens also in the manufacturing domain. Future Smart Manufacturing infrastructures are faced with the digitalisation and virtualisation of objects enhanced with sensors, processors, memory and communication devices. That is providing the ability to communicate coactively and to exchange information independently through a reactive, predictive behaviour [6]. Massmann et all [19] described a framework for data analytics in Data -Driven Planning. That's addressing the major challenges in the context of analytics activities and the resulting requirements. Along with the four layers of analytics projects, the framework proposes procedures and methods that support the planning and implementation of a successful data analysis in product planning. Research has proven that it is advantageous to employ algorithms with self-learning abilities as their predictive abilities often increase over time with an increase in the size of the data [9-11]. Besides, it can reveal new failure modes and give insights into the asset reliability model [2-4]. Machine learning algorithms have become more and more popular over the last decade for production applications, which can lead to better-suited recommendations for decision-making managers[12]Because of high changeability in organizations surrounding companies are looking for methods for risk mitigations and being resilient. Supply chain resilience was discussed in literature widely. Hosseini et al [11] reviewed quantitative methods , technologies and key drivers of supply chain resilience. Hosseini, S. and Ivanov, D., [10] proposed resilience measure as a function of supplier vulnerability and recoverability using a Bayesian network and considering disruption propagation .That allows to uncover higher-risk suppliers to develop recommendations to control the ripple effect. In literature. Many different methods and approaches in fixing buffers under different situations can be found in literature. Aleotti and Qassim [2] concluded that holding inventory in the intermediate levels which only reduce the frequency of stockout is not economical. Li and Li [17] showed a dynamic model of the safety stock. Only the variability of demand is considered in this model. Authors also presented another method for a multilevel MRP system. The relation between safety stock and different system measures like service level, schedule variability, and total cost in different methods has been provided. Bahareh and Bhuiyan [6] present a general safety stock optimization model with the objective of logistics cost minimization by considering both internal and external variabilities. Authors also consider part availability (First Fill Rate FFR). Demand and Supply variability are addressed in [19]. Authors provide research about the required amount of safety stock or the length of a safety lead time influenced by the level of uncertainty experienced in a production unit. Karaesmen et al [16] present that there is an impact of increased un certainty in demand and supply variability to decrease delivery performance. Recent reviews on managing uncertainties in MRP environments show that, to date, studies have been largely restricted to a single source of uncertainty, related to either supply or demand. Hedvall [18]identified and constitute the foundation for buffer management in: Balance management (Demand and Supply), Resource management (Materials and Capacity), Risk management (Regular and Safety), Hierarchical management(Structural, Aggregate, Detailed and Execution). That hierarchical split is then shown in additional 4 dimensions- Material Management (MM) and Capacity Management(CM) with regular and safety approach – That gives sixteen components of buffer management. No use case or practical aspect was shown. Amirjabbari and Bhuiyana [5] presented a safety stock optimization model with the objective function of total logistic costs minimization with an optimal level and location of safety stock across the supply chain.

The available research publications use mostly standard data like ERP and do not cover complex buffer model addressing both supply and demand variability with manufacturing aspects in internal process and additional data availability. Dynamic buffer modelling with Machine Learning algorithm sand a wider view based on new data view from Industry 4.0 systems for securing production planning is presented in this paper. This industrial problem represents another interesting and challenging research opportunity especially due to the resilience aspect igh variability, responsiveness and flexibility expectancy with continuous cost perspective.

Framework

Analytics solutions in production and supply planning for a manufacturing company need strong data-driven intelligence based on Industry 4.0 systems. The analytics framework schema is shown in Figure 1.

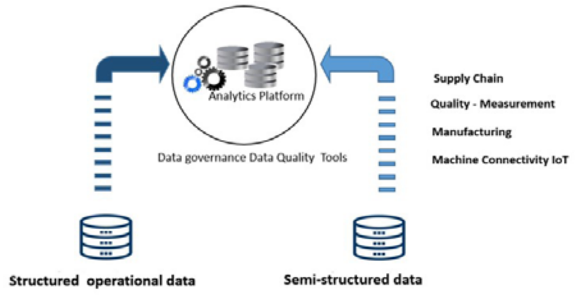

Fig. 1. Analytics framework

Analytics platform gathers, combine, cleanse and enhance data from two types. Except for structured operational data e.g. ERP system data and other supporting ones which extend business data framework needs to address also those less-structured ones. Those data are coming from Industry 4.0 systems like Machine Connectivity, Manufacturing IoT, Measurements, MOS. IoT data like machineries signals providing detailed information about the way that manufacturing organization works may also give valuable information in terms of production planning and raw material availability.

The below framework can be consumed by various users and tools shown in a Fig. 2.

Analytics models as a computed portion of data with detailed information prepared with a business goal are consumed by Self-Service solutions. They ensure data re-use for personal /ad-hoc data exploration, outside of formal projects. Data investigations in self-serve mode serve for generating initiatives and projects. Analytical tools help to improve process and information flow. They are reusing data collected and stored in Analytics framework. Advances Analytic sis a decision support as the ultimate goal of analytics solutions – data driven decision making based on recommendations found in data. The process of manufacturing data modelling is shown in Fig. 3.

Data modelling for defined questions based on Machine Learning algorithms needs strong and scalable data acquisition and storage steps. Then data pre-processing for preparing and cleaning is set. Process definition and key variable identification is the next element. Then data exploration and data training is performed. Model development is the last step.

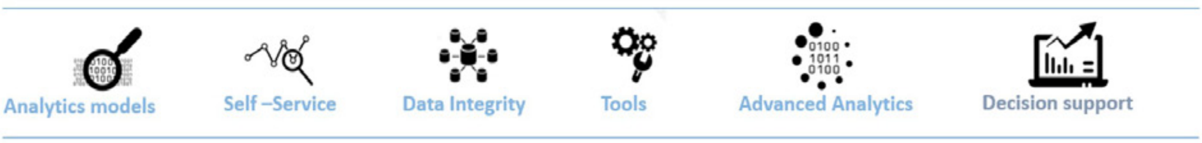

Fig. 2. Data consumption

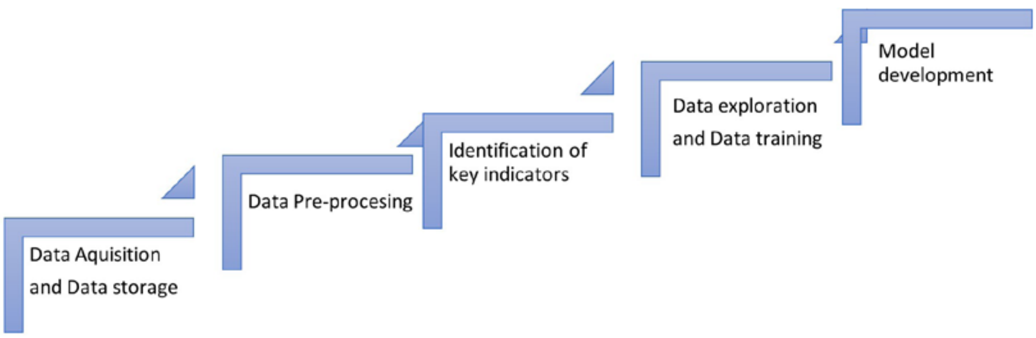

Fig. 3. Data modelling process-Machine Learning

Methodology and model

Effective buffer management (right places, levels and types) is the key element for manufacturing risk management for production and supply environment and a variability on both sides. All parts availability on time allows to finish assembly on time for customer demand and provide resources workload according to plan. Lack of components at any point of production leads to material flow distortions. Risk management in that area is evaluated thought buffer management. That is guaranteed through safety stock (SS) or safety time (ST) or mixing policy. Buffer level, type and location should also consider the optimized level of costs. Costs of resource waiting, the material flow stops and customer waiting should be compared to the cost of additional inventory storage. The research was carried out on data coming from company A – for the purpose of confidentiality. A is a manufacturing company. A has a complex multi-level bills of material, high demand variability and long lead times. Numbers of suppliers, procurements, manufacturing, final assembly, and customers (internal and external) are different nodes of the A's supply chain. That advanced system focuses significant attention on setting and positioning buffers. Data used in research covers two years history of inventory levels, overdue, shortage history gathered in weekly snapshots. Based on CRM, ERP demand variability was calculated. Historical parts availability is calculated based on ERP and Manufacturing systems. Data are additionally cleaned from used buffer methods to have full visibility in the real environment. Additionally a big number of another parameter and variables gathered in Industry 4.0 systems were included in modelling. The results are limited to the selected Final Assembly family composed of 29 part numbers that represents one of A's production lines. Sample Bill of Material for particular Finish Good (FG) assembly is shown in Fig. 4. The green colour indicated raw materials (RM), blue are manufactured (MFG)

The objective is to minimise the overdue of raw material and subassembly for production and thus avoiding production material flow breaks and assembly picking issues for on-time delivers to the customer while not exceeding the level of cost. Parameters and variables are listed in Tab. 1. Those variables affect the final state of material availability and create the integrated model. Used variables impact on a buffer management model.

Table 1. Parameters and variables

M	Number of Final Assembly i
N	Number of Sub-Assembly j
O	Number of Component k
p	Date
a_k	Number of Supplier for Component k
b_{kp}	Planned delivery time of Component k
c_{kp}	Inventory-stock of Component k in historical snapshot p
d_{kp}	Overdue-Missed parts of Component k in historical snapshot p
w_{knp}	Balance of Component k in weeks n in historical snapshot p
e_{kp}	Overdue deepness – Missed parts of Component k in weeks for historical snapshot p
f_{kp}	if item d_k<0 , 0 otherwisein historical snapshot p
w_{kp}	Demand of item k [Weekly – average for next 8 weeks] for historical snapshot p
g_k	Demand variability for Component k
h_k	Supply variability for Component k
l_{kp}	Number of Production Orders that cannot start because of lack of k for historical snapshot
m_k	Segment volume for Component k
n_k	Bill of Material level for Component k
r_k	Cost Segment for Component k
s_k	Volume Segment for Component k
t_{kp}	Component k availability measurement (FFR) in historical dates
T_{mp}	Final Assembly m availability measurement (FFR) in historical dates
u_{kp}	Type of Component k in historical dates
z_{kp}	First Pass Yield (FPY) Quality grade of k in historical dates
C_k	Cost of shortage for Component k in historical snapshot p – resource waiting
O_k	Cost of overstock for Component k in historical snapshot p – inventory

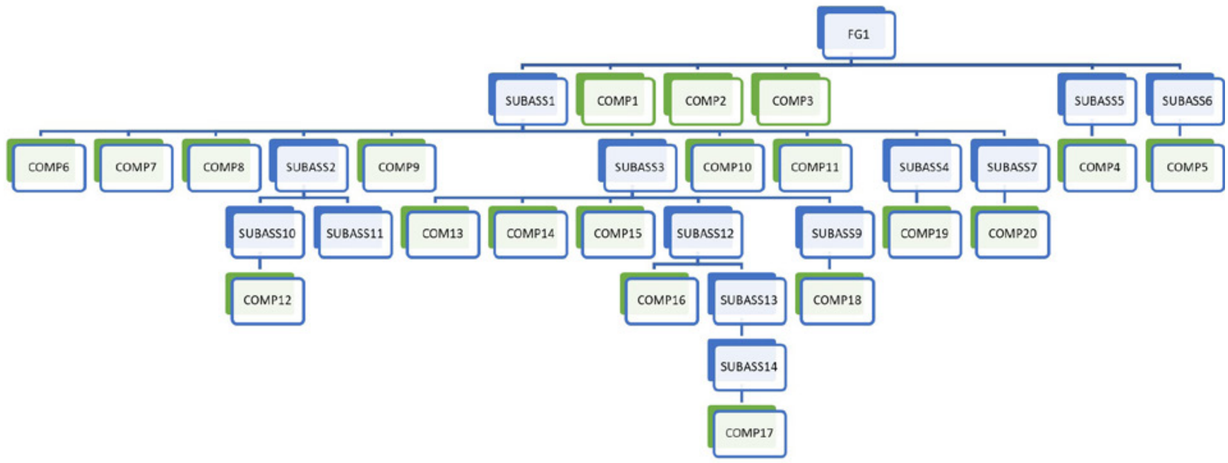

Fig. 4. Sample Bill of Material

Multilevel bill of materials for 29 Final Assembly Parts *i* with an average 35 Components *k* and an average 13 Sub-Assembly j is a complex modules model framework. Place in BOM structure n_k impact significantly material availability. Historical datashow structure forthe deepness of overdue e_{kp} and accompanying values of demand level w_{kp}, supply and demand variability g_k, h_k, quality z_{kp} in that period. Also parts parameters for that period were included like Planned delivery time (LT) b_{kp}, type u_{kp}.Those elements have multiple sources (suppliers a_k or manufacturing lines), prices r_k and volume segments m_k that determine the costs of inventory. For buffer calculations were included also costs of shortage. Data used to create that information are coming from Industry 4.0 systems. Machine waiting and manpower resources waiting costs calculated based on above data. The complex module structures cause multiple shortage issues. For example – We may have available 100% components on time and still will not be able to provide part on time because of quality or resources problems. That is why we also include FFR value for Subassembly *j* and Final assembly *i* in snapshot (*p*).

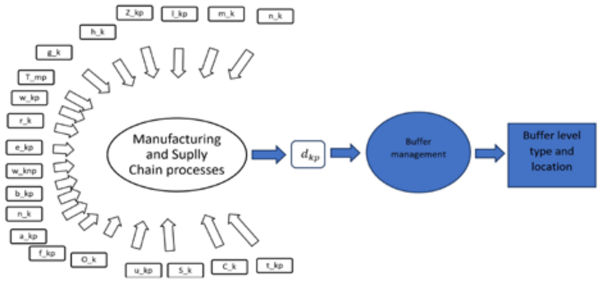

Fig. 5. Buffer management module

Output from Manufacturing and Supply Processes is reflected in material balance /Overdue d_{kp} as a material availability score in snapshot p. It is a balance of stock level and past requirements for component *k*. The result variable has a distribution shown in Fig. 5. Values d_{kp}<0 means that there is a shortage and planned orders cannot be converted into Work In Process.

Data distribution for d_{kp} result by components is shown in Fig. 6.

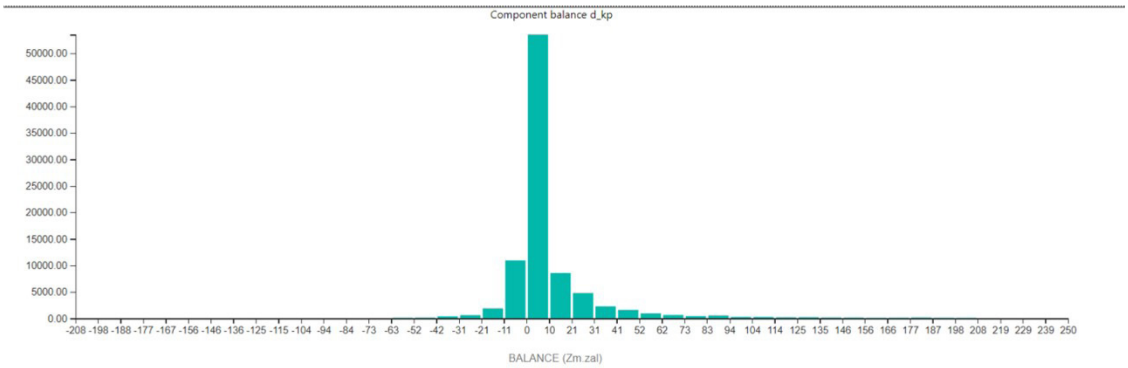

Fig. 6. Material balance d_{kp} data distribution

For better visibility one particular final assembly components distribution is shown in Fig. 7.

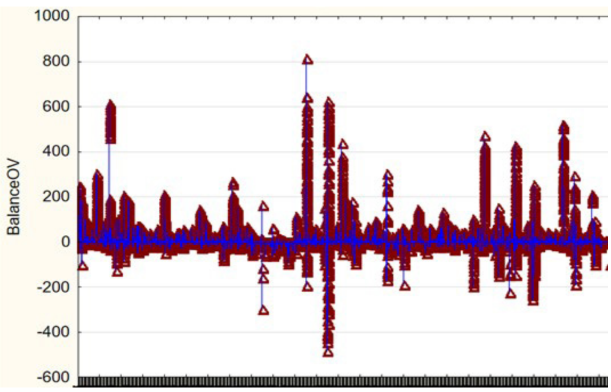

Fig. 7. Data distribution for d_{kp}

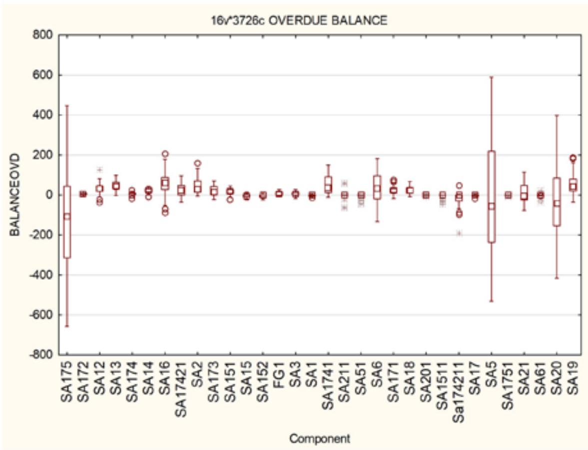

Fig. 8. Overdue boxplot

The first conclusion about buffer allocations can be made for those components that have a median below 0. Recommended buffer level needs additional data modelling. As a result of the production and supply environment and a variability on both sides it is the key element for manufacturing risk management to provide buffer management in the right places, levels and types. The Machine learning model is proposed to create a dynamic self-learning algorithm to predict future material balance for shortage cases based on mentioned set of parameters and variables. That model could predict future level of balance on components and then provide the answer in buffer allocation to mitigate that risk and guaranty material availability.

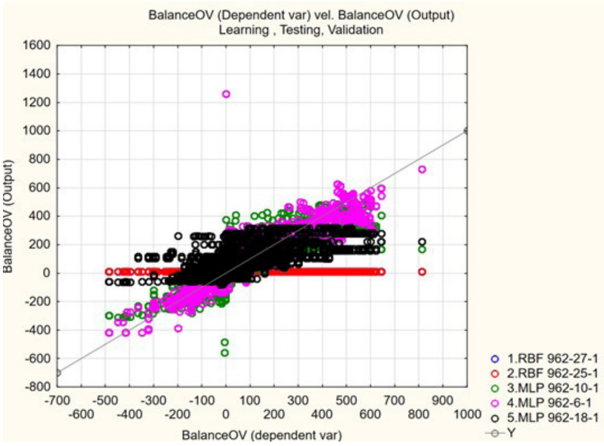

Fig. 10. NN Learning results graph comparison

Results present analyses

Artificial Neutron Network MLP

An artificial neural network (ANN) was developed to predict the material balance d_{kp} for components in time. ANN structure consists of input, hidden, and output layers for the estimation of material availability. The hidden layers consist of different nodes for the estimation of the output. For the development of ANN, 21 parameters were considered as inputs including: demand and supply variability in last period, Component FG, average demand for next 8 weeks, supplier, Planned LT, Batch size, FPY in the last period, Bom level and Bom structure. Linear functions were used as the transfer function in the hidden layer. The optimum ANN topology was obtained by trial and error, and the ANN structure is shown in Fig. 9. As seen, the ANN takes multiple parameters as the inputs, and estimates the material balance d_{kp} as the output. *Statistica 13.3* software was used for performing the ANN analysis.

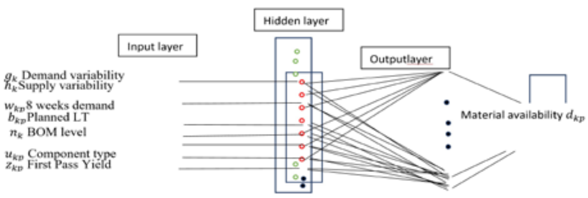

Fig. 9. ANN structure

Data were divided into learning (70%), training (15%) and validation (15%).ANN Model results are shown in Tab. 2 and Fig.10

The best results are captured in network 4 with Exponential activation (hidden). It is a Multilayer Perceptron type of network. The used algorithm is BFGS 6754.Re-alvaluescomparable to those produced by winning network 4 are shown in Fig. 11.

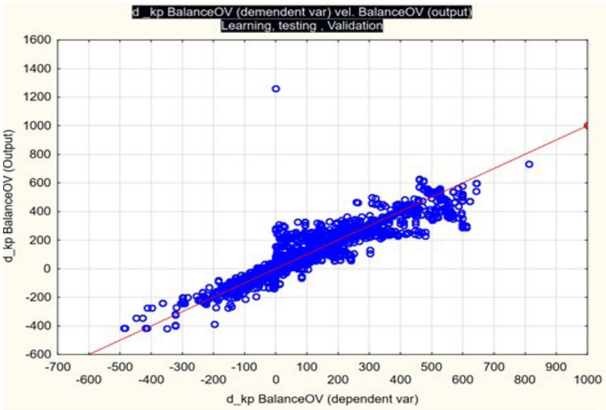

Fig. 11. Winning network-data comparison

The results show that MLP can provide very good rules in future projections based on data. The difference between captured real data and those produced by Neutral Networksis 6.5% (93.5% accurate).The detailed information shows a great opportunity to use trained Network to provide projections for future levels of components balance d_{kp}. The structure of differences between captured and projected data for the data set is presented in Fig.12.

Table 2. ANN Learning results comparison

Id sieci	Nazwa sieci	Jakość (uczenie)	Jakość (testowanie)	Jakość (walidacja)	Błąd (uczenie)	Błąd (testowanie)	Błąd (walidacja)	Algorytm uczenia	Funkcja błędu	Aktywacja (ukryte)
1	RBF 962-27-1	0.000000	0.000000	0.000000	854.1504	911.3160	983.0272	RBFT	SOS	Gaussa
2	RBF 962-25-1	-0.000000	0.000000	0.000000	854.1504	911.3160	983.0272	RBFT	SOS	Gaussa
3	MLP 962-10-1	0.899685	0.885158	0.892778	163.2220	197.4026	199.9295	BFGS 95	SOS	Logistyczna
4	MLP 962-6-1	0.952398	0.944205	0.916645	79.3877	98.8196	158.5997	BFGS 6754	SOS	Wykładnicza
5	MLP 962-18-1	0.764975	0.780491	0.762031	354.3135	356.7371	412.2092	BFGS 161	SOS	Liniowa

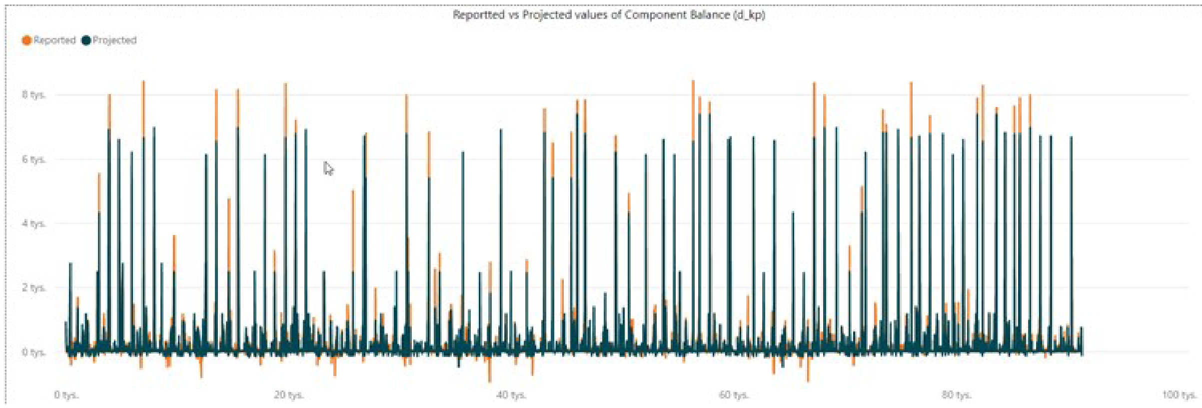

Fig. 12. Reported and Projected values

For better visibility data for individual component 403 is shown in Figure 13

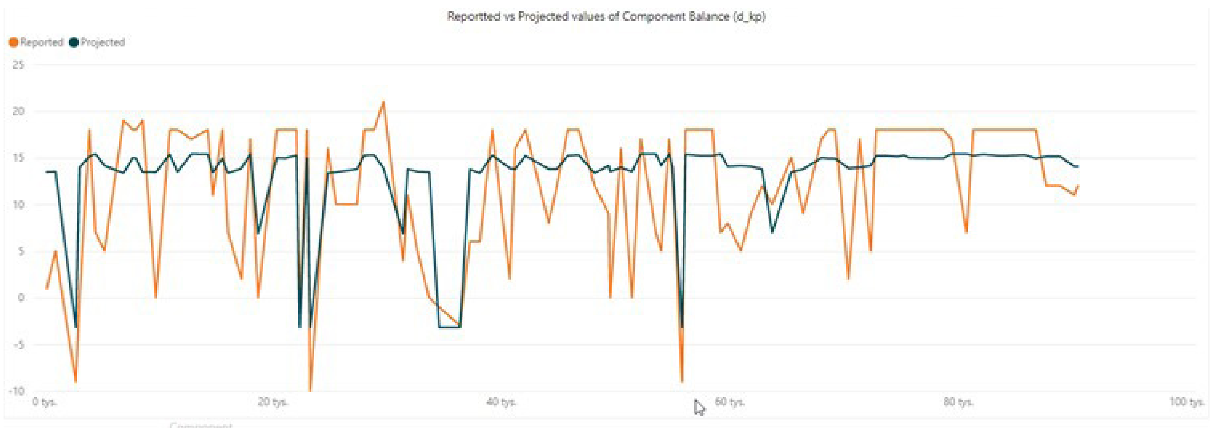

Fig. 13. Component 403 reported and projected values

That means that better than any other statistical method or approach Neutron Network can predict how violable market will perform in way of the balance of material. Having that information and combining it with other variables is a key element for risk mitigation by recommending levels and locations of buffers.

Neutron Network data consumption to buffer levels recommendation

Projected values from Neutron Network and other defined variables are included to build an analytics model to recommend buffer levels, location and types. Key elements considered in modelling:

- *Projected values from Neutron Network*

When projected values are below 0 (shortage) they need to be secured by implementing a buffer strategy. The recommended levels will exceed it to provide week up to three weeks of buffer depending on other variables

- *Median value from Historical Data*

In a quickly changing environment it's critical to react quickly. If the median value for Component balance is below 0 then a physical inventory buffer will be proposed in the Safety Stock type of buffer. If shortage situation is frequent and median is around 0 and overdue is more connected to supply variability then safety time (ST) will be proposed. When the shortage situation is rare and median is high then a more elastic form of the buffer will be recommended like Dynamic Safety Stock (coverage profile in ERP).

- *Cost aspect*

As mentioned in the literature review it is economical and organizational profitable to keep buffers. The components from high cost segment will have a lower buffer then those medium or low. The situation where the costs of inventory offset costs of shortage and low delivery performance also were included.

- *Component parameters*

Lead times, batch sizes, type of component, supplier type also impact buffer management policy.

Analytics Model is prepared to work dynamically with ANN. Model is produced on the platform described in Figure1. Kampen et all [23] present research for using Safety stock and Safety Time depending form the source of variability. Partially it finds confirmation in this paper. Static forms of buffer were proposed on locations where we see the projection of shortage and it happened often in history based on median. Safety stock (SS) was proposed there where ANN forecasts shortage and historical median set shortage frequent. Safety time (ST) was proposed in low levels on projected balance with historical shortage situations. The rest of the population was covered by Dynamic Safety stock. They are defined by Coverage profile which works on average daily requirements. It is calculated depending on the requirements within a specified period (e.g. 6 months) and the range of coverage (e.g. 3 weeks). That elastic form of buffer matches demand. Additionally working in a range of coverage it works from the minimum up to the maximum level being very elastic and guarantying on time material availability.

The results of experiments show that the received target inventory value level is lower than firstly predicted in NN. That show that thanks to Machine Learning and Mathematical programming and modelling it is possible to guaranty material availability by mitigating the risk of shortage with correct buffer levels, location and type without additional investment. Reducing big numbers of inventory in one place and setting buffers is a key to the proposed dynamic approach. The projected level of balance (planned inventory) was firstly 482.36 KPLN. The new Buffer structure will recure a maximum of 349.02 KPLN. Difference values split for Final Assemblies is provided in Fig. 14.

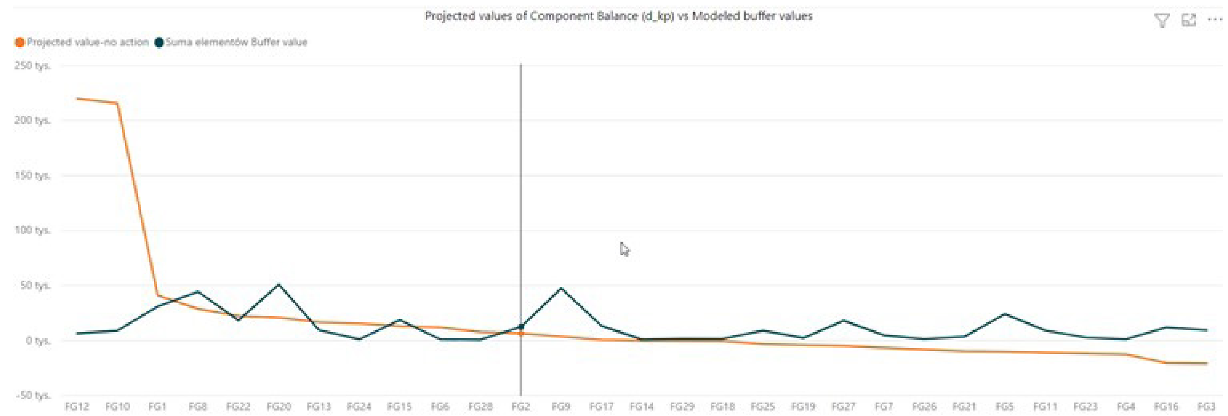

Fig. 14. Comparison of projected inventory and new buffer value

Used buffer types split is shown in Fig. 15.

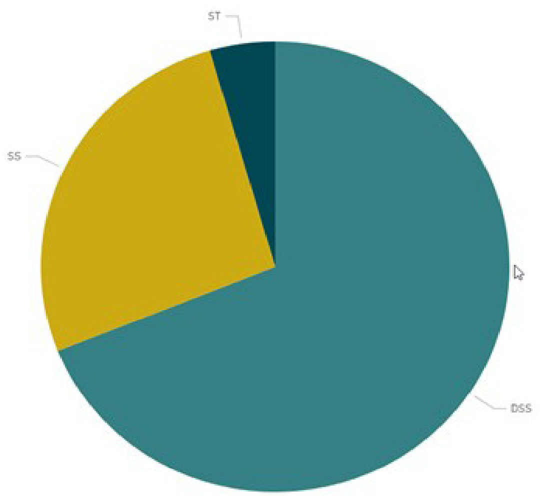

Fig. 15. Buffer types split

The above analyses show that Machine Learning combined with analytical modelling can give organizations new possibilities to optimize buffer management process, increase performance and profit.

Conclusions and future research opportunities

In this research, a dynamic and data driven buffer management optimalization model is provided with the objective function on buffer location, levels and types. Modelling is based on predictions from Neutron Network for future material balance (inventory or shortage) combined with other variables defined. Practical real-world problem with different value streams was used during research. The proposed methodology which joins Machine Learning algorithms and risk mitigation analytical modelling make the system less vulnerable to demand and supply changes.

In this paper, we presented an approach that optimizes the buffers placement in a manufacturing company production line. We find in our experiments that thanks to a data-driven approach combining Machine Learning and other algorithms we may guaranty on time delivery without additional investments. Target inventory levels should be rearranged due to demand change. Buffer realignment based on dynamic modelling should be adjusted when data and trends are changing as fast as possible. By enhancing the visibility and control of key elements in value stream in the chain, the optimization model can be applied for each specific part. By increasing the accessibility of the data, and new data views it is possible to bring more information from the data and using them for optimizing products and processes in the company.

Several promising directions for further research remain like factors of waiting time for receiving the late parts, safety stock for the finished assembled product, and build ahead in making the decision for the buffer placement. An another direction for further research is extending the applied methodology for other processes in Production Planning and Control.

References

[1] Aissani, N., Bekrar, A., Trentesaux, D. and Beldjilali, B. 2012."Dynamic scheduling for multi-site companies: A decisional approach based on reinforcement multi--agent learning". Journal of Intelligent Manufacturing 23(6): 2513–2529.

[2] Aleotti M., L.O.,Qassim, R.Y. 1998. "Minimum cost safety stocks for frequently delivery manufacturing". International Journal of Production Economics 62(3): 233–236.

[3] Altaf, M. S., Bouferguene, A., Liu, H., Al-Hussein, M. and Yu, H..2018 ."Integrated production planning and control system for a panelized home prefabrication facility using simulation and RFID". Automation in Construction 85: 369–383.

[4] Alzubaidi, L., Zhang, J., Humaidi, A.J. et al . 2021."Review of deep learning: concepts, CNN architectures, challenges, applications, future directions", J Big Data 8: 53

[5] Amirjabbari, B., Bhuiyan, N.. 2014. Determining supply chain safety stock level and location. Journal of Industrial Engineering and Management 10. 10.3926/jiem.543.

[6] Bergmann, S., Feldkamp, N. and Strassburger, S. 2015."Approximation of dispatching rules for manufacturing simulation using data mining methods". Winter Simulation Conference. Huntington Beach, USA, 2329–2340.

[7] Carvajal Soto, J. A., Tavakolizadeh, F. and Gyulai, D. 2019. "An online machine learning framework for early detection of product failures in an Industry 4.0 context".. International Journal of Computer Integrated Manufacturing 32: 1–14.

–

[9] Dolgui, A. ,Prodhon, C.. 2007."Supply planning under uncertainties in MRP environments: a state of the art." Annual Reviews in Control 31 (2): 269–279.

[10] Hosseini, S., Barker, K.,2016."A Bayesian network model for resilience-based supplier selection". International Journal of Production Economics 180: 68–87.

[11] Hosseini, S., Ivanov, D., 2019. " A new resilience measure for supply networks with the ripple effect considerations: a Bayesian network approach". Annals of Operations Research. Springer US.

[12] Hosseini, S., Ivanov, D. ,Dolgui, A., 2019. "Review of quantitative methods for supply chain resilience analysis". Transportation Research Part E: Logistics and Transportation Review 125, 285–307.

[13] Daniyan, I., Bello, E.,Ogedengbe, T., Mpofu, K.. 2020. "Use of Central Composite Design and Artificial Neural Network for Predicting the Yield of Biodiesel". Procedia CIRP. 89. 59-67. 10.1016/j.procir.2020.05.119.

[14] Daniyan, I.,Muvunzi, R.,Mpofu, K. 2021." Artificial intelligence system for enhancing product's performance during its life cycle in a railcar industry". Procedia CIRP. 98. 482-487. 10.1016/j.procir.2021.01.138.

[15] Kunnumkal, S., Topaloglu, H. 2008. "Price discounts in exchange for reduced customer demand variability and applications to advance demand information acquisition". International Journal of Production Economics 111 (2): 543–561.

[16] Karaesmen, F.,. 2003. " Inventory systems with advance demand information and random replenishment times" Proceedings of the fourth Aegean international conference on analysis of manufacturing systems, 1–4 July Samos Island, Greece, 151–160. Karaesmen, F., Liberopoulos, G., and Dallery, Y., 2004. The value of advance demand information in production/inventory systems. Annals of Operations Research, 126 (1–4), 135–157

[17] Li, Q.Y., Li, S.J. 2009."A dynamic model of the safety stock under VMI". Proceedings ofthe Eighth International Conference on Machine Learning and Cybernetics, 1304-1308.

[18] Hedvall, L.,Wikner, J.,Hilletofth, P. 2017. "Introducing Buffer Management in a Manufacturing Planning and Control Framework". 366-373. 10.1007/978-3-319-66926-7_42.

[19] Massmann, M., Meyer, Maurice,F.M., von Enzberg, S.,Kühn, A.,Dumitrescu, R. 2020. "Framework for Data Analytics in Data-Driven Product Planning". Procedia Manufacturing 52. 10.1016/j.promfg.2020.11.058.

[20] Nagorny, K., Monteiro, P., Barata, J., Colombo, A.. 2017. "Big Data Analysis in Smart Manufacturing: A Review". International Journal of Communications, Network and System Sciences 10. 31-58. 10.4236/ijcns.2017.103003.

[21] O. T., Adesina, T., Jamiru, I. A., Daniyan, E. R., Sadiku, O. F., Ogunbiyi, O. S., Adesina & L. W. Beneke.2020." Mechanical property prediction of SPS processed GNP/PLA polymer nanocomposite using Artificial Neural Network". Cogent Engineering 7(1720894):1-17.

[22] Partha S.Ghosal, Ashok K.Gupta. 2016." Enhanced efficiency of ANN using non-linear regression for modelling adsorptive removal of fluoride by calcined Ca-Al-(NO3)--LDH". Journal of Molecular Liquids 222: 564-570

[23] Rahman, Md.A., Karim, M.2021."Designing a Modelto Study Data Mining in Distributed Environment". Journal of Data Analysis and Information Processing 9: 23–29.

[24] van Kampen, T. J., van Donk, Dirk P., van der Zee, Durk-Jouke. 2010. "Safety stock or safety lead time: coping with unreliability in demand and supply". International Journal of Production Research 48: 24, 7463 —7481

[25] Y. H. Ali, 2018, "Artificial Intelligence application in machine monitoring and fault diagnosis". Intech Open, Artificial Intelligence - Emerging Trends and Applications: 276–291.

mgr inż. Maria Laciuga – Doctoral School of Engineering and Technical Sciences at the Rzeszow University of Technology, Rzeszów University of Technology ,
Al, Powstańców Warszawy 12, 35-309 Rzeszów, Poland
e-mail: d499@stud.prz.edu.pl

prof. dr hab. inż. Jarosław Sęp,
Rzeszów University of Technology ,
Al Powstańców Warszawy 12 , 35-309 Rzeszów, Poland

Z PRASY ZAGRANICZNEJ

Tytuły i streszczenia artykułów zamieszczonych w miesięczniku naukowo-technicznym **„Sborka v mashinostroenii priborostroenii”** (Wydawnictwo Maszynostrojenije, Moskwa, Rosja)

Sborka nr 7, 2020

1. The question of forecasting residual resource artillery weapons
Authors: Pushkarëv A.M., Muralev A.A.

The issue of forecasting the technical condition of the object, on the example of artillery weapons, is considered. The criterial relations of the working condition of the object are analyzed. A methodology for predicting the residual life of weapons products is proposed, which allows you to assign the maximum tolerance of the determining parameter for long-term operation of the products.

2. Integration of information business systems and management systems in assembly production
Authors: Nuzhdin G.A., Nujdin M.G.

Issues of the implementation of the "Strategy for the Development of the Information Society in the Russian Federation for 2017—2030" in terms of the implementation of information business systems and their integration with management systems of industrial enterprises are presented. The module components of the APS system, its capabilities and limitations in terms of implementation in an industrial enterprise are considered. The special relevance and necessity of integration with functioning ERP systems and management systems in order to ensure a systematic approach and performance was noted.

3. Mathematical model of a robotized assembly in the presence of vibrations and gripper rotation
Authors: Vartanov M.V., Chan Chung Ta

The assembly method using the effect of rotational motion and vibration is considered. The presence of rotation allows to significantly reducing the friction force in connection, which prevents the assembly process. The effect is achieved due to using the rotation of robot gripper and the vibrating device. A mathematical dynamics model of the robotic assembly process is presented.

4. The assembly of the controller
Authors: Mikaeva A.S., Mikaeva S.A.

The assembly of the control controller for controlling an electronic star t-up control device is described. The technical characteristics of the controller are given. The list of commands supported by the controller when exchanging via the RS485 interface and additional discrete controller signals is presented.

5. The assembling of machine tool’s change gear quadrants based on modernized sets of gears
Author: Fot A.P.

A method of assembling the twin-paired change gear quadrant with variable center distance that used on different metalworking machine tools is proposed. The possibility to increase the quality and reducing time of gears adjustment is proved — increase number of gear ratios provided by the modernized set of change gears while the number of change gears in set remains constant. Sets are created based on software tool executing the adjustment of twin-paired change gear quadrants regarding the primary kinematic and design constraints of a machine. The analytical methods and methods of computer modeling are used.

6. Sealing critical connections of the cylinder head with adhesives
Authors: Zaharova M.E., Vasileva P.YU., Arsenov N.A.

The classification of adhesive compositions is considered. The requirements for adhesive compositions that provide a given joint strength are given. The design of the cylinder head and its components is described and the use of adhesive composition as a means of sealing is justified. The criteria for selecting the optimal adhesive connection are presented. A comparative analysis of adhesive compositions of different brands is presented.

7. Analysis of existing diagnostic systems to control the vibration level of locomotive components
Authors: Gubarev P.V., Bolshikh I.V., Shabaev V.V.

The existing installations and systems used in locomotive depots for their diagnosis are analyzed. New devices and technologies are proposed. The approximate composition of the diagnostic complex is given.

8. The influence of specific lubricants on the friction and wear properties of titanium aluminum nitride + solid carbon two-layer coating investigation
Authors: Buyanovsky I.A., Samusenko V.D., Pilatskaya S.S., Levchenko V.A.

The influence of three model lubricants (inactive, surface-active and chemically active) on the friction-wear characteristics of steel—steel friction pairs, steel—coating of titanium aluminum nitride and steel—two-layer coating of titanium aluminum nitride + hard carbon coating is studied. The minimum coefficient of friction and the minimum diameters of the wear spot were established for the combination of steel-two-layer coating of titanium aluminum nitride + hard carbon coating-orientant in compared media.

9. **System with two degrees of freedom in the problem of damping frictional oscillations taking into account nonlinearities of passive forces**
   Author: Erlich B.M.

The actual problem of damping frictional oscillations taking into account the nonlinearities of passive forces in a system with two degrees of freedom is considered. As an active influence during vibration damping two power impacts of a special structure are used simultaneously, providing steady fluctuations of lower intensity. The calculation confirm the effectiveness of the proposed solution to the problem under consideration.

10. **Influence of the characteristics surface layer of the tool and composition technological lubricant on the coefficient of friction in methods combined mandreling of holes**
    Authors: Schedrin A.V., Bekaev A.A., Chikhacheva N.Yu.

The influence of the nature and parameters microgeometry of the surface layer tool on the sliding friction coefficient in the combined methods opening under the conditions of using metal-coating lubricants, which implement the effect of wear-free friction of Garkunov—Kragelsky, is studied comparatively using the theoretical provisions of the adhesive deformation theory of friction.

Link: http://www.mashin.ru/eshop/journals/sborka_v_mashinostroenii_priborostroenii/2026/22/

Sborka nr 8, 2020

1. **Improving the reliability of robotic assembly based on optimization of locating charts**
   Authors: Vartanov M.V., Petrov V.K., Troshina O.V.

A comparison of locating charts with passive adaptation and hard basing for robotic assembly of cylindrical parts of the "shaft—bushing" type is presented. The results of a physical experiment and an analytical solution to the problem using the original models of the robotic assembly in a quasistatic setting are compared. The reactions at the contact points that occur during the coupling process are determined.

2. **Assembly of metal-ceramic cases integrated circuit**
   Authors: Ivanov A.A., Kretinin O.V.

Technological processes of assembly of the most mass metal-ceramic IC cases with planar and pin contact conclusions on the automatic modular line are considered. It is proposed for the automated shop of assembly of cases to combine the assembly line and a site of automatic cassetting it into a single transport-accumulative system. The introduction of the IC hull assembly line into production provides an increase in labor productivity by 3...5 times while reducing the number of service personnel by an average of 3 times.

3. **High precision multi-spindle wrench for automated sealing of joints during assembly of products operating at high pressures**
   Authors: Zhitnikov Y.Z., Zhitnikov B.Yu., Matrosov A.E.

Based on the theoretical and experimental analysis of achievable accuracy and stability of main forces of automated tightening of threaded joints, a multi-spindle nut has been developed, which ensures tightness of joints of articles operating at high pressures.

4. **Ensuring high-quality tightening of threaded connections according to dynamic criteria**
   Authors: Shuvaev V.G., Kryilova I.N.

The options of normalized tightening of threaded connections in the process of ultrasonic assembly according to the tightening the system's response to the impact applied to the threaded connection during tightening are discussed. The original scheme of the device for monitoring the quality of tightening of a threaded connection by a dynamic criterion in the nonlinear domain is presented.

5. **Assembling a medical recirculator**
   Authors: Brysin A.N., Mikaeva A.S., Mikaeva S.A., Larshina E.L.

The assembly of a recirculator designed for decontamination of indoor air of all categories in the presence and absence of people are described. Potential consumer of the recirculator is junior nursing staff of medical and preventive, preschool, school, industrial, public and other organizations. The curve of bactericidal action of ultraviolet radiation and technical characteristics of the recirculator are presented.

6. **Predicting the values of average stresses during the ice–water phase transition in mesoporous silicon-based structures in the temperature range 233...273 K**
Authors: Bardushkin V.V., Kochetygov A.A., Shilyaeva YU.I., Volovlikova O.V.

Theoretical model has been developed for predicting the average stress values during melting of water frozen in silicon-based mesoporous structures in the temperature range 233...273 K, caused by the difference in the thermal expansion coefficients of the heterogeneity elements in the materials studied. Numerical calculations were carried out using and dependences of the average stress tensor components on the volumetric water content in the mesoporous silicon matrix were investigated.

7. **Formation of boundary lubricating films in the presence of complexing additives**
Authors: Boiko M.V., Kolesnikov I.V., Ermakov S.F., Boyko T.G., Bicherov A.A.

The formation of boundary lubricating films on the surface of steel during friction in the presence of substances forming complex compounds with iron — dipyridyl, o-phenanthroline, 8-hydroxyquinoline, and ethylenediaminetetraacetic acid, is considered. Boundary layers formed in the presence of complexones increase the antifriction properties of the lubricant at low loads. It has been established that surface films are formed predominantly from base oil molecules.

8. **Construction of manipulator movements in two-handed robotic systems when assembling of cylindrical joints**
Authors: Vorobev E.I., Morgunenko K.O., Koneva E.E.

The problem of constructing movements with manipulators with five degrees of freedom when capturing a cylindrical part, transferring it to a given position for the process of connecting parts are considered. Cyclograms of movement of manipulators during assembly are constructed.

9. **The methodology for determining the minimum allowable and maximum possible tooth lift when designing broaches for processing face holes with a side of more than 60 mm**
Authors: Kochergin V.S., Kuts V.V., Razumov M.S.

The methodology for determining the minimum allowable feed per tooth and maximum possible tooth lift is presented. Given the fact that with a decrease in the thickness of the metal layer being cut, the specific cutting force increases, in order to reduce the pulling force when designing broaches, it is necessary to strive to choose the maximum possible tooth lift.

10. **Dimensional chains for ensuring that the assembled axisymmetric housing is inserted into the guide hole**
Authors: Rodionova E.N., Yamnikov A.S., Matveev I.A.

Dimension chains were calculated using the example of a jet engine housing entering the launch tube. It was found that the method used does not take into account the actual values of losses and requires significant reliability in the radical run-out of the collected rocket engine case. A method for controlling radial run-out in prisms is also considered.

Link: http://www.mashin.ru/eshop/journals/sborka_v_mashinostroenii_priborostroenii/2026/23/

Sborka nr 9, 2020

1. **Development of a new method for assembling adjustable cylindrical joints**
Authors: Zaharova M.E., Tarasov D.R.

A new method for assembling cylindrical joints with a horizontal axis of assembly using adhesive compositions with the ability to regulate the relative position of the mating parts was developed. A constructive scheme of the assembly using the developed method is proposed.

2. **Analyze the allowances for the diameter for centering of lenses**
Authors: Kutenkova E.YU., Larina T.V.

The allowances for the diameter of lenses, from the general nomenclature of parts manufactured at JSC NPZ were analysis, and three groups of details were identified: 1) well-centered lenses on which the allowance is assigned traditionally; 2) lenses with a thin edge; 3) poorly centered.

3. **Mechanical and tribological properties of solid lubricant composites based on thermoplastic polyimide loaded with PTFE and surface modified carbon fibers**
Authors: Panin S.V., Tszyankun Lo, Buslovich D.G., Aleksenko V.O., Kornienko L.A.

The mechanical and tribological properties of thermoplastic polyimide based composites loaded with polytetrafluoroethylene and milled carbon fi bers, annealed and functionalized with a KH550 silane-coupling agent were studied. It has been revealed that, compared with neat PI, the composite with annealed carbon fi bers and PTFE particles possessed the highest wear resistance. Reinforcing carbon fibers of hundreds micron size increase the elastic modulus by 2 times; while all other physical and mechanical properties remain at the level of unfilled PI.

4. Tribological properties of structural alloys for the heat exchange equipment parts subjected to fretting

Authors: Martsenko E.A., Khrushchov M.M., Kaplunov S.M., Panov V.A.

Tribological characteristics of sliding friction in stainless steel and titanium alloys in dry and water lubricated conditions have been determined. The character of the coefficient of friction variation with load and the duration of tests have confirmed the prevailing wear mechanism in these materials to be frictional fatigue fracture that in the case of titanium alloys is accompanied with adhesive interaction and plastic plowing. The frictional fatigue curves built in a result of this investigation make possible to estimate the materials tribological longevity.

5. Active change in the state of self-oscillations in machines and mechanisms in a system with various types of nonlinearities of an arbitrary structure under the action of an impulse or harmonic disturbing force

Author: Erlich B.M.

The method of actively changing the state of self--oscillations in machines and mechanisms in a system with various types of nonlinearities of an arbitrary structure under the action of external periodic perturbations was proposed. The differential equations of the method take into account two types of external force periodic disturbances: impulse and harmonic.

6. Improving the tribological characteristics of lubricants by introduction of an additive of zinc phosphorovolframate

Authors: Savenkova M.A., Volyanik S.A., SHehov V.P., Avilov V.V., Sychev A.P., Koroleva A.I.

The results of the application of an inorganic polymer of zinc phosphorovolframate as an antifriction and anti-wear additive introduced into vaseline and glycerine, used as a dispersion medium for created lubricants are presented. It was found that the introduction of this type of additive into such dispersion media improves the tribological properties of lubricants without reducing the operational parameters.

7. Development of engineering calculation methods of a vibration isolation mechanism with stiffness compensation of the main elastic element

Authors: Glushko S.P., Pudovkin YU.A.

The design and verification calculation of the vibration-isolating mechanism of a pneumatic riveting hammer with stiffness compensation of the main elastic element is devoted. Graphs of the frequency response and amplitude-stiffness characteristics are given. Conclusions about the effectiveness of the vibration-isolating mechanism are made.

8. A necessary additions to GOST 21495—76 “Basing and bases in mechanical engineering, terms and definitions"

Authors: Melnikov A.S., Tamarkin M.A., Tishchenko E.E.

Additional terms are proposes, the use of which will avoid ambiguous interpretation of rules of selection of technological bases and quantify the achieved accuracy of installation of a part in a product or billets in a technological system.

9. Scissor car lift design optimization

Authors: Samarkin A.I., Dementev A.M., Dmitriev S.I., Samarkina E.I., Evgenyeva E.A.

The problem of the optimal application and load of the scissor lift drive is considered.

Link: http://www.mashin.ru/eshop/journals/sborka_v_mashinostroenii_priborostroenii/2026/24/

ASSEMBLY AUTOMATION

Emerald Publishing Limited
Howard House
Wagon Lane
Bingley BD16 1WA
United Kingdom
e-mail: emerald@emeraldinsight.com

Volume 40, Issue 4
ABSTRACTS:

1. An interference discrimination method for assembly sequence planning and assembly simulation

Authors: Wenlei Zhang, Mingxu Ma, Haiyan Li, Jiapeng Yu, Zhenwei Zhang

The purpose of this paper is to discriminate fake interference caused by polygonal approximation so as to achieve accurate assembly sequence planning and assembly simulation.

An approximation zone model is proposed to formulate polygonal approximation. Fake interference is discriminated from hard interference by evaluating if polygonal models intersect within corresponding approximation zones. To reduce the computation, the surface-surface, surface-end face and end face-end face intersection test methods have been developed to evaluate the intersection and obtain collision data. An updated collision detection algorithm with this method is presented, which is implemented by a system named AutoAssem.

This method has been applied to a set of products such as a valve for assembly interference matrix generation, static and dynamic collision detection. The results show that it ensures the accuracy of assembly sequence planning and assembly simulation for polygonal models.

This method facilitates assembly design in the virtual environment with polygonal models. It can also be applied to computer aided design systems to achieve quick and accurate collision detection.

Fake interference between polygonal models may result in serious errors in assembly sequence planning and assembly simulation. Assembly zone model and novel polygon intersection verification methods have been proposed to effectively tackle this problem. Compared to current methods, this method considers valid penetration direction and approximation difference, does not need to process complicated auxiliary data and can be easily integrated with current collision detection methods.

2. A measurement method of free-form tube based on multi-view vision for industrial assembly

Authors: Tianyi Wu, Jian Hua Liu, Shaoli Liu, Peng Jin, Hao Huang, Wei Liu

This paper aims to solve the problem of free-form tubes' machining errors which are caused by their complex geometries and material properties.

In this paper, the authors propose a multi-view vision-based method for measuring free-form tubes. The authors apply photogrammetry theory to construct the initial model and then optimize the model using an energy function. The energy function is based on the features of the image of the tube. Solving the energy function allows to use the gray features of the images to reconstruct centerline point clouds and thus obtain the pertinent geometric parameters.

According to the experiments, the measurement process takes less than 2 min and the precision of the proposed system is 0.2 mm. The authors used simple operations to carry out the measurements, and the process is fully automatic.

The paper proposes a method for measuring free-form tubes based on multi-view vision, which has not been attempted to the best of authors' knowledge. This method differs from traditional multi-view vision measurement methods, because it does not rely on the data of the design model of the tube. The application of the energy function also avoids the problem of matching corresponding points and thus simplifying the calculation and improving its stability.

3. An angle-changeable tracked robot with human-robot interaction in unstructured environments

Authors: Chengguo Zong, Zhijian Ji, Junzhi Yu, Haisheng Yu

The purpose of this paper is to study the adaptability of the tracked robot in complex working environment. It proposes an angle-changeable tracked robot with human–robot interaction in unstructured environment. The study aims to present the mechanical structure and human–robot interaction control system of the tracked robot and analyze the static stability of the robot working in three terrains, i.e. rugged terrain, sloped terrain and stairs.

The paper presents the mechanical structure and human–robot interaction control system of the tracked robot. To prevent the detachment of the tracks during obstacle navigation, a new type of passively adaptive device based on the relationship between the track's variable angle and the forces is presented. Then three types of rough terrain are chosen to analyze the static stability of the tracked robot, i.e. rugged terrain, sloped terrain and stairs.

This paper provides the design method of the tracked robot. Owing to its appropriate dimensions, good mass distribution and limited velocity, the tracked robot remains stable on the complex terrains. The experimental results verify the effectiveness of the design method.

The theoretical analysis of this paper provides basic reference for the structural design of tracked robots.

4. Mechanism and quantitative evaluation model of slip-induced loosening for bolted joints

Authors: Qingchao Sun, Qingyuan Lin, Bin Yang, Xianlian Zhang, Lintao Wang

Bolted joints are the most common type of mechanical connections, and improving the anti-loosening performance of bolts for the reliable performance of mechanical and building structures is highly significant.

Because of the lack of sufficient theoretical basis for the evaluation and design of anti-loosening bolts, a quantitative evaluation model exhibiting the following two evaluation criteria for anti-loosening bolts is introduced: bolt rotation angular acceleration criterion and critical transverse load criterion. Based on the relationship among bolt tension, transverse load and bolt rotation angular acceleration, a critical transverse load calculation model is put forward, and the mechanism by which the critical transverse load increases with the increase of bolt tension is revealed.

Based on the above model, a new type of anti-loosening bolt is designed, which generates additional bolt tension when the transverse load increases, and then improves the critical transverse load of the bolt. The effectiveness of the new type of anti-loosening bolt is verified by theoretical calculations and experiments.

The proposed model and method set a preliminary theoretical foundation for the evaluation of bolt anti-loosening performance and the design of a new anti-loosening bolt.

5. Design of H_/H∞ fault detection observer for closed-loop nonlinear system with disturbance

Authors: Zhengquan Chen, Lu Han, Yandong Hou

This paper proposes a novel method of fault detection, which is based on H_/H∞ Runge–Kutta observer and an adaptive threshold for a class of closed-loop non-linear systems. The purpose of this paper is to improve the rapidity and accuracy of fault detection.

First, the authors design the H_/H∞ Runge–Kutta fault detection observer, which is used as a residual generator to decouple the residual from the input. The H_ performance index metric in the specified frequency domain is used to describe how sensitive the residual to the fault. The H∞ norm is used to describe the residual robustness to the external disturbance of the systems. The residual generator is designed to achieve the best tradeoff between robustness against unknown disturbances but sensitivity to faults, thus realizing the accurate detection of the fault by suppressing the influence of noise and disturbance on the residual. Next, the design of the H_/H∞ fault detection observer is transformed into a convex optimization problem and solved by linear matrix inequality. Then, a new adaptive threshold is designed to improve the accuracy of fault detection.

This paper presents a novel approach to improve the accuracy and rapidity of fault detection for closed-loop non-linear system with disturbances and noise.

6. A fuzzy-regression-PSO based hybrid method for selecting welding conditions in robotic gas metal arc welding

Authors: Amruta Rout, Deepak Bbvl, Bibhuti B. Biswal, Golak Bihari Mahanta

This paper aims to propose fuzzy-regression-particle swarm optimization (PSO) based hybrid optimization approach for getting maximum weld quality in terms of weld strength and bead depth of penetration.

The prediction of welding quality to achieve best of it is not possible by any single optimization technique. Therefore, fuzzy technique has been applied to predict the weld quality in terms of weld strength and weld bead geometry in combination with a multi-performance characteristic index (MPCI). Then regression analysis has been applied to develop relation between the MPCI output value and the input welding process parameters. Finally, PSO method has been used to get the optimal welding condition by maximizing the MPCI value.

The predicted weld quality or the MPCI values in terms of combined weld strength and bead geometry has been found to be highly co-related with the weld process parameters. Therefore, it makes the process easy for setting of weld process parameters for achieving best weld quality, as there is no need to finding the relation for individual weld quality parameter and weld process parameters although they are co-related in a complicated manner.

In this paper, a new hybrid approach for predicting the weld quality in terms of both mechanical properties and weld geometry and optimizing the same has been proposed. As these parameters are highly correlated and dependent on the weld process parameters the proposed approach can effectively analyzing the ambiguity and significance of each process and performance parameter.

7. Active disturbance rejection control strategy for airborne radar stabilization platform based on cascade extended state observer

Authors: Dong Mei, Zhu-Qing Yu

This paper aims to improve the anti-interference ability of the airborne radar stabilization platform, especially the ability to suppress continuous disturbance under complex air conditions to ensure the clarity and stability of airborne radar imaging.

This paper proposes a new active disturbance rejection control (ADRC) strategy based on the cascade extended state observer (ESO) for airborne radar stabilization platform, which adopts two first-order ESOs to estimate the angular velocity value and the angular position value of the stabilized platform. Then makes the error signal which subtracts the estimated value of ESO from the output signal of the tracking-differentiator as the input signal of the nonlinear state error feedback (NLSEF), and according to the output signal of the NLSEF and the value which dynamically compensated the total disturbances estimated by the two ESO to produce the final control signal.

The simulation results show that, compared with the classical ADRC, the ADRC based on the cascade ESO not only estimates the unknown disturbance more accurately but also improves the delay of disturbance observation effectively due to the increase of the order of the observer. In addition, compared with the classical PID control and the classical ADRC, it has made great progress in response performance and anti-interference ability, especially in the complex air conditions.

The originality of the paper is the adoption of a new ADRC control strategy based on the cascade ESO to ameliorate the anti-interference ability of the airborne radar stabilization platform, especially the ability to suppress continuous interference under complex air conditions.

8. A flexible planning methodology for product family assembly line based on improved NSGA_II

Authors: Yongming Wu, Xudong Zhao, Yanxia Xu, Yuling Chen

The product family assembly line (PFAL) is a mixed model-assembly line, which is widely used in mass customization and intelligent manufacturing. The purpose of this paper is to study the problem of PFAL, a flexible (evolution) planning method to respond to product evolution for PFAL, to focus on product data analysis and evolution planning method.

The evolution balancing model for PFAL is established and an improved NSGA_II (INSGA_II) is proposed. From the perspective of data analysis, dynamic characteristics of PFAL are researched and analyzed. Especially the tasks, which stability is considered, can be divided into a platform and individual task. In INSGA_II algorithm, a new density selection and a decoding method based on sorting algorithms are proposed to compensate for the lack of traditional algorithms.

The effectiveness and feasibility of the method are validated by an example of PFAL evolution planning for a family of similar mechanical products. The optimized efficiency is significantly improved using INSGA_II proposed in this paper and the evolution planning model proposed has a stronger ability to respond to product evolution, which maximizes business performance over an effective period of time.

The assembly line designers and managers in discrete manufacturing companies can obtain an optimal solution for PFAL planning through the evolution planning model and INSGA-II proposed in this paper. Then, this planning model and optimization method have been successfully applied in the production of small wheel loaders.

9. Haptic-enabled virtual planning and assessment of product assembly

Authors: Enrique Gallegos-Nieto, Hugo I. Medellin-Castillo, Yan Xiu-Tian, Jonathan Corney

This study aims to present a new haptic-enabled virtual assembly system for the automatic generation and objective assessment of assembly plans. The system is intended to be used as an assembly planning tool along the product development process.

The generation of product assembly plans is based on the analysis of the assembly movements and operations performed by the user during the virtual assembly execution, and the objective assessment of product assembly is based on the definition and computation of new proposed assembly metrics.

To evaluate the system, a case study corresponding to the assembly of a mechanical component is presented and analyzed. The results demonstrate that the proposed system is an effective tool to plan and evaluate different product assembly strategies in a more practical and objective approach than existing assembly planning methods.

Although the virtual assembly execution time is larger than the real assembly execution time, the assembly planning and evaluation results provided by the system are valid. However, the development of higher performance collision detection algorithms is needed to reduce the simulation time.

The proposed virtual assembly system is able to not only simulate and automatically generate assembly plans but also objectively assess them from the virtual assembly task execution. The introduction and use of several assembly performance metrics to objectively evaluate assembly strategies in virtual assembly also represents a novel contribution.

10. 3D long-term recurrent convolutional networks for human sub-assembly recognition in human-robot collaboration

Authors: Xianhe Wen, Heping Chen

Human assembly process recognition in human–robot collaboration (HRC) has been studied recently. However, most research works do not cover high-precision and long-timespan sub-assembly recognition. Hence this paper aims to deal with this problem.

To deal with the above-mentioned problem, the authors propose a 3D long-term recurrent convolutional networks (LRCN) by combining 3D convolutional neural networks (CNN) with long short-term memory (LSTM). 3D CNN behaves well in human action recognition. But when it comes to human sub-assembly recognition, the accuracy of 3D CNN is very low and the number of model parameters is huge, which limits its application in human sub-assembly recognition. Meanwhile, LSTM has the incomparable superiority of long-time memory and time dimensionality compression ability. Hence, by combining 3D CNN with LSTM, the new approach can greatly improve the recognition accuracy and reduce the number of model parameters.

Experiments were performed to validate the proposed method and preferable results have been obtained, where the recognition accuracy increases from 82% to 99%, recall ratio increases from 95% to 100% and the number of model parameters is reduced more than 8 times.

The authors focus on a new problem of high-precision and long-timespan sub-assembly recognition in the area of human assembly process recognition. Then, the 3D LRCN method is a new method with high-precision and long-timespan recognition ability for human sub-assembly recognition compared to 3D CNN method. It is extraordinarily valuable for the robot in HRC. It can help the robot understand what the sub-assembly human co-operator has done in HRC.

TiAM
kwartalnik naukowo-techniczny
TECHNOLOGIA I AUTOMATYZACJA MONTAŻU
ZESPOŁÓW • MASZYN • URZĄDZEŃ

ASSEMBLY TECHNIQUES AND TECHNOLOGIES

INFORMATION FOR AUTHORS

Please submit to the editorial office author's application form with contact details, a title of the proposed article, number of pages, illustrations and tables and a brief abstract. After receiving information about the acceptance of the proposed paper submit the entire text prepared according to the editorial instructions as well as a complete declaration form.
Submitted articles are subjected to editorial assessment and receive a formal editorial identification number used in further stages of the editorial process. Every submitted article is reviewed. Publication is possible after receiving positive reviews (see review procedure).
The editorial office does not pay royalties.

GUIDELINES FOR PREPARING PAPERS

- Articles for publication in Assembly Techniques and Technologies should have scientific and research character and deal with current issues of the industry.
- Articles must be original, not previously published (if the article is a part of another work i.e. PhD thesis, Habilitation etc. the information about that should be placed in the reference section) .
- The article should involve a narrow topic but treated thoroughly without repeating general knowledge information included in the widely known literature.
- If the problem is extensive break it into articles for separate publications.
- Articles should be of a clear and logical structure: the material should be divided into parts with titles reflecting its content. The conclusions should be clearly stated at the end of the paper.
- The article should be adequately supplemented with illustrations, photographs, tables etc. however, their number should be limited to absolute necessity.
- The title of the article should be given in Polish and English as well as the abstract and key words.
- The article should not exceed 8 pages (1 page – 1 800 characters).
- The article should include mailing and e-mail addresses of the author(s).
- The article should be electronically submitted in * doc or * docx format. Equations should be written in the editors, with a clear distinction between 0 and O. If the equations exceed the width of column (8 cm) they must be moved, otherwise use double width column (16 cm).
- The editorial staff does not rewrite the texts or prepare illustrations. Apart from doc, * docx formats it is recommended to submit the source files of illustrations (in *.eps, *jpg or * tif format).
- Drawings and graphs must be clear, taking into account the fact that the width of the columns in the magazine is 8 cm, width of the single column - 17 cm, height of the column - 24.5 cm.
- The text on the drawings cut to the size must be legible and not less than 2 mm.
- The authors are required to give at the end of the article a full list of sources used for the paper. The text must include citation references to the position of cited work in the bibliography. The bibliography prepared according to the references in the text must include: books – surname and first letter of the author's name, title, publisher, year and a place of publication (optionally page numbers), magazines – author's name and surname, title of the article, title of the magazine, number, year and optionally page numbers. The bibliography should present the current state of knowledge and take into account publications of world literature.
- The authors guarantee that the contents of the paper and the drawings are originally their property (if not, the source should be indicated). The authors who submit the paper, will receive the following documents from the Publisher SIGMA-NOT to be signed by them:
  - The declaration on granting a licence
  - The licence agreement
  - The Authors' agreement

  on the right of the Publisher to:
  a) Preservation and reproduction of the article, via production of its copies by paper and electronic way,
  b) Turnover of the copies on which the article has been preserved – by introduction to market, lending or lease of the copies,
  c) Making available to the public, including the Internet pages,
  d) Dissemination as a whole or of its parts for advertisement and/or promotional purposes.
- The editorial staff will document all forms of scientific misconduct, especially violations of the rules of ethics applicable in science.


WYDAWNICTWO SIGMA-NOT
ponad 70 LAT NA RYNKU
34 TYTUŁY
129 000 PUBLIKACJI
WYGODNY DOSTĘP
DO ARTYKUŁÓW FACHOWYCH
Nowy
PORTAL INFORMACJI TECHNICZNEJ
www.sigma-not.pl
Zmieniamy się dla Ciebie